University of Cape Town: Department of Environmental and Geographical Science

African Climate and Development Initiative (ACDI)

Attribution-based Parametric Insurance: Towards Affordable Premiums

By: Sylvia Saygbay Diamond Dorbor

DRBDIA001

Thesis

Submitted in partial fulfillment for the degree of

Master of Science

specializing in

Climate Change and Sustainable Development

DECEMBER 2019

Supervisor: Professor Mark New

Co-supervisor: Dr. Romaric C. Odoulami

Declaration

This dissertation is presented for the approval of Senate in partial fulfilment for the requirements of the Master of Science degree specializing in Climate Change and Sustainable Development in coursework and minor dissertation. I, Sylvia S.D. Dorbor, hereby declare that I have read and understood the regulations governing the submission of MSc dissertation specializing in Climate Change and Sustainable Development, including those relating to length and plagiarism, as contained in the rules of the university, and that this minor dissertation conforms to those regulations, and in any other case thereof, a communication will be provided.

Acknowledgements

I would like to be grateful to the almighty God for granting me the wisdom and strength used to complete this work. He is truly an amazing God. A big thanks and appreciation go to my parents, siblings and family for their financial, moral and emotional support throughout my studies. I would also like to say a special thanks to my amazing "super-advisor", Professor Mark New, for guiding me through this process and to my co-supervisor, Dr. Romaric Odoulami, for all the technical support that made this work a huge success. To African Risk Capacity Insurance Limited for the partnership, resources and facilities made available; to the AXA/BNP group here at UCT and the University of Oxford; and to the life-long family I made here at ACDI; thank you all so much. A special thanks also goes out to my friend, Setsabile Thwala, for all her support given to me during my first few months in Cape Town.

Finally, I would like to say thank you to everyone else who supported, encouraged and wished me well along my journey. This is truly a story of resilience!

Dedication

This work is dedicated to the memory of my late grandmother, Saygbay Dorbor. She was always fond of asking, "When will my namesake finish the big school?" Well, I am almost there. I just need to be Dr. Saygbay Dorbor.

Abstract

To deal with the adverse impacts of climate change, index-based or parametric insurance has been recognized as an adaptation technique to compensate farmers for economic losses from extreme weather events. The insurance can be either private or sovereign. African Risk Capacity Insurance (ARC Ltd) offers the latter to African countries against drought events through contingency planning, risk pooling and transfer facilities. While the ARC insurance initiative seems promising, the current approaches used to estimate risk and determine premiums do not consider the change in risk from anthropogenic climate change. As the frequency of extreme weather events changes, the price of insurance premiums is likely to rise. Representing a cutting-edge science from weather to impact attribution, this study links attribution modelling with parametric insurance modelling to quantify how the probability of drought events has changed due to human influence on the climate system and translates the impacts into actual costs. To quantify this change, global climate models consisting of both factual and counterfactual world (with and without human forcing of climate, respectively) experiments were post-processed and used as rainfall inputs into an insurance risk modelling software, Africa *RiskView*. Estimated response costs needed for drought assistance in a world with and without climate change were calculated in Malawi, Zimbabwe, Senegal and Mauritania for the last 30 years. The empirical cumulative distribution function plots show that the distributions of models that represent the counterfactual natural world estimate lesser drought-affected population and lower response costs for assistance than those of the factual world distributions. The results suggest that climate change is likely to increase the price of insurance premiums. Therefore, there is a need for blended financing models that integrate international climate funds generated on a responsibility-based approach to cater for the added cost brought in by climate change.

Table of Contents

List of Figures

List of Tables

List of Acronyms

ARC- African Risk Capacity

ARC2- African Rainfall Climatology Version 2

ARV- Africa *RiskView*

AU- African Union

CDF- Cumulative Distribution Function

COP- Conference of the Parties

CMIP5- Coupled Models Intercomparison Project Version 5

ECDF- Empirical Cumulative Distribution Function

FAO- Food and Agriculture Organization

FAR- Fractional Attributable Risk

GCF- Green Climate Fund

GCM- Global Climate Model

IDA- Image Display Analysis

IFAD- International Fund for Agricultural Development

IPCC- Intergovernmental Panel on Climate Change

LDC-Least Developed Country

NOAA- National Ocean and Atmospheric Administration

NDVI- Normalized Difference Vegetation Index

PEA- Probabilistic Event Attribution

PDF- Probability Distribution Function

RCM- Regional Climate Model

RR- Risk Ratio

SSTs- Sea Surface Temperatures

TAMSAT- Tropical Applications of Meteorology using SATellite data and ground-based observations

UN- United Nations

UNDP- United Nations Development Program

UNFCCC- United Nations Framework Convention on Climate Change

WIM- Warsaw International Mechanism

WFP- World Food Program

XCF- Extreme Climate Facility

Chapter One: Introduction

1.1 Introduction to the Study

Anthropogenic climate change provides a key challenge for mankind and affects many sectors including the agricultural sector, which is a critical pillar for sustainable economic development (UNGA, 2015; Myers et al., 2017). This is particularly challenging in regions of Africa, where agriculture is highly dependent on rainfall and per capita food production is declining due to the increase in demand from the rapidly growing population (FAO, 2017; Myers et al., 2017). Although farmers have always had to deal with weather variations due to drought being a natural part of climatic variability in Africa (Masih, Maskey & Trambauer, 2014), an increasingly frequent occurrence of extreme weather events is further exacerbating the challenge of food production (IPCC, 2013; Myers et al., 2017). Dawson, Perryman & Osborne (2016) reported that climate change is estimated to put approximately 1.7 billion people globally at risk of undernourishment by 2050. Furthermore, every one in four persons in Africa currently lacks access to adequate food to sustain a healthy and an active lifestyle (FAO, 2015), and with a population that is projected to rise to 2.4 billion by 2052 (UN, 2015), there is an urgent need to build a resilient agricultural system that adapts to changes in the climate system.

To help farmers cope with extreme events impacts and ensure that the demand for food is sustainably met, a combination of climate risk reduction and risk response strategies is needed to manage challenges posed to the agricultural sector. While some of the challenges can be addressed through technical and other 'on-farm' approaches, such as shifting to drought resistant crops, those approaches alone cannot "climate-proof" society (Dow et al., 2013). Therefore, insurance has been recognized as a form of risk management that has been widely used in agriculture, through which those insured are compensated for loss and damage incurred from extreme weather events, as well as other hazards such as pest and price fluctuations (Alderman & Haque, 2007; UNFCCC, 2008). In the last decade, there has been a shift from traditional indemnity agriculture insurance schemes, which compensate farmers after assets have been depleted, to index-based or parametric insurance schemes, which compensate

farmers by addressing immediate losses (Cole et al., 2012; Adiku et al., 2017). Index-based or parametric weather insurance schemes bring along a proactive lens and use rainfall levels, crops yield or a vegetation index as objective parameters which trigger payments when a specified threshold is exceeded (IFAD, 2011). An advantage of parametric insurance is there is no assessment of losses, so payouts are faster and timely. The insurance can either be private, where private losses are insured or on a sovereign level, where countries insure against national scale damage (IFAD, 2011; Richards & Schalatek, 2017).

African Risk Capacity Insurance (ARC Ltd), under the auspices of the African Union (AU), offers parametric insurance at a sovereign level to African countries against extreme weather events (drought in this case) through contingency planning, risk pooling and risk transfer facilities (ARC, 2018a). In recent years, the following countries have joined the ARC risk pools: Kenya, Mauritania, Niger, Senegal, The Gambia, Mali, Malawi, Burkina Faso and Cote d'Ivoire. To estimate drought risk, ARC Ltd uses the Africa *RiskView* (ARV) model (ARC, n.d.). The number of people affected in a given area from a drought event, as well as the response costs for assistance are estimated using ARV. The modelled national drought response costs underlie the basis of parametric insurance products and premiums that are negotiated with governments and insurance partners (ARC, n.d.).

While parametric insurance seems to be a promising initiative, the current approaches used do not consider the change in risks of extreme events due to human influence on the climate system. This change in risks ultimately impacts on the cost of insurance, and this has both business and ethical implications.

For the insurance industry, if insurance premiums get too high, state and private actors in vulnerable developing countries may not be able to afford insurance, and this might reduce the insurance market base to unviable levels. From an ethical perspective, although heavily debated, it has been outlined in the Paris Agreement and the Warsaw International Mechanism (WIM) of the United Nations Framework Convention on Climate Change (UNFCCC) that direct compensation be given to vulnerable countries to address socio-economic losses from climate change (Richards & Schalatek, 2017). Therefore, is it fair under the terms of the UNFCCC and the

Paris Agreement that developing countries should carry the additional cost of insurance arising from climate change?

While no one thus far can attribute an event entirely to human-induced climate change, the frequency and magnitude of events are changing dramatically, predominantly due to human-induced greenhouse gas emissions (IPCC, 2001, 2013). Moreover, assessing the role of human activities in the likelihood of occurrence of extreme events is now possible through the emerging field of Probabilistic Event Attribution (PEA) science (Stott et al., 2016).

The challenge thus lies in finding a way to make parametric weather insurance attractive to insurers, farmers and policymakers. Attribution science works by modelling two alternative worlds: the factual world (the reality) and a counterfactual world (without greenhouse gas emissions and other human forcing factors) to estimate the probability of a given event occurring in a world without human-induced climate change (Allen, 2003; Stott, Stone & Allen, 2004; Stott et al., 2016).

Using the lens of attribution science could enable us to ascertain if the risks of drought events have changed due to human influence on the present-day climate, and if so, how the change in risks translates into expected damage. If a fraction of the risks can be attributed to human-induced climate change, evidence can be provided on how climate change has altered the cost of insurance, providing a basis to argue that the developing countries should be compensated for the added cost of the insurance due to climate change.

1.2 Rationale and Aim of the Study

Event Attribution is a new field of science that is still rapidly developing, and studies in Africa are limited, with focus being placed mainly on the East African droughts (Funk et al., 2013, 2014; Lott, Christidis & Stott, 2013; Marthews et al., 2015; Uhe et al., 2018). Going from weather to impact attribution is at the cutting edge of science, with two European study papers being published so far (Mitchell et al., 2016; Schaller et al., 2016). The potential to use attribution science to improve risk assessments has long been recognized but has not been adopted (Richards & Schalatek, 2017). This study offers the opportunity to move from weather event to impact attribution in an

African setting, and for the first time, expresses this impact in economic terms. It brings forth a novel idea, with scientific and developmental objectives, to merge the cutting edge of attribution science modelling with parametric insurance modelling. It aims to address both the business and ethical implications of climate change on parametric insurance, bringing forth an argument that there should be a blend of international climate funds such as the Green Climate Fund (GCF) to account for the cost of the added risk from climate change, to make insurance premiums more affordable for developing countries in climate vulnerable settings.

1.3 Research Question

This project seeks to answer the following research question:

Can attribution science be used to apportion the damage estimates used in insurance underwriting between that expected from a natural climate and that added through climate change?

1.4 Objectives of the Study

To answer the above research question, this study has the following specific objectives:

1. Use of a weather or climate attribution approach to assess if the rainfall levels used in ARC Ltd risk models have changed due to human influence on the present-day climate.

2. Quantify how this changed probability translates into expected damage calculated in the risk model used by ARC Ltd to inform its underwriting calculations.

1.5 Thesis Outline

The rest of this thesis is structured as follows, with five chapters. The second chapter reviews the literature and identifies the knowledge gaps that need to be filled. The third chapter explains the methodologies used in this study. The fourth chapter presents the results or findings of this study and the fifth chapter discusses the implications of the findings.

Chapter Two: Literature Review

2.1 Introduction

This chapter discusses what has already been said in the literature with regards to climate change, loss and damage, event attribution and index-based insurance and identifies existing gaps that are intended to be filled by this project. It starts off by giving an overview on the impacts of climate change on the frequency, magnitude and intensity of extreme weather events. It further describes the emerging field of weather or climate attribution science, its prominence in Africa and its relevance for impact attribution. It also discusses the socio-economic risks associated with extreme events impacts, various strategies and instruments that are used to address loss and damage from extreme events and explains how insurance has been proposed as a financial instrument popular to the loss and damage approach currently. With insurance in the spotlight, it further explains parametric index-based weather insurance schemes, including those offered by ARC Ltd, in terms of its meaning, types and levels. It finally links both attribution and parametric insurance concepts to portray how human influence on the climate system is altering the damage estimates in insurance underwriting.

2.2 An Overview of Climate Change and Extreme Events

Extreme weather events such as floods and droughts have been occurring in the earth's record long before humans' fingerprints on the climate system began to accumulate (IPCC, 2001). Those events led to famine and other socio-economic impacts that affected people during and even before the Stone Age. However, over the last several decades, the frequency, magnitude and intensity at which these extreme events are occurring are dramatically changing. Since the industrial revolution, human activities have caused major changes to the climate system through the emission of greenhouse gases and have accumulated enough effects to push extreme events beyond the bounds of natural variability (IPCC, 2001, 2013, 2014). According to the IPCC Fifth Assessment-Report (AR5), *"since 1950, changes in many extreme weather and climate events have been observed"* (IPCC, 2014). Moreover, CO_2, a major greenhouse gas, level in the

atmosphere has increased from 280 ppm in pre-industrial times (O'Hare, Sweeney & Wilby, 2005) to 414.7 ppm in the 21st century (NOAA, 2019) and is expected to increase to 540 ppm and 970 ppm under different Representative Concentration Pathways (RCP) scenarios (Moss et al., 2010). According to scientists from the National Ocean and Atmospheric Administration (NOAA), the monthly average surpassing 414 ppm in May 2019 is the highest seasonal peak observed in the last 61 years of observational data (NOAA, 2019). Climate change is expected to increase the frequency and intensity of extreme events and as global temperatures increase, so will the likelihood of the world encountering *"severe, passive and irreversible"* impacts from climate change (IPCC, 2014).

2.3 Attribution of Extreme Weather and Climate Events

Whenever an extreme event occurs, there is always some public concern and media interest to know whether humans played a role in the occurrence of that event (Allen, 2003). Extreme events, which parametric index-based insurance schemes protect against, are rare, by definition, and in practice, there is limited knowledge on how the climate is changing. The weather is all that can be observed, and a short observational record alone does not enable one to assess whether or not extreme events have increased (Allen, 2003). However, the influence of human-activities on the long-term record is evident and is already changing high impact weather and climate events (IPCC, 2013; Fischer & Knutti, 2015). Although the change in climate might reduce the risks of some extremes such as cold spells; the negative, most damaging extremes such as droughts, floods, heat waves and storm surges are more likely to increase, especially in vulnerable developing countries (IPCC, 2013). As more extreme events occur, the public demand to know the role of human-influence will increase.

The field of attributing extreme events to human influence has gained momentum both in the scientific and public space and this could perhaps be due to its ability to provide evidence that seemingly links the abstract concept of climate change to the more tangible everyday weather impacts that are felt.

Attribution is defined as *"the process of evaluating the relative contributions of multiple causal factors to a change or event with an assignment of a statistical confidence"* (Hegerl et al., 2010:2; Stott et al., 2016:24). Attribution studies are currently grouped into three types: the attribution of long-term changes in climate parameters, the attribution of extreme weather or climate events and the attribution of climate-related impacts (Knutson et al., 2017; Zhai, Zhou & Chen, 2018). Attributing long-term trends in the observed record, especially using temperature, has been investigated since the IPCC Second Assessment-Report in 1995 (Otto, 2016). Initially, attribution was based on investigating human influences on long-term changes in the climate (Zhai, Zhou & Chen, 2018), and attributing individual extreme event was deemed as impossible (Otto, 2016).

2.3.1 Probabilistic Event Attribution Science

Assessing the role of human-influence on individual extreme event is now possible under a relatively new field of science known as Probabilistic Event Attribution (PEA). PEA seeks to estimate how the change in risks of extreme events has been impacted by human-induced climate change (Allen, 2003; Stott et al., 2013; Otto et al., 2015).

Factual versus the Counterfactual World

As with other forms of attribution, executing a PEA approach is based on two alternative worlds: the actual world with simulations that are as realistic as possible, and a counterfactual 'natural' world that represents a world that may have been, had we not increased our greenhouse gas levels (Allen, 2003; Stott et al., 2016). The counterfactual simulation is generated by running the same climate model with the anthropogenic forcing agents removed (Otto et al., 2015). The fraction of attributable risk due to human influence on the climate system is calculated using an ensemble of climate model simulation representing the probability of an event happening in the actual world, compared to the probability of the same event occurring in a world without climate change (Allen, 2003). The core concept of PEA is to compare both worlds to assess how human influence has altered the probability or the magnitude of a particular event (Pall et al., 2011; Otto et al., 2015; Stott et al., 2016).

The exact method used to remove human-induced climate change drivers from the model simulations will significantly influence the result (Otto et al., 2015). Different methodologies may lead to equally robust results, but how the risks are quantified may differ.

2.3.2 Methodologies in Event Attribution Science

Fractional Attributable Risk (FAR) and Risk-Ratio

The concept of Fraction of Attributable Risk (FAR) is used to provide a link between human-induced climate change and an extreme weather or climate event (Allen, 2003; Stott et al., 2013). The probability of an event occurring in the actual world, denoted by (P_1) is quantified and compared to the probability of the same event occurring in a counterfactual 'natural' world, had human forcing on the climate been absent, denoted by (P_0). The probabilities of both worlds' scenarios are expressed as a risk-ratio ($RR=P_1 / P_0$) or as a FAR ($FAR=1- P_0 /P_1$), which are used to measure the extent of human influence on the changes in the probability and intensity of extreme events (Allen, 2003; Stott, Stone & Allen, 2004; Fischer & Knutti, 2015). The role of human influence is quantified by comparing the likelihoods of occurrence. When the FAR exceeds a particular threshold, it indicates that a probability that is attributable to anthropogenic forcing has increased (Pall et al., 2011). This method of attribution has been widely used for mainly temperature and precipitation parameters (Stott et al., 2016).

Individual Methods

There are two main methods used for extreme weather and climate events attributions: methods that employ observational data to estimate changes in extreme events and methods that employ climate model simulations to compare differences in extremes using different approaches to simulate factual and counterfactual worlds (Stott et al., 2016; Zhai, Zhou & Chen, 2018). Methods based on observations include the analogue and empirical methods, which consider the overall effects of climate trends (Stott et al., 2016). The analogue approach considers observed circulation characteristics by identifying analogues of the characteristics of an observed event to determine how similar types of events have changed. The empirical approach estimates how secular climate change is affecting the return times of extreme events, by using long-term data

to determine the changes in the likelihood of an observed event with time (Stott et al., 2016). However, PEA studies rely on robust model simulations to account for changes in extreme event. Therefore, analyzing changes in the frequency and magnitude of extreme events, as well as the fraction of attributable risks due to external forcing such as human-induced greenhouse gas emissions, requires large ensembles of climate model simulations (Otto et al., 2013). This paper discusses methods that make use of climate models to make robust attribution statements using climate models.

Coupled-Model Approach

This method uses coupled ocean-atmosphere Global Circulation Models (GCMs) which simulate all major components of the climate system – including the land, atmosphere, ocean, and other biological and chemical processes – at relatively high resolution. Coupled GCMs provide the most comprehensive simulations of the overall climate system (Stott et al., 2016). The assessment is done using large datasets containing many ensembles (i.e. Coupled Model Inter-comparison Project phase 5 (CMIP5)) with different forcings that represent the actual world and a counterfactual world, using a climate variable of interest.

Use of these archived GCMs is advantageous due to their provision of existing data to enable rapid assessments as soon as an event occurs. The changing likelihood of extremes is estimated with reference to a specified threshold of the climatic variable investigated (e.g. a rainfall threshold). The estimates can also be computed over different range of thresholds to make attribution information available for future event occurrence (Stott et al., 2016). In some instances, event attribution is done conditionally by considering features that were present in the climate at the time the event occurred. When using this approach, the models must be rigorously evaluated against observations to factor in statistical uncertainties (Stott et al., 2016).

Sea-Surface Temperature (SST) Forced Atmosphere-only Model Approach

This approach also uses large model datasets but with atmosphere-only GCMS (AGCMs), forced by prescribed Sea-surface Temperatures (SSTs) and sea ice, mainly simulating the changes in atmospheric composition (Stott et al., 2016). It relies on the model's ability to simulate conditions present during the occurrence of an event and recognizes the variations in SST conditions are a

key driver of seasonal and shorter-term variability within which extreme events are embedded. The actual world scenario is simulated using observed SSTs and sea ice concentrations, while the counterfactual 'natural' world is simulated using SSTs with the human influence removed as well as pre-industrial greenhouse gas and aerosols levels (Christidis et al., 2012). Whereas removing human-induced greenhouse gas and aerosol forcing from a model is straight forward, estimating the pattern of warming to be removed from the observed SSTs and sea ice is not as simple. The warming signal is obtained from coupled GCMs by subtracting their actual world SSTs simulations and the natural world simulations. Some argue it is important to use more than one counterfactual 'natural' world SST pattern, since human influence on the event may be sensitive to the differences in patterns. To overcome this, SST patterns based on observations rather than models, can be used to test its validity (Stott et al., 2016).

This method is advantageous due to its relatively cheap nature to run model simulations, thereby producing more outputs of ensembles that result in a better representation of an event due to its improved "signal-to-noise" ratio (Stott et al., 2016). It is however limited due to its inability to represent events that are strongly affected by atmosphere-ocean coupling (as opposed to forcing), since it runs on atmosphere-only models (Stott et al., 2016).

Multi-method Approaches

Some studies use multi-method approach. With a multi-method approach, studies can make use of observations from stations and gridded datasets, coupled-climate models and atmosphere-only models for analysis (Otto et al., 2018). When different methods yield a consistent or similar result, confidence is boosted in the study. A recent study that used this method was the attribution study on the Western Cape drought in South Africa by Otto et al. (2018). The observational analyses relied on 18 meteorological stations, and a global station-based gridded data set (CRU) was used to compare observations to models. Two coupled climate models and two SST atmosphere-only models were also utilized to understand the dynamic and thermodynamic changes (Otto et al., 2018). All the methods used for attribution have their advantages and disadvantages. If one were to use all methods to study and event, and they all

agree, the attribution evidence is robust (either there is a human influence or not), but if all methods do not agree, then the attribution statement is not robust enough.

2.3.3 Operational Attribution

With varying PEA methods deployed, efforts have been made to develop operational attribution systems (Hoerling et al., 2013; Zhai, Zhou & Chen, 2018). Previous approaches in PEA generated results that were available months or even years after an event occurs. Christidis et al. (2012) argued that attribution is performed on past events and does not require predictability. However, given the growing public awareness on the role of climate change every time an extreme event occurs, an attribution statement based on fast, yet robust analysis of the extreme event, is desired. Science is based on current understanding and is liable to changes as our understanding on a certain topic improves. Therefore, a new method which assesses the fraction of attributable risk of an event due to an external driver was proposed by Haustein et al. (2016). It employs weather@home modelling experiments created at the University of Oxford for event attribution to produce fast track assessments (Haustein et al., 2016). Instead of using observational data, this method uses seasonal forecast SSTs and sea ice concentration based on an atmosphere-only model. With this method, possible weather can be simulated before an extreme event occurs, enabling users to provide rapid attribution statement after an event occurs, based on scientific evidence (Haustein et al., 2016).

2.3.4 Prominence of PEA

Quantifying human influences on an individual event was first applied about 14 years ago on the European heat wave of 2003 (Stott, Stone & Allen, 2004). The study showed that the likelihood of the event occurring was at least doubled by human-influence (Stott, Stone & Allen, 2004). With the concept of event attribution still in its early or trial stages, it took another individual extreme event that had severe socio-economic impacts, for practitioners in the scientific community to evaluate events, and further explore ways they could be analyzed (Otto, 2016). This event was the Russian heat waves of 2010, which stimulated two attribution studies that yielded different results; at least that was the initial thought until Otto et al. (2012) reconciled their apparently

contradictory results. One of the studies by Dole et al. (2011) looked at the magnitude of the event and concluded that human-influence did not play a role in the event, and the other study by Rahmstorf & Coumou (2011) investigated the frequency of the event and concluded that human-influence increased the likelihood of the event by five-fold. None of the two studies was wrong as they were both complementary aspects of the event (Otto et al., 2012). The way each attribution question is framed or designed can potentially influence the results generated (Otto et al., 2012).

With growing interests, increasing concerns and the advancement in models and methods, there has been an increase in attribution studies (Zhai, Zhou & Chen, 2018). Issues looking at how human-induced climate change may have affected individual events were published for the first time in 2012 in the Bulletin of American Meteorological Society (BAMS) (Peterson, Stott & Herring, 2012), with subsequent BAMS publications thereafter (Peterson et al., 2013; Herring et al., 2014, 2015, 2018). Even though there has been an improvement in attribution studies globally, there have been relatively few studies in Africa (Lott, Christidis & Stott, 2013; Otto et al., 2013, 2015; Marthews et al., 2015).

2.3.5 Review of Attribution Studies in Africa

Africa is often considered to be the most vulnerable continent to climate change (IPCC, 2013); yet its climate system has received a lack of research attention: both in general, and in the case of extreme event attribution (Otto et al., 2015; Parker et al., 2017).

Africa has a large-scale monsoon system that is more responsive to globally distributed ocean temperatures than any other monsoon system (Hoerling et al., 2006). An investigation considering whether the attribution of rainfall trends observed in Africa in the 20th century can be attributed to ocean-atmosphere interactions that were influenced by human forcing was done by Hoerling et al. (2006). Through investigating the sensitivity of rainfall to variations in global Sea Surface Temperatures (SSTs) using climate models, they found that drying trends in Africa from 1950 - 1990 were directly attributable to the fluctuations in the SSTs field observed globally.

Even then, studies suggest a role of climate change in the frequency, intensity, and magnitude of events in areas such as Australia that has similar climatology to Southern Africa (Herring et al., 2014).

Studies on event attribution are still rare in Africa, with focus being placed mainly on the East African droughts (Funk et al., 2013, 2014; Lott, Christidis & Stott, 2013; Marthews et al., 2015; Uhe et al., 2018). The first PEA study in Africa was done on the 2011 East African drought by Lott, Christidis & Stott (2013); they found that human influence increased the long rainy season but there was no evidence of human-influence on the short rainy season in East Africa. Attribution studies other than the East African droughts include: a precipitation study in the Congo basin area (Otto et al., 2013), which showed that PEA studies can be robust in data sparse regions; the attribution of floods in the Okavango basin, Southern Africa, which showed that human-influence increased the probability of the event occurrence (Wolski et al., 2014); and most recently, an attribution study on the Western Cape drought in South Africa by Otto et al. (2018) (see Table 1). Reasons why event attribution studies are rare in Africa have alluded to the lack of technical expertise, lack of observations from weather stations to identify extreme events and validate the climate model (Otto et al., 2015). However, gridded observational datasets are made available through satellite imagery that can further aid work to reduce reliance on directly observed data. Table 1 below provides examples of different attribution studies from around the world, using the different methodologies discussed.

Table 1: Examples of Event Attribution Studies Using Different Methodologies

Study	Methodology	Outcome	Reference
Western Cape drought (South Africa)	**Risk-based multi-method** Observational analysis (Empirical) Coupled climate models SST atmosphere-land models	Anthropogenic climate change significantly increased the likelihood of such a drought to occur by a factor of 3	(Otto et al., 2018)
Attributing extreme precipitation in the Netherlands	Observational analysis Coupled- global climate models and regional climate model	Observations- anthropogenic forcing significantly increased the intensity and frequency of the event. considerably smaller trends seen in the models	(Eden et al., 2018)
Attribution of summer 2013 heat waves in Korea	**Risk-based multi-method** Coupled- climate models Atmosphere-only models	Anthropogenic influence had an important role in the extreme heat event over Korea, and increased the chance of heat waves occurrence by 20 %	(Kim et al., 2018)
Extreme European summer of 2012	**Multi-method approach** Observational analysis (Analogue, Empirical) Coupled-climate models SST atmosphere-only models	Consensus across all methods that climate change significantly increased the risk of hot and dry summers in Southern Europe. No clear robust indication of climate change in Northern Europe	(Wilcox et al., 2018)
Attributing record wet winter in South East Australia	SST atmosphere-only models' approach	Minimal role of human-influence. Warmth in East Indian Ocean increased the likelihood of the event by a factor of 2	(King, 2018)
Attributing extreme rainfall from Hurricane Harvey in Texas	**Multi-method approach** Observational analysis (Empirical) Coupled- global climate models SST forced atmosphere-only models	Global warming over the last century, primarily caused by greenhouse gas emissions, increased the probability of the given rainfall event.	(van Oldenborgh et al., 2018)
Attributing 2012 West African heavy rainfall	**Multi-method approach** Coupled-climate models SST atmosphere-only models Observations – for models' validation	Human influence decreased the probability of high precipitation across most of the model ensembles.	(Parker et al., 2017)
Drivers of the 2016 Kenyan drought	**Multi-method approach** Observational analysis (Empirical) Coupled-climate models SST Atmosphere-only models' approach	No consistent signal from climate change. Event was more likely due to specific SSTs.	(Uhe et al., 2018)
Extreme precipitation in Boulder, Colorado	**Multi-method approach** Observational analysis (Analogue, Empirical) Coupled-climate models' approach SST atmosphere-only models' approach	Anthropogenic forcing increased the likelihood of extreme one-day-precipitation. Unable to detect five-day-precipitation	(Eden et al., 2016)
Attributing the 2014 drought in the horn of Africa, East Africa	Atmosphere-only-models approach (Weather@home regional model)	No anthropogenic influence on the likelihood of low rainfall but clear signal in other drought drivers	(Marthews et al., 2015)
Attributing past dry and wet rainy season over Southern Africa and South America	Coupled-climate models' approach Observations- for model validation	Not enough evidence to make a robust attribution statement over South America. Southern Africa- unusually dry summers (2002/3) likely due to climate change; unusually wet austral summer (1999/20000) less likely due to climate change	(Bellprat et al., 2015)
Floods in the Okavango basin, Botswana	Risk-based approach Atmosphere-only-models approach Hydrological models	Probability of occurrence of floods is likely lower than it would have been in a world without climate change	(Wolski et al., 2014)
Attributing the 2011 East African drought	SST atmosphere-only model approach Observations-for model validation	Human influence increased the long rains to be as dry as 2011. N0 evidence for the short rains in 2010	(Lott, Christidis & Stott, 2013)
Precipitation patterns in African rainforests (Congo Basin)	SST atmosphere-only model approach Observations- for model validation	No significant changes in the risk of low extreme precipitation extremes during the June-July-August dry season. Highlights that there is a potential for attribution studies to be done in region with sparse data	(Otto et al., 2013)

2.3.6 From Weather to Impact Attribution

Weather attribution considers attributing the occurrence of extreme events to anthropogenic forcing or natural variability; while impact attribution considers attributing the potential contribution of those extreme events to loss and damage associated with climate change impacts (IPCC, 2014; Otto, James & Allen, 2014). Loss and damage from human-induced climate change goes beyond what people can adapt to and increases their vulnerability and exposure level (IPCC, 2014; Mechler et al., 2014, 2019). To make a scientific association between human-induced climate change and loss and damage, two links need to be made: a link between greenhouse gas

emissions and meteorological change and a link between the meteorological change and the impacts it would have on society (Otto, James & Allen, 2014). However, according to the Fifth Assessment-Report of the IPCC, there have been limited studies done on the impact of climate change on human systems, with more focus being placed on the natural system (IPCC, 2014). Given that the earth is a coupled system consisting of both the human and natural system, this study focuses on attributing the actual impact of drought on food production in the coupled natural-human food system.

2.4 Climate Change Adaptation: Addressing Loss and Damage from Extreme Events

The risks associated with extreme weather and climate-related events are of major socio-economic concern, especially in the light of climate change (Müller, Johnson & Kreuer, 2017). Since climate change is expected to increase the frequency of extreme events and those events are linked to 'loss and damage' impacts, it is crucial to plan for adaptation to reduce the level of exposure to those risks.

Loss and damage in the context of climate change refers to *"irreversible losses and damages of significant economic cost that are caused, at least in part, by climate change"* (Durand et al., 2016). When an agricultural system is heavily dependent on rainfall for crops production, drought-related extremes can cause major economic damages to farmers (Burke, De Janvry & Quintero, 2010; Winkler, Gessner & Hochschild, 2017). For example, crop failures due to the low level of rainfall during both the short and long rainy seasons in East Africa contributed to famine in Somalia in 2013 (Funk et al., 2013).

Extreme weather events can have compounded effects on the lives and livelihoods of people, most especially poor vulnerable groups. They trigger farming through crop failures, displace families through flooding events and lead to the loss of slowly-built assets to deal with these impacts (Alderman & Haque, 2007). The damage also extends to transfer poverty across generations through scenarios that lead to children being dropped out of school due to loss of income from agriculture (Alderman & Haque, 2007).

Loss and damage (i.e. climate-related risks and damages) from weather and climate-related extreme events have been addressed mainly using market-based and solidarity instruments (Linnerooth-Bayer & Hochrainer-Stigler, 2015; Gewirtzman et al., 2018). The market instruments place responsibility on the population at risk (Gewirtzman et al., 2018). For example, African countries paying insurance premium to ARC Ltd to cover drought is a form of market instrument. Whereas, solidarity instruments transfer bulk of the responsibility to the international community, which includes countries responsible for most of historical greenhouse gases emissions (UNFCCC, 2008; Gewirtzman et al., 2018). Unlike developed countries, which have capabilities to provide immediate relief to disaster victims through funds and other relief items, responding to natural and climate-related disasters in developing countries has not always been timely or fair, as it should be, with victims having to bear most of the costs from the losses (Richards & Schalatek, 2017). When governments appeal for aid, it is done largely on an *ad hoc* basis, after a disaster has struck, and in most cases, governments are compelled to reallocate funds from their national budgets for quick response (Cole et al., 2012). At most times, the crisis response, which is mostly solidarity-based comes in late when livelihoods and lives have already been affected (Linnerooth-Bayer & Mechler, 2006; Linnerooth-Bayer & Hochrainer-Stigler, 2015; ARC 2018a). And as the frequency and intensity of extreme events change in response to climate change, these challenges will be further exacerbated.

2.4.1 International Frameworks

Addressing loss and damage through international efforts first emerged in 1991 at the international climate negotiations when a proposal was made to compensate developing countries and small island states dealing with sea level rise (Vanhala & Hestbaek, 2016). After being in the spotlight for years, it was agreed in 2013 at the 19th Conference of Parties (COP) to establish arrangements on loss and damage, through which the Warsaw International Mechanism (WIM) on loss and damage, associated with climate impacts, was established (UNFCCC, 2014). At the following COP 20 in 2014, a work plan was adopted to explore a direction for the next two years, but enhancing action and support, mainly through finance was neglected (Richards & Schalatek, 2017).

At COP 21 in 2015, the Paris Agreement emerged, and a full article was devoted to loss and damage. Article 8 of the Paris Agreement states that *"Parties should enhance understanding, action and support, including through the Warsaw International Mechanism, as appropriate, on a cooperative and facilitative basis for loss and damage"* (UNFCCC, 2015:8.3). However, no basis was provided for any compensation, and opportunities for gathering support are limited since 'loss and damage' is not mentioned in the finance section of the Paris Agreement (van Asselt et al., 2016). Thus, international efforts on addressing loss and damage from climate change, particularly regarding the question of how they would be funded, have not shown substantial efforts yet.

Nevertheless, there is a growing architecture of climate finance and funding that come in from different sources through means such as pledges, grants, loans and aids to 'help' developing countries adapt climate-resilient pathways (Watson & Schalatek, 2019).

2.4.2 Global Climate Funds: Climate Funds Architecture in Africa

The Global climate finance architecture is a complex and ever-evolving architecture that includes funds from multilateral, bilateral, regional and national sources in and out of the spheres of the UNFCCC and the Paris Agreement to help developing countries adopt climate-resilient development pathways to adapt to the adverse impacts of climate change (CFU, 2019). The 2015 Paris Agreement has reinforced the case for developed countries to take the lead in mobilizing climate finance and a collective goal of USD 100 billion was set to be reached annually by 2020 (Watson and Schalatek, 2019). The Green Climate Fund (GCF) is by far the biggest climate fund allocated for adaptation in sub-Saharan Africa (CFU, 2019). As a financial mechanism of the UNFCCC, the GCF was adopted by 194 nation states to support adaptation in developing countries, especially countries that are particularly vulnerable to the adverse effects of climate change (ADB, 2019). It is expected to become a primary source through which international public climate finance will flow to developing countries.

The GCF approved a total of 93 projects with USD 4.6 billion in funding commitments as of November 2018 but sub-Saharan Africa remains a '*paddling pool*' when it comes to receiving

climate finance for adaptation. The GCF works by having accredited entities (national, non-governmental organizations, international) in different countries through which countries are allowed direct access to climate finance. As of November 2018, the GCF has a total of 75 accredited entities in developing countries (Watson & Schalatek, 2019). Of those, only 10 African countries are accredited as national implementation entities and 5 African countries with accreditation from GCF.

There has been a deficit in the number of African countries that have received funding from the GCF. According to a survey done for the Africa Climate week 2018, more than half of the countries in Africa have faced problems with mobilizing climate funds (UNDP, 2019). Not only do climate funds have developmental significance, they also have ethical and political significance, reflecting the responsibility and commitment of developed industrialized countries to aid developing countries to adapt to the adverse impacts of climate change caused by their development pathways (CFU, 2019). This project seeks to find ways through which international climate funds, not based on aid or charity, can be accessed for loss and damage impacts.

2.5 Addressing Loss and Damage Using Financial Instruments

Building the resilience of vulnerable people to weather and climate-related risks using financial instruments has been crucial for disaster risk management and climate change adaptation (Linnerooth-Bayer & Hochrainer-Stigler, 2015; Richards & Schalatek, 2017). Linnerooth-Bayer & Hochrainer-Stigler (2015) divided financial instruments for disasters into two major categories: traditional post-disaster financial instruments and non-traditional pre-disaster instruments. The traditional financial instruments include:

- *Solidarity*- whereby vulnerable people rely on governmental and donor assistance to cope with disasters
- *Savings and credit*- an instrument by which disaster victims use up their savings or get a loan to cope with disasters
- *Informal risk sharing*- whereby victims rely on kinship ties and their social capital

- *Traditional insurance mechanisms*- which pools risks across communities and regions (Linnerooth-Bayer & Hochrainer-Stigler, 2015)

The non-traditional, novel financing mechanisms include risk transfer mechanisms such as: index-based insurance, which uses parameters and trigger points for pay-outs; public sector risk transfer, national insurance programs, insurance pools among small states, donors' insurance, catastrophe bonds and contingency credits. Therefore, financial instruments for dealing with loss and damage, in their view, consisted of both solidarity-based instruments and market-based instruments.

With insights from the executive committee of WIM, financial instruments investigated consisted of mainly market-based instruments such as risk pooling, catastrophic risk insurance, contingency finance, climate-themed bonds and catastrophe bonds (Gewirtzman et al., 2018). While all these approaches lead to addressing loss and damage, and are currently being used, there is a need for a shift from a more solidarity-based approach to an approach where developed countries can own up to take responsibilities of funding market-based instruments (Richards and Schalatek, 2019). For instance, a developing country with other developmental priorities and low finance may not be able to put aside money for contingency financing.

Insurance schemes have been widely proposed as a market-based instrument for addressing loss and damage (Gewirtzman et al., 2018) but it may not be reliable over time as it burdens vulnerable countries. Even though insurance is not a 'one size fits all' approach for dealing with loss and damage and has been described as the "*band-aid for a much deeper injury"* (Richards & Schalatek, 2017) because it does not fully cover all losses, it is a scheme sold out in the international arena as it fits within an overall 'market friendly' approach (Richards & Schalatek, 2017).

2.6 Insurance as a form of Adaptation Tool

Agricultural insurance is a form of adaptation practice through which compensations are made to farmers insured for the economic impacts from extreme events (Hazell, 1992; Alderman & Haque, 2007). However, the uptake of insurance remains low in developing countries, and an

average of 2 % of total losses pertaining to weather or climate events are insured (Binswanger-mkhize, 2012; Cole et al., 2012; Hoeppe, 2016). There is also a lower uptake of insurance by women farmers than men farmers due to lack of access to finance, education and other farming services (Akter et al., 2016). A study done in Bangladesh showed that financial education and building trust in the insurance entities led to differences in uptake of the insurance observed between men and women, with male dominance (Akter et al., 2016). It is argued that small-holder farmers usually face the problem of affording insurance cost, while large scale farmers self-insure their crops through on-farm approaches such as crop diversification and storage, traditional management practices and social safety-nets (Binswanger-mkhize, 2012). However, those 'on-farm' and technical approaches alone cannot "climate-proof" society (Dow et al., 2013). To address these challenges, insurance covers are sometimes undertaken by international organizations on behalf of farmers in a region or country, or by the government, as in the case of the insurance provided by ARC Ltd.

The traditional form of indemnity insurance relies on measuring the loss and damage incurred from an event on an individual farm, and has proven to be expensive and non-transparent, since it involves complex logistics and time to verify each individual claim (Cole et al., 2012). Parametric index-based insurance serves a response by using objective parameters which trigger payments when a specified threshold is exceeded (IFAD, 2011). Earlier efforts of using indemnity insurance on individuals failed due to transaction costs and weight of "asymmetric information" (Hazell, 1992; Barnett, Barrett & Skees, 2008). Nevertheless, the rise in technology, remote sensing and prior idea of area-yield insurance ignited efforts to use a measured index for payments for a group, rather than individuals (Cole et al., 2012; Tadesse, Shiferaw & Erenstein, 2015). Index-based insurance emerged with a pro-active lens that provides rapid pay-out with no required monitoring costs (Barnett, Barrett & Skees, 2008).

2.6.1 Parametric or Index-based Insurance

Parametric or index-based insurance can be accessed by households (micro-scale), community groups or businesses (meso-scale) or on a national level (macro-scale) (Tadesse, Shiferaw &

Erenstein, 2015). Examples of micro-insurance on climate risks include the ACRE Africa weather index micro-insurance and the R4 Rural Resilience Initiative supplied by Oxfam and the World Food Program (WFP) in Ethiopia (Richards & Schalatek, 2017). International aid may also decide to buy insurance coverage to act as a disaster relief for vulnerable countries at the meso-scale. For example, WFP bought insurance coverage for Ethiopian farmers in 2006 (IFAD, 2011). Example of a macro-scale insurance scheme is ARC Ltd, which this study makes use of.

There are three different types of agricultural index-based insurance: weather index-based insurance, area-yield index-based insurance and the NDVI/satellite index-based insurance (IFAD, 2011; Turvey & Mclaurin, 2012; Tadesse, Shiferaw & Erenstein, 2015).

Weather index-based insurance

This scheme was first introduced in the early 1900s as a form of index-based insurance which uses measurable weather event (rainfall level, wind speed, heat content) as objective parameters which trigger payments when a specified threshold is exceeded (IFAD, 2011; Adiku et al., 2017). Insurance premiums are calculated by defining a threshold for a single peril, below which pay-outs are made (Adiku et al., 2017). Payments are triggered when the realized value of the index falls below or surpasses that of the pre-specified threshold at a specific rainfall gauge or station (Tadesse, Shiferaw & Erenstein, 2015). For example, if a threshold of 200 mm for rainfall level is chosen, payments are made whenever rainfall goes below 200 mm. It is advantageous in that it gives out rapid pay-outs, and the rate of payment is the same regardless of the losses sustained by the insurer (IFAD, 2011). However, this form of insurance can be disadvantaged by basis risk (which will be further discussed), which occurs when rainfall level on a farm differs from that at the station used as reference (Gommes & Göbel, 2013). This form of index-based insurance will be used purposely for this study.

Area-yield index-based insurance

This scheme was first introduced in the 1950s as a form of index-based insurance which uses average crop yields realized in a certain area as a proxy for pay-outs, and covers everything that may have caused low crop yields (Cole et al., 2012; Liesivaara & Myyrä, 2015). The insurance agreement is developed based on historical yield data in an area, upon which the normal average

yield and the insured yield are generated, by the insurers and partners involved. Pay-outs are made when the average yield realized is less than the insured yield in an area, regardless of the average yield on individual farms (Tadesse, Shiferaw & Erenstein, 2015). This form of insurance may be disadvantageous when there are different conditions for crop production such as different topographies or soils, which lead to different yields on individual farms (Tadesse, Shiferaw & Erenstein, 2015). However, one can evaluate the efficacy of area-yield based insurance by comparing yield levels on an individual farm with general yields in the broad geographical area (Liesivaara & Myyrä, 2015), but this may be time-consuming.

Normalized Difference Vegetation Index (NDVI)

The vegetation or satellite index-based insurance scheme is not as common as the previous forms of index-based insurance discussed, but it has been used, and mainly applied in pastoral systems as a form of livestock index-insurance (Chantarat et al., 2013; Tadesse, Shiferaw & Erenstein, 2015). Other forms of index-based insurance rely on station data for payments, but NDVI is promoted as a form of index-based insurance that overcomes the challenge of relying on station data by using satellite products (Turvey & Mclaurin, 2012). For example, due to sparse station data, NDVI was used as a proxy for forage scarcity to determine livestock mortality in pastoral systems in Kenya (Chantarat et al., 2013). The indices are generated using time-series remote sensing imagery that measures how green the vegetation is on the earth's surface, and pay-outs are triggered based on the NDVI, which relates to the deficit in moisture. By measuring the *'greenness'* of the earth, the health of the vegetation which correlates with crop yields can be described at any given time (Turvey & Mclaurin, 2012). With the NDVI, a more comprehensive data on crop health can be gathered, rather than relying on weather variables alone, which vary from time to time.

Critiques of Weather Index-based Insurance

The growth of weather index-based insurance has been limited by the lack of weather data, technical expertise, and mainly basis risks (IFAD, 2011). **Basis risk** refers to the lack of correlation between crop yield at a farm level and the output projected by a weather derivative (e.g. rainfall) at the station used to create and settle pay-outs (Gommes & Göbel, 2013). Basis risk can be a

geographical basis risk that results from different weather patterns at the weather station and on the farm (IFAD, 2011). For instance, rainfall level could be higher at a weather station than at a farm that is several kilometers away. Basis risk can also be a production basis risk, which results from the correlation between yield loss on farms and weather index (IFAD, 2011). This occurs when pay-outs are not perfectly correlated with the agricultural losses faced by farmers. However, since rainfall index is also used as a proxy, mapping for a crop-specific coverage may reduce basis risk if done more precisely, decreasing the mismatch between the index and the actual losses that were incurred (Cole et al., 2012). There is an interaction of other factors such as pests, diseases and fire, which are not directly related to weather but affect yield. Basis risk may decrease demand for insurance, especially for high levels of risk aversion individuals (Gommes & Göbel, 2013); however, index insurance could perhaps have great benefits for risk adverse individuals even with basis risk.

With the great benefits that can be explored from index-based insurance, the affordability of insurance premiums remains a major problem affecting demand, especially for poor farmers (Binswanger-mkhize, 2012).

2.7 Climate Change and Insurance

The insurance sector is a particularly important sector for managing anticipated risks such as climate-related risks in society (Mills, 2009). Not only does the insurance industry get to insure clients against disasters, the industry itself needs to adapt to the changing climate. The largest insurance firm in the world, Munich Re, allocated its 24 billion losses in the California wildfires to global warming and warned that climate change could make insurance too expensive for people, according to the Guardian News (Neslen, 2019).

Insurers have traditionally depended on historical data to calculate and price future risks; if future risks are underestimated, a serious threat is posed to the sustainability of business, and if future risks are included, the price of premiums will go high (Ernst & Young, 2008; Gewirtzman et al., 2018). To address the concern of underestimation, new approaches are being identified to incorporate climate change impacts into catastrophe models by modelling future climate to yield

more robust results. However not much has being done for the rise in insurance premiums due to climate change. Gewirtzman et al. (2018) argued that even though insurance schemes play a major role in managing loss and damage from events, they may not be reliable over time as the burdens fall on the most vulnerable countries. As explained by Linnerooth-bayer et al. (2019), insurance may fall short of meeting the goals of addressing loss and damage, unless other interventions such as subsidies are put into place to make insurance more affordable to poor clients.

The concept of using insurance as a mechanism through which developed nations can compensate developing nations for their historic contribution to climate change first surfaced in 1991 when the Alliance of Small Island Sates (AOSIS) demanded that developed nations fund an international insurance pool to compensate small-islands and low-lying developing countries for loss and damage from sea level-rise (Mechler et al., 2019). Then emerged other proposals addressing rather sudden-onset weather events (e.g. floods and tropical cyclones) such as the Müller proposal which advocated for relief funds to be centrally administered and funded up-front rather than voluntarily (Müller, 2002); and the Germanwatch proposal to form a global catastrophic insurance funded by developed countries and administered by a public or private entity (Bals, Warner & Butzengeiger, 2006).

These proposals brought a new thinking into ways insurance can be used to address climate change impacts, bringing in a compensatory layer through which developed countries can finance climate attributed risks. Although it was challenged by not differentiating between climate-attributed risks and other risk drivers (Linnerooth-Bayer & Mechler, 2006), it informed many international discussions and insurance has been prominently featured in the UNFCCC workplans. Insurance schemes at different levels have been applied as a strategy for loss and damage from climate-related risks (Richards & Schalatek, 2017). Two examples depicting sovereign-level insurance risk pools are the Caribbean Catastrophe risk pool which offers insurance to Caribbean countries (CCRIF, 2019) and the African Risk Capacity Ltd, which offers insurance to African countries to ensure timely and rapid payouts to address loss and damage

from extreme events (ARC 2018a). The latter form of sovereign risk pool insurance is used in this study.

2.8 African Risk Capacity Insurance (ARC Ltd)

The African Risk Capacity Insurance (ARC Ltd) is a financial affiliate of the African Risk Capacity (ARC), a specialized agency of the African union (AU). Sovereign-level insurance against climate and weather-related risks are offered to African countries by ARC Ltd through contingency planning, risk pooling and transfer facilities (ARC 2018a). The aim of this insurance scheme is to develop a risk-pooling and transfer instrument using weather-based index insurance to pre-finance disaster risks for affected member parties in Africa (ARC 2018a). The insurance currently deals with drought-related events; nevertheless, models for other extreme events such as floods and tropical cyclones are being developed to deal with those events (ARC 2018a). The insurance scheme has cut-cross across a few African nations which include Malawi, Senegal, Mali, Niger, the Gambia, Mauritania, Burkina Faso, Kenya and Cote d'Ivoire (ARC, 2018b; ARC, 2019). ARC has received more than USD 400 million in drought risk coverage and has paid out over USD 35 million in pay-out for early responses to four countries assisting over two million affected people. ARC Ltd also proposed a financing mechanism known as the Extreme Climate Facility (XCF) to secure direct access to climate finance through bonds for African governments already involved in managing risks through ARC Ltd. The funds will be given to countries who have experienced more frequent extreme events to aid with adaptation (ARC, 2018a).

If widely implemented across Africa, ARC Ltd has the capability to serve as a very important risk management system that will allow African countries to reduce reliance on international aid, and reduce the high social cost from delayed responses, by providing fast and timely pay-outs (ARC, 2018a). The insurance relies on a state-of-the-art technology known as the Africa *RiskView* (ARV) software, originally developed by the United Nations World Food Program (WFP) to calculate response costs to drought events and price premiums (ARC, 2018b). Even though ARV is the technical engine of ARC Ltd, there are other steps required in developing an insurance offering and allowing a country to participate in the risk pool (Figure 1). Each country intending to join

the risk pool provides a contingency plan - which includes the operation implementation plans, outlining how the funds, if paid, will be distributed to the population insured. While ARC operates at a sovereign level, it seeks to reduce disaster risk at the individual level; therefore, the distribution of funds or other relief materials to the number of people affected from a disaster is a relevant criterion.

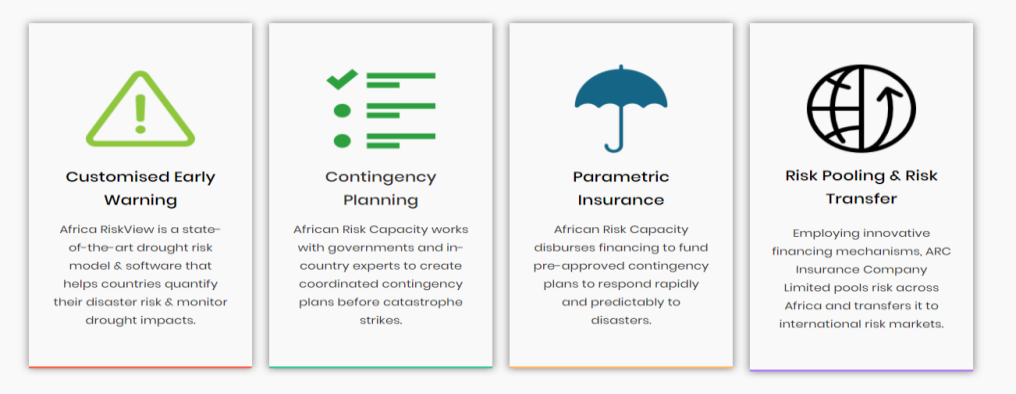

Figure 1: Methodology for getting insurance coverage with ARC Ltd. The early warning system is used to inform countries about drought risks and if countries choose to insure farmers, a contingency plan stating how the funds, if distributed, will be used is developed before a country can join the risk pool and transfer risk. Source: (www.africanriskcapacity.org).

2.8.1 Africa *RiskView* Software (ARV)

The technical engine behind ARC Ltd is a proprietary modelling software, Africa *RiskView*, which is designed to work within national frameworks, allowing governments to carry out country-specific risk analyses, by defining their management strategy and determining their level of participation in the risk pool (ARC, 2018a).

ARC Ltd then uses ARV to estimate drought and populations at risk, as input to its underwriting calculations. The main objective of ARV is to estimate the number of people affected by a drought event during an agricultural season and the USD cost necessary to assist those people in a timely manner. To do so, ARV uses historical rainfall data to estimate an agricultural drought measure, and overlays this with population vulnerability information to produce a first order estimate of

the drought-affected population and the amount required for assistance as illustrated in Figure 2.

Customization Stages in Africa *RiskView*

There are four major phases in the customization process via ARV (Figure 2) and they are discussed below:

Rainfall

As part of its parametric insurance calculation, ARC Ltd uses dekadal (10-daily) satellite-based rainfall data to calculate cumulative rainfall in an area and define a rainfall threshold for a growing season. The default dataset used is the Rainfall Estimates (RFE) 2.0. Alternative rainfall datasets include African Rainfall Climatology Version 2 (ARC2) and TAMSAT. Countries are allowed to choose the dataset that best reflect the rainfall estimates in their country (ARC, n.d.). Rainfall is the only real-time varying input that is placed into ARV (ARC, n.d.).

Drought Index

The drought model used in ARV is the Water Requirements Satisfaction Index (WRSI), and it requires relatively few parameters for calculation. The rainfall estimates selected by users, along with other static inputs such as potential evapotranspiration and soil water holding capacity, are translated into a spatial drought index called WRSI, originally developed by the Food and Agriculture Organization (FAO). The index serves as an indicator of crop performance based on the amount of water available to a crop during a growing season. The model monitors water deficits throughout a growing season and accounts for the amount, distribution and timing of rainfall on staple annual rain-fed crops. The index ranges from 0-100, with 100 indicating no water deficit and an excellent growing season, and 0 indicating a situation where not enough rainfall was available for planting. Any number below 100 indicates some water deficit. WRSI is calculated at each pixel per rainfall data and the final WRSI value at each pixel is expressed as some function over all the WRSI values calculated for a growing season. Users choose whether this function is the first, average or maximum planting opportunity found. To determine if the drought conditions are more severe than expected at the end of a growing season, the

aggregated WRSI is compared to its expected level (benchmark). The default benchmark in ARV is the median WRSI value of the previous five years (ARC, n.d.).

Estimated Population Affected

The WRSI is aggregated at vulnerability polygons, which represent geographical units within a country with available information on household vulnerability, to estimate populations affected from a drought index. Once the final index is compared to its benchmark and the 'relative severity' of a drought is defined, the drought index is overlaid with social indicators such as population vulnerability information to estimate the populations affected by a drought event. The vulnerability profile of a population is determined by the population's resilience and exposure to drought risks. Each drought ratio (WRSI/Benchmark) is compared to each specific polygon vulnerability profile to determine the number of drought-affected population in that polygon. The vulnerability profiles are determined by four main points: the drought detection point, the 1st impact calibration point, the second impact calibration point and the third impact calibration point. When the drought ratio is above the drought detection point, there is no drought and the estimated population affected is zero. If the drought ratio value is below the third drought impact calibration point, the estimated population affection is equal to the population affected by a drought severity at the third impact calibration point (ARC, n.d.).

Estimated Response Costs

The last phase in the ARV customization is to calculate the response costs needed to assist the estimated drought-affected population. This step is by far the simplest in the customization process as it involves a simple multiplier of the estimated population affected by response cost per person. The default response cost per person for a rainfall season is USD 100 per person for countries with unimodal rainy season and USD 50 per person for countries bimodal rainy seasons. The cost is lower for a bimodal season, which means two rainy seasons because the customization process in any given case would cover both seasons in a year and have a total cost as the cost of a unimodal season. However, the final response cost per person differs across countries and requires discussion that involves governments and insurance partners. The final costs also depend on the country's planning activities, in terms of costs required to respond to

drought events, especially in a case where ARC Ltd pay-out will only cover a fraction of the costs required to respond to a drought event. The response costs may also vary based on the drought severity. The national modelled drought response costs underlie the basis of the parametric insurance products and it is the last step this study covers (ARC, 2018a). Once the customization process is complete and the final model settings are validated, countries decide their risk transfer parameters and decide what portion of its total modelled drought risk it wants to transfer in the insurance risk pool (ARC, n.d.).

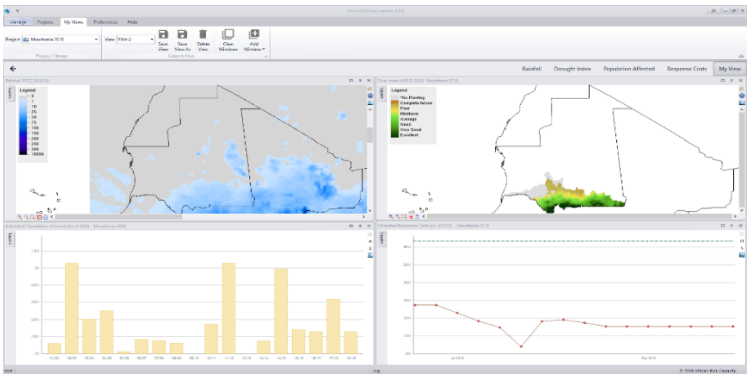

Figure 2: Africa RiskView v4.4.6 display of Mauritania 2018 Growing Season. The top left panel shows the rainfall data used as inputs into ARV; the bluer the diagram, the more rain there is in an area. The top right panel shows the drought index that has been calculated based on the rainfall data; the brown color represents a likelihood of a drought event while the green color shows excellent growing conditions with enough water available for a growing season. The bottom left panel shows the estimated population affected from drought events and the bottom right panel shows the estimated response costs for assistance in each dekad over the year.

2.8.2 Prospects of ARC Ltd

Nine countries to date have purchased insurance premiums from ARC Ltd, and a pay-out of about USD 60.3 million have been paid to drought-affected countries (USD 26 million collectively to Mauritania, Senegal and Niger in 2015; USD 8 million to Malawi in 2017; USD 2.4 million to Mauritania in 2018, USD 23.1 million to Senegal in 2019; and USD 758,135 to Cote d'Ivoire in 2019), assisting over 2.1 million people and over a million livestock (ARC, 2018b, ARC, 2019) (Table 2). Even though parametric insurance through ARC Ltd is a great initiative that could reduce the loss of lives and livelihoods from extreme events, the current approach does not consider the change in weather and climate risks, which ultimately affects the costs of insurance

premiums. To support the continued refinement and improvement of the parametric insurance, and offer potential value to its policy, a distinction needs to be made between the background risk from natural variability and the added risk from human-induced climate change using attribution science.

Table 2: Countries That Have Taken Up Insurance with ARC Ltd with Pay-out Years (ARC, 2018a)

Countries that have taken up insurance	**Year joined**	**Year of pay-out**
Kenya	2014/15; 2015/16	
Mauritania	2014/15; 2015/16; 2016/17; 2017/18	2015,2017
Niger	2014/15; 2015/16; 2016/17	2015
Senegal	2014/15; 2015/16; 2016/17; 2017/18;2018/19	2015,2019
The Gambia	2015/16; 2016/17; 2017/18	
Mali	2015/16; 2016/17; 2017/18	
Malawi	2015/16	2016
Burkina Faso	2016/17; 2017/18	
Cote d'Ivoire	2018/19	2019

2.9 Synthesis of the Literature Review

Findings from the literature review showed that climate change and its associated weather risks are affecting the agricultural sector, leading to loss and damage impacts. Parametric weather or index-based insurance is being used as a risk-management tool to deal with weather related disasters as other risk reduction approaches, such as crop diversification, alone cannot *'climate proof'* society. However, parametric insurance is being challenged by the change in risk of extreme events from human-induced climate change. If insurance premiums become too expensive from the added risk from climate change, vulnerable African countries will face a challenge in adopting parametric insurance as a risk management tool. Nevertheless, there is a potential to blend international climate funds to help cover this increased risk. And to do so, the

lens of attribution science, which estimates the role of human influence in the occurrence of extreme events, can be used to estimate the added risk and hence how much climate funds should contribute to the cost of parametric weather insurance.

Chapter Three: Research Methodology

3.1 Introduction

To recap, this study seeks to address the business and ethical implications of climate change on weather-related insurance and answer the following research question: "Can attribution science be used to apportion the damage estimates used in insurance underwriting between that expected from a natural climate and that added through climate change?" It will do this by meeting the following specific objectives:

1. Use of a weather or climate attribution approach to assess if the rainfall levels used in ARC Ltd risk models have changed due to human influence on the present-day climate.

2. Quantify how this changed probability translates into expected damage calculated in the risk model used by ARC Ltd to inform its underwriting calculations.

Therefore, this methodology section describes the steps in achieving these objectives:

1. Access the reference observation and model simulations of the two worlds (factual and counterfactual)
2. Process and bias correct the models so that the inputs to ARV match (in terms of means and variance) what ARV has been calibrated on (that is ARC2)
3. Evaluate the model inputs before and after bias-correction
4. Choose countries to be used in this study
5. Run ARV with attribution inputs
6. Assess the differences in damage probabilities

This study is purely quantitative and was undertaken in two major phases: post-processing of Global Climate Model (GCM) data into formats appropriate for use into Africa *RiskView* and the use of Africa *RiskView* to estimate response costs due to water stress in a given growing season.

3.2 Data Collection

3.2.1 Reference Observation

The observational dataset used is the African Rainfall Climatology version 2 (ARC2), one of the three satellite-based datasets used in the ARV software. It is provided by the National Ocean and Atmospheric Administration (NOAA) climate prediction center and consists of daily rainfall data over the Africa wide domain with a resolution of 1.0^{o} (Novella & Thiaw, 2013). ARC2 rainfall data from the last 30-years 1989-2018 were extracted from the Climate System Analysis Group (CSAG)- at the University of Cape Town for analysis.

3.2.2 Global Climate Models

Daily rainfall data from 15 GCMs, representing both the factual (historical simulations, with both natural and human forcing) and counterfactual (natural forcing only) worlds were extracted from the archive of the Coupled Model Intercomparison Project phase 5 (CMIP5). The CMIP5 models were chosen for the purpose of this mini dissertation since they are the easiest to access, compare to other experiments such as weather@home (Massey et al., 2015) or C20C+ (Stone et al., 2019) and are sufficient for a proof of concept work such as this.

The different CMIP5 models are used to test the data validity and enable a robust assessment of rainfall patterns in the models. Valid data include models that capture the regional rainfall patterns, seasonality and interannual variability in a way that makes us confident they can be used to attribute human influence on rainfall. Since this project seeks to proof a concept, one ensemble member from each model is used to validate the model data. Both the natural and historical runs begin in 1989 and continue through to 2005. The historical runs were extended by using the Representative Concentration Pathways (RCP8.5) simulations up to 2018 because up to today, the forcing of climate in the real world has followed very closely that of the RCPs. The natural runs consist of rainfall data for the last available 30 years since the models are not made based on ‘real-time’ (Taylor, Stouffer & Meehl, 2012).

Table 3: The 15 CMIP5 Models Used in this Study

Models	Horizontal Resolution (latitude x longitude)	Institution	Reference
ACCESS 1-3	1.25° x 1.875°	CSIRO-BOM, Australia	Hui-Jun et al., 2015
BNU-ESM	2.78° × 2.81°	BNU, China	Hui-Jun et al., 2015
CanESM2	2.78° × 2.81°	CCCMA, Canada	Arora et al., 2011; Hui-Jun et al., 2015
CESM1-CAM5	0.94° X 1.25°	NSF-DOE-NCAR, USA	Meehl et al., 2013
CCSM4	3.75° x 3.75°	NSF-DOE-NCAR, USA	Gent et al., 2011; Shields et al., 2012
CNRM-CM5	1.39° × 1.40°	CNRM-CERFACS, France	Hui-Jun et al., 2015
CSIRO Mk3-6-0	1.86° × 1.87°	CSIRO-QCCCE, Australia	Collier et al., 2011; Hui-Jun et al., 2015
GFDL-CM3	2.0° × 2.5°	NOAA-GFDL, USA	Donner et al., 2011; Griffies et al., 2011
GFDL-ESM2M	2.0° × 2.5°	NOAA-GFDL, USA	Donner et al., 2011; Griffies et al., 2011
HadGEM2-ES	1.25° x 1.875°	UKMO, UK	Collins et al., 2011
IPSL-CM5-LR	1.89° × 3.75°	IPSL, France	Dufresne et al., 2013; Hui-Jun et al., 2015
IPSL-CM5-MR	1.268° × 2.5°	IPSL, France	Dufresne et al., 2013; Hui-Jun et al., 2015
MIROC-ESM-CHEM	2.78° × 2.81°	AORI-NIES-JAMSTEC, Japan	Watanabe et al., 2011; Hui-Jun et al., 2015
MIROC-ESM	2.78° × 2.81°	AORI-NIES-JAMSTEC, Japan	Watanabe et al., 2011; Hui-Jun et al., 2015
MRI-CGCM3	1.1° × 1.1°	MRI, Japan	Yukimoto et al., 2011

3.3 Data Post-Processing

The model data for both the factual and counterfactual worlds were regridded to the spatial resolution of the observations (1.0^o) and the domain size of the observations (-40^o S 40^o N; -20^o W -55^{o}E) corresponding to 751 pixels in the east-west direction and 801 pixels in the south-north direction. The regridding method used is the bilinear method of regridding using a batch script in the Linux system. Having both the models and observations on the same spatial scale and resolution allowed the models to be evaluated and bias-corrected against the observations; thereby, allowing systematic errors to be removed from the models. Since Africa *RiskView* takes dekadal rainfall datasets, both models and observations were converted from daily to 10-daily rainfall, resulting in three dekads per month. The first ten days of a given month were summed, followed by the next 10 days, and the rest of the days in that month for each year.

Missing Values

ARC2 had some missing values; there were no missing data in the climate models. In order to fill those missing values, the following method was used: in the period (1989-2018), the missing data were replaced with the arithmetic mean of the available historical data for that day and the relevant pixel in that period (1989-2018). The arithmetic mean is calculated using symmetric rounding of the raw daily ARC2 data for everyday and pixel to the nearest eighth decimal place. Africa *RiskView* also takes rainfall inputs as integers with a maximum value of 253 mm. All the models and observational datasets were rounded to the nearest integer using symmetric arithmetic rounding, and any dekadal rainfall value higher than 253 mm was replaced by 253 mm to produce the final ARC2 data used in ARV.

3.4 Model Evaluation

The evaluation of the models was completed in two stages: evaluation before and after bias-correction. Rainfall levels were evaluated based on comparisons between the uncorrected models and ARC2 on a seasonal, monthly and dekadal basis to investigate whether the models simulated similar precipitation patterns as ARC2. Taylor Diagrams (seasonal), Annual Cycles (monthly means) and Q-Q plots (10-daily) were plotted to visually identify any potential problems in the GCM data. The evaluation done on the 10-daily rainfall results are attached as Q-Q plots in Appendix 3. The seasonal evaluation was done over two regions: West and Southern Africa. The monthly and daily evaluations were done in four cities in the four countries (Malawi, Zimbabwe, Senegal & Mauritania). The numeric tests also carried out for this evaluation are listed below. Note that all model datasets were standardized by subtracting the value of the model from the value of the observation. For instance, a standard deviation of 2 for a model indicates that the model falls 2 standard deviations above the observation value.

Pearson Correlation Coefficient (r)– was calculated on the Taylor Diagrams (Taylor, 2001) to show correlation of the seasonal mean over space between the models and the reference observation for each season in both West and Southern Africa (Appendix A).

Absolute Mean – represents the point-by-point differences between the model and the observations. The standardized means of each CMIP5 model was calculated as a difference between the model and the observation. The absolute value was taken for each model since a 'negative' mean value represents a wet year in the model. The closer the mean is to the observation, the better (Appendix A).

Root Mean Square Error (RMSE) – calculated to compare the seasonal mean over a given domain. It showed how spread out the residuals (prediction errors) were. It showed the relative errors in each CMIP5 model compared to the observation (Appendix A).

Normalized standard deviation difference- calculated on the Taylor Diagrams (Taylor, 2001) to show how dispersed the values are about the mean. The standard deviation of all grid points in the model was calculated and represented as the ratio of the standard deviation across the grid points in the observations (Appendix A).

Coefficient of Variation (CV) – was calculated as percentages to show the ratio of the standard deviation to the mean to know how dispersed the values were about the mean (Appendix A).

3.4.5 Kolmogorov-Simonov test – a non-parametric 'goodness of fit' test was carried out on the 10-daily data sets to investigate if the models and observation followed a specified distribution. (Appendix A). Below are the following conditions for this test:

The null hypothesis H_o- states the data follow a specified distribution

The alternative hypothesis H_a- states the data do not follow a specified distribution

The p-values (Appendix C) represent the closeness between the models and observations distributions were calculated. If the p-value is less than 0.05, the null hypothesis is rejected.

3.5 Bias-Correction

The regridded models were bias-corrected to match the statistical characteristics of the observations on a point-by-point basis (0.1^o) over an Africa-wide domain (-40^o:40^o lat, -20^o:55^o lon). The bias-correction was done using the quantile-quantile mapping method (Cannon, Sobie

& Murdock, 2015) in R, which plots cumulative distribution functions (CDFs) of both the model and observations and matches the precipitation quantiles for the model with the corresponding quantile in the observations (Appendix F). The mapping was done on a monthly basis to avoid seasonal biases in the models being replicated in the output data.

For the factual world, the CDF of the model was bias-corrected directly against the observations; whereas, for the counterfactual natural world, the model data were first quantile matched to the model factual data before being bias-corrected against the observation. This approach was deemed as appropriate to preserve the absence of climate change signal (e.g. greenhouse gases) in the attribution (counterfactual) runs. The quantile-quantile mapping was done using an 'R' script in the 'R' software (See Appendix F).

3.6 Bias-corrected Model Validation

After the GCMs were regridded and bias-corrected, they were again validated against the observational dataset to investigate whether they simulated or retained similar rainfall patterns as the observations. This second phase of evaluation was done more robustly and holistically as the model data were now in their final forms for use in the insurance software. At this point, the biases were removed from the models and their distributions were to be close or as close enough as possible to the observations. The evaluation was based on comparisons between the bias-corrected models and ARC2 on a seasonal, monthly and dekadal basis to validate the bias-correction methodology. Similar tests carried out in the first evaluation phase were repeated. All the CMIP5 models were chosen to be used in this study because none of them incorrectly captured the rainfall patterns and seasonality.

3.7 Conversion of Gridded Rainfall Datasets to Image Display Analysis

The bias-corrected model data were converted into IDA format, which is that used in ARV, using the Geospatial Data Abstraction Library (GDAL) image conversion tool, installed as part of QGIS OSGEO application installation, which can be downloaded from https://qgis.org/en/site/forusers/download.html. Each IDA file was named according to the following convention

required for ARV: yyyy_m_d.img e.g. 1989_01_1.img (1989-January_1) for months 1-9; and 1989_10_1.img (1989-October_ 1) for months 10-12. YYYY represents each year (1989-2018), m represents the months (January - December) and d represents the dekads (1-3).

3.8 Country Selection

In choosing a set of countries to apply the attribution data to, the following criteria were chosen (i) the country should have already been parametrized in ARV, through ARC's customization process; (ii) countries should have consistent drying or wetting pattern in the observed and projected rainfall datasets over Africa.

3.8.1 ARV Customized Countries

Countries that have been customized (i.e. population affected, and response costs estimated) for insurance via Africa *RiskView* were obtained from the Africa *RiskView* model and represented in the table below.

Table 4: Countries that have been customized by ARV as of 2019. Note that customization does not mean they have joined the risk pool. The customization serves as an early warning tool.

Countries that have been customized via ARV		
Burkina Faso	Madagascar	Senegal
Chad	Malawi	Togo
Cote d'Ivoire	Mali	Zimbabwe
The Gambia	Mauritania	
Kenya	Niger	

3.8.2 Consistent Drying and Wetting patterns

Countries with consistent drying or wetting patterns were identified using observed trends and projected percentage change in precipitation over Africa from the IPCC Fifth Assessment-Report

(IPCC, 2014). Spatial maps showing the observed and future projected percentage change in rainfall relative to 1986-2005 were extracted from Chapter 12 (long-term projections) and chapter 22 (Africa) of the Report. Two Representative Concentration Pathways (RCP2.6 and RCP8.5) were used in the projections of percentage precipitation change relative to 1986-2005. Areas of high and low precipitation were highlighted using different colors as indicators; the browner, the direr and the bluer, the wetter (Appendix D).

Based on the observations and projected percentage change (both RCPs), there is a consistent but statistically insignificant drying pattern in the north eastern part of Southern Africa, which includes ARC customized countries such as Zimbabwe and Malawi. In the south eastern part of West Africa, there is a wetting pattern. In the north western part of West Africa, which includes ARC countries such as Senegal and Mauritania, there is a consistent drying pattern in both the observed trend and the projected percentage change relative to 1986-2005. There is a statistically insignificant drying pattern in areas of East Africa where the observed trends were computed. The projections showed wetting patterns all through the mid and late 21st century; indicating inconsistency in the observed and projected patterns for this region. Further, when seasonal rainfall was examined in East Africa, additional consistencies were noted (IPCC, 2014) (Appendix D).

3.8.3 Consistent Drying Patterns

Countries with consistent drying patterns were delineated to investigate the attributable risk. This is because Africa *RiskView* uses satellite-based historical rainfall dataset to estimate risks, and part of this study includes using rainfall data from a world without climate change to calculate insurance premiums. Thus, countries with potential worsening climate change signal were required for an attribution statement to be made. Based on the observations and projected percentage change, the two potential regions to work in are Southern Africa and West Africa. Even though a wetting pattern is projected in most areas in West Africa, Senegal and Mauritania have significant drying patterns (Appendix D). Therefore, Malawi, Zimbabwe, Senegal and Mauritania were chosen as case studies.

3.9 Calculation of the Damage Costs: Insurance Modelling via ARV

The second phase of the analysis was completed using Africa *RiskView* to calculate estimated response costs for a recent insurance estimation in Malawi, Zimbabwe, Senegal and Mauritania. The pre-existing customization of ARC specific to each country was retained and only the rainfall dataset was substituted. The estimation was done using the following steps:

1. Place the IDA files in the ARV directory: Each CMIP5 model dataset consisted of 2160 IDA files comprising 1080 files (3 dekads x 12 months x 30 years) for a world without climate change, and 1080 files (3 dekads x 12 months x 30 years) for a world with climate change. Each file was named as (model_hist) for the natural world and (model Nat) for the counterfactual world and placed in the following ARV directory: RiskView directory: C:\Users\{{user}}\AppData\Local\WFP\ RiskView2 \data\rain.

2. Add Display Name for ARV: Add a text file 'dataset.ini' whose contents identify the datasets. This was done in each of the thirty folders, named as *DisplayName= model_hist/Nat.*

3. Make a copy of Recent Country Customization- ARV consists of many projects for different countries over different years. To make changes to any existing project, a copy of that project must be made.

4: Estimate Damage Costs- Open copy of the project and in each project setting, substitute only the rainfall datasets of your choice from the drop-down menu of files that were created. Each rainfall scenario was placed separately to calculate the final drought index (WRSI), estimate the population affected by drought and the costs needed for assistance. Thus, for each country, thirty estimates of damage were calculated, one factual and one counterfactual per CMIP5 model.

Analysis

The rainfall input data, WRSI, estimated population affected and estimated response costs from each CMIP5 model were analyzed by plotting empirical Cumulative Distribution Function (CDF) plots to know how the damage varied between a world with and without climate change and

according to different insurance conditions for each country. Risk-ratios were calculated for the population in each country and represented in a box and whisker plotted in R.

Chapter Four: Results

4.1 Introduction

This chapter shows the results of the model evaluation, the difference in rainfall levels between the world with and without climate change as well as the four stages which form part of parametric weather insurance modelling. It starts with the model evaluation done on the uncorrected models and their bias-corrected forms on a seasonal, monthly and 10-daily basis. The difference in rainfall levels for both the world with climate change and the world without climate change is also plotted as spatial maps. All 15 models evaluated were used for risk modelling via Africa *RiskView.* Thereafter, results illustrating the four major steps that precede parametric weather insurance modelling as discussed in Chapter 2 are shown in the sequence of i.) cumulative rainfall of both world scenarios ii.) drought index represented by the final WRSI value; iii). the population affected using Africa RiskView vulnerability polygons and iv.) the estimated response costs for assistance (cost per person)

4.2 Model Evaluation (Uncorrected and Bias-Corrected)

4.2.1 Taylor Diagrams

The Taylor Diagrams plotted over the two regions – West Africa and Southern Africa (Figure 3) consist of two major features: (i) the Pearson correlation coefficient (r), which shows the association between the models and the observations based on the pattern or point-wise correlation of the mean seasonal rainfall in the models and the observations; and (ii) the normalized Standard Deviation (SD), which is the ratio of the SD across of mean grid point values in the models to the SD of same in the observations. A good correlation coefficient value is 1.0– the closer the value is to 1, the more correlated the models are with the observations. A good SD value is close to 1.0– values above 1.0 suggest that the model data have a spread of higher values from the observations and values below 1.0 suggest a spread of lower values from the observations.

West Africa

For all the seasons, the model simulations are more scattered and dispersed from the observations for the uncorrected models (top) than the bias-corrected models (bottom). However, after bias-correction, the models become more clustered around the observations. For the JJA rainy season specifically, the models are clustered at a point approximately (r = 0.90, SD = 0.90) close to the observations. The only outlier is IPSL-CM5A-MR, which equally shows high correlation but is more dispersed around the mean. For the SON rainy season in West Africa, the models with the most dispersion (SD= 1.7) are HadGEM2-ES and MIROC-ESM-CHEM; all the other models are clustered at a point approximately (r = 0.95, SD = 1.0) (Figure 3).

Southern Africa

Similarly, the models are more scattered and dispersed from the observations before bias correction and become more clustered around the observations after bias-correction. For the rainy seasons (DJF and MAM) in **Southern Africa**, the model simulations are more clustered towards the observations than the dry season months (JJA, SON). The models find it harder to agree in the dry season, even with bias-correction, and this is because the rainfall patterns tend to be more "random" and not as strongly controlled by the larger scale dynamics in the wet seasons. However, after bias-correction, the models showed the most improvement for the DJF rainy season in Southern Africa, with all the models clustered at a point approximately (r = 0.95, SD = 0.97). The models also showed similar improvement for the MAM rainy season in Southern Africa but with models HadGEM2-ES (SD = 1.6) and IPSL-CM5A-MR (SD = 2.5) showing more dispersion (Figure 3).

Overall, the models that showed the least improvement were consistent in both regions and none of the models was negatively correlated to the reference observation for all seasons. Therefore, all of the models evaluated showed improvement after being bias-corrected to somewhat represent reality (Figure 3).

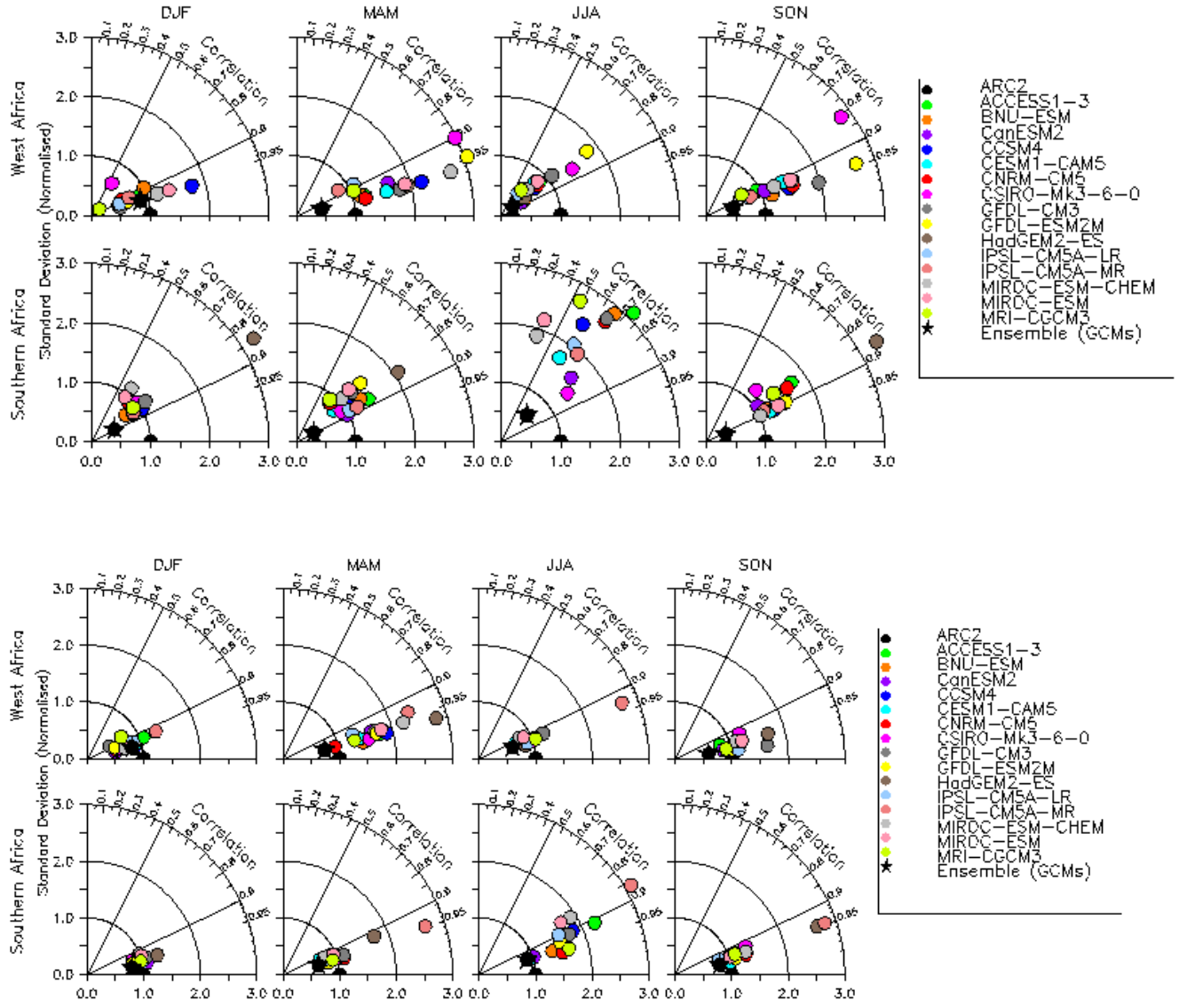

Figure 3: Taylor diagrams showing the normalized standard deviation (x and y axis) and the correlation coefficients (along curve) of mean seasonal precipitation (mm/season) for four seasons over West and Southern Africa from 1989-2018 using 15 models and a reference observation. Top (Uncorrected models); Bottom (Biased-corrected models).

4.2.2 Annual Cycles

The annual cycles below show the mean monthly total precipitation in four cities in Malawi, Zimbabwe, Senegal and Mauritania respectively (Figure 4). These four cities were chosen to capture a spread of locations across each country.

Southern Africa

The total monthly rainfall in each of the city ranged from approximately 100 mm to 450 mm. Most of the models in their uncorrected forms simulated higher rainfall than what was observed. After bias-correction, the rainfall level ranged from approximately 200 mm – 300 mm in cities in Malawi and from 150 mm to 220 mm in cities in Zimbabwe. The rainfall levels were however reduced to match the reality of rainfall observed in the cities through bias-correction (Figure 4).

Malawi and Zimbabwe

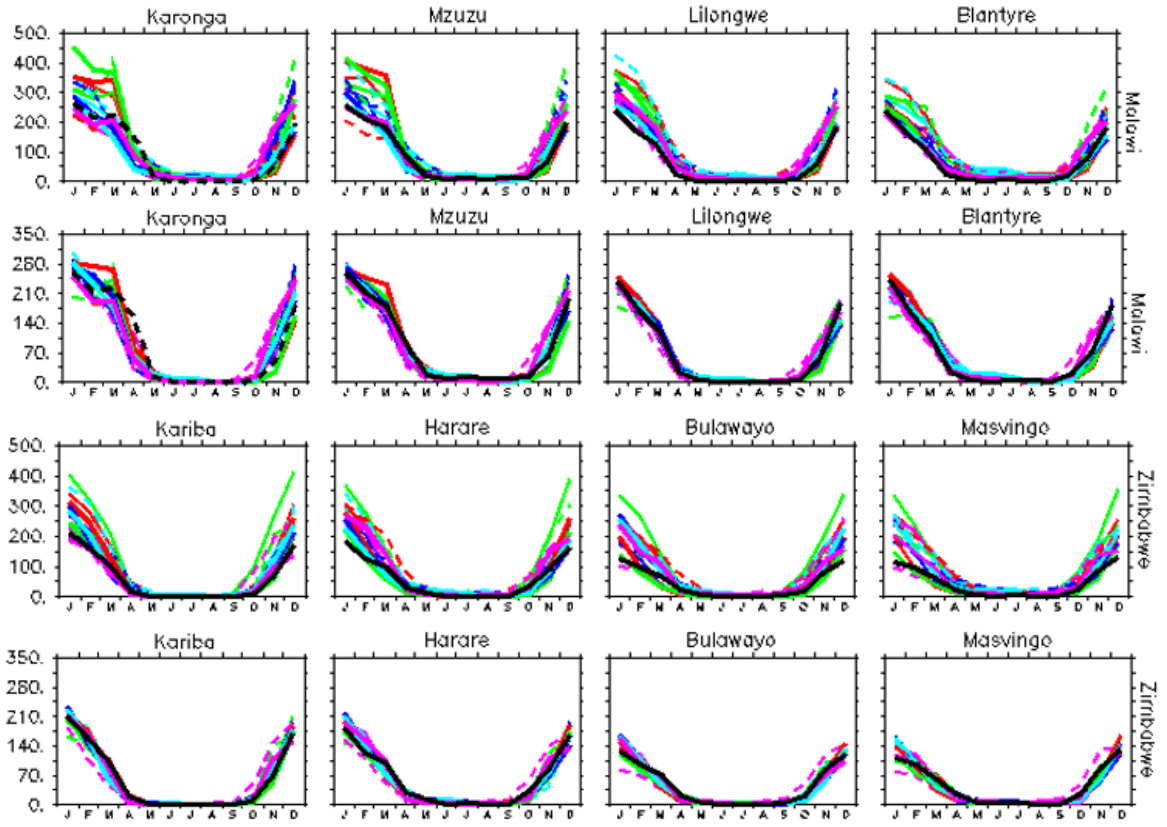

Figure 4: Annual cycles showing monthly total precipitation (mm/month) over four cities in Malawi and Zimbabwe respectively from 1989-2018 using 15 models and a reference observation. Top (Uncorrected models); Bottom (Corrected models). The solid black line represents the observations and the rest of the colors represent the 15 models.

West Africa

The total monthly rainfall ranged from 0-200 mm in Senegal, and from 0-100 mm in Mauritania (Figure 5). Unlike Southern Africa, most models in their uncorrected forms simulated lesser rainfall than what was observed, with three models (GFDL-ESM2M, BNU-ESM, CSIRO-MK3-6-0) consistently over-estimating the rainfall levels. In Senegal, the three models (GFDL-ESM2M, BNU-ESM, CSIRO-MK3-6-0) over-estimated the rainfall level up to 500 mm. However, after bias-correction, the rainfall level in Senegal ranged from 0-280 mm, with more rainfall received in southern parts (Sedhiou & Tambacounda) of the country. In Mauritania, the models consistently over-estimated the rainfall levels up to 300 mm. After bias-correction, the rainfall level in Mauritania however ranged from 0-100 mm, with more rainfall received in eastern parts (Kiffa & Bassikounou) of the country. All the models that over-estimated rainfall levels in the cities improved after bias-correction (Figure 5).

Senegal and Mauritania

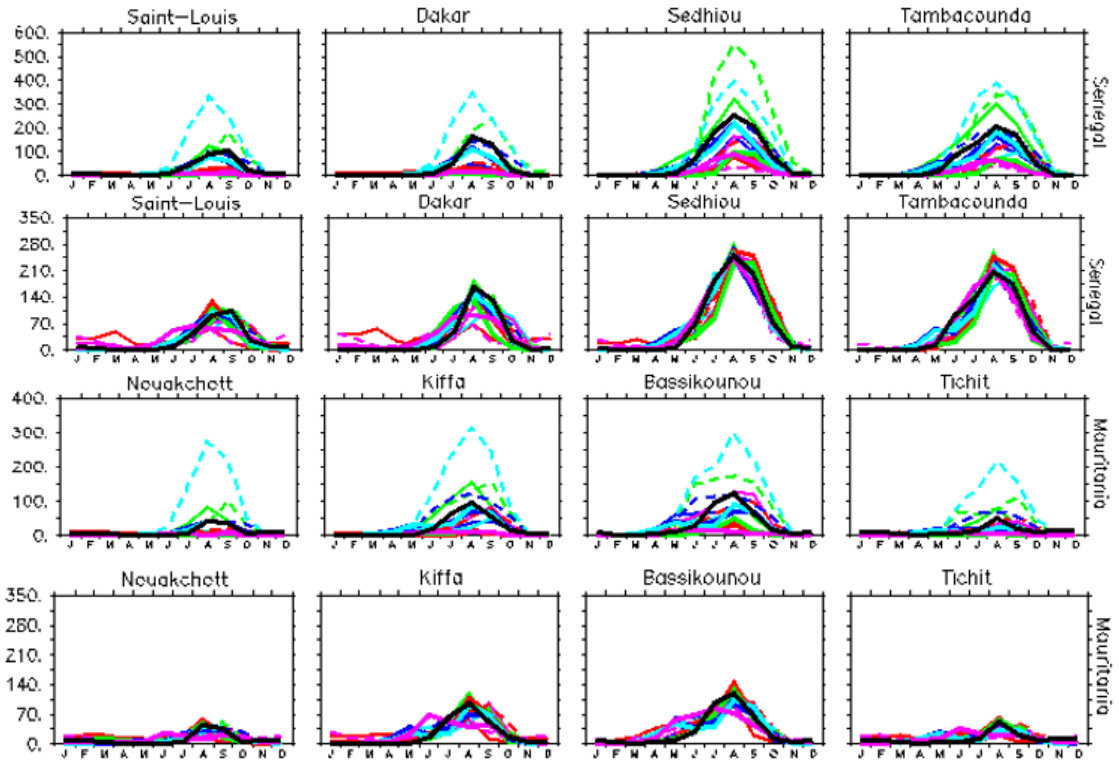

Figure 5: Annual cycles showing monthly total precipitation (mm/month) over four cities in Senegal and Mauritania respectively from 1989-2018 for 15 models and a reference observation. Top (Uncorrected models); Bottom (Corrected models). The solid black line represents the observations and the rest of the colors represent the 15 models.

Overall, the models captured the seasonality of rainfall in the respective regions before and after bias-correction and the models' performance improved after bias-correction, most especially in the southern African countries (Figure 3). This is because the bias-correction did well in shifting the simulated monthly rainfall values to those expected from the observed.

4.3 Factual and Counterfactual World Seasonal Rainfall Differences

Here, I investigated the change in rainfall levels due to anthropogenic forcing on the climate system. Figure 6 shows the simulated rainfall in the factual and counterfactual world and their difference with a focus on a regional scale covering broadly defined areas of West Africa (-20^{o} S: 20^{o} N) and Southern Africa (0^{o} W:25^{o} W).

4.3.1 West Africa

The spatial maps below show the difference in the 1989-2018 seasonal mean (mm/season) for only the rainy seasons (JJA and SON) in **West Africa** and this is because we are interested in water deficit during a growing season (Figure 6). The purple color represents very low rainfall; green-yellow represent intermediate rainfall levels and red represents high rainfall levels. Factual represents the reality; counterfactual, the world void of greenhouse gas emissions; and difference, the difference between both the factual and counterfactual worlds. The brown color represents low rainfall levels, which indicates more rainfall in the counterfactual world while the grey color represents high rainfall levels, which indicates less rainfall in the counterfactual world. The three sub-headings (Factual, Counterfactual, Difference) produced different rainfall levels over each rainy season in West Africa. The Sahel region which consists of two of the countries (Senegal and Mauritania) studied received the least rainfall, with little difference between the factual and the counterfactual worlds. Most of the models simulated higher rainfall in the counterfactual world (Figure 6). A better representation and more in-depth explanation of the rainfall distributions is in the next section on risk modelling.

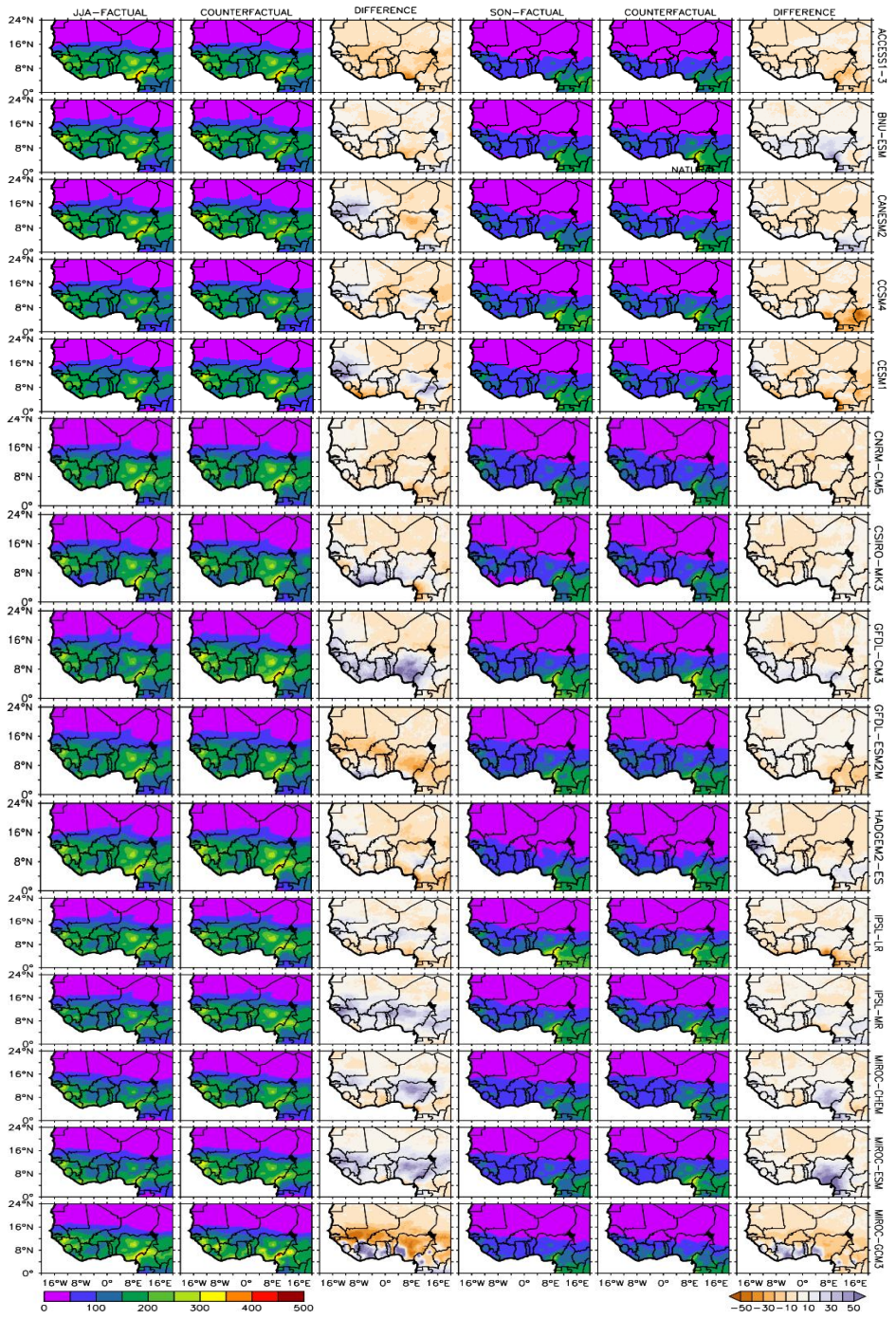

Figure 6: Difference in the rainfall levels in the factual and counterfactual worlds for JJA & SON seasons in West Africa using 15 models.

4.3.2 Southern Africa

The spatial maps below show the difference in the 1989-2018 seasonal mean (mm/season) for the rainy seasons (DJF & MAM) in southern Africa (Figure 7). The purple color represents a very low rainfall; green-yellow represent intermediate rainfall levels and red represents high rainfall levels. Factual represents the reality; counterfactual, the world void of greenhouse gas emissions; and difference, the difference between both worlds. The brown color represents low rainfall levels, which indicates more rainfall in the counterfactual world while the grey color represents high rainfall levels, which indicates less rainfall in the counterfactual world. The three sub-headings (Factual, Counterfactual, Difference) produced different rainfall levels over each rainy season in Southern Africa. Malawi and Zimbabwe showed more difference between the factual world with climate change and the counterfactual world without climate change than the West African countries, with more rainfall levels in the counterfactual world. A large percentage of the models simulated higher rainfall in the counterfactual than the factual world (Figure 7). A better representation and more in-depth explanation of the rainfall distributions is in the next section on risk modelling.

Figure 7: Difference in the rainfall levels in the factual and counterfactual worlds for JJA & SON seasons in Southern Africa using 15 models.

4.4 Q-Q Plots

The quantile-quantile plots below were done by plotting the quantiles of the models against the observations as a non-parametric approach to determine the association of the underlying distributions of the 10-daily rainfall (mm/dekad) data in the climate models and observations. Similar distributions are indicated when the points fall along a straight line. Different distributions are indicated when there is some skewness in the plot. Like the monthly evaluation, four cities were evaluated in each of the four countries to represent a spread across the countries. However, only one city from Malawi and Senegal respectively is shown here due to space limitation (Figures 8 & 9). The rest of the plots can be found in Appendix B.

Malawi- Figure 8 shows the q-q plots for Lilongwe's 10-daily rainfall from 1989-2018 before bias-correction (left) and after bias-correction (right). Before bias-correction, the plots showed some skewness suggesting that the distributions are not closely related. However, there is a close relationship in the distributions of both datasets at rainfall values of approximately 0-130 mm/dekad. The change in relationship is mainly seen at rainfall values above 150 mm through to 250 mm/dekad. The models estimated approximately 50 mm more rainfall than the observations. After bias-correction, the points are more sorted on a straight line, indicating a linear relationship between both the values that the models simulated and what was observed. Similarly, there are outliers at high rainfall values above 200 mm, indicating that the models had some extreme rainfall values (Figure 8). Similar patterns are seen in other cities such as Karonga, Mzuzu and Blantyre (See Appendix B). **Zimbabwe-** Similar patterns are evident in cities such as Harare, Kariba, Bulawayo and Masvingo. The observations estimated about 50 mm less rainfall than the models (See Appendix B).

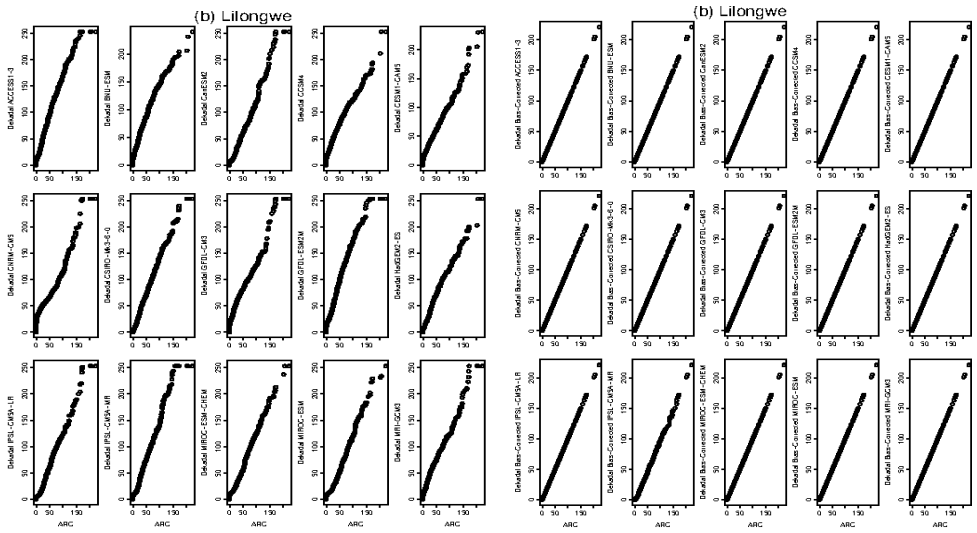

Figure 8: Q-Q plots of the 10-daily rainfall data in Lilongwe from 1989-2018 for 15 climate models against the reference observations. A straight line represents a linear relationship between the models and the observations.

Senegal- Figure 9 shows the q-q plots for Dakar's 10-daily rainfall from 1989-2018 before bias-correction (left) and after bias-correction (right). Before bias-correction, the plots showed non-uniformity suggesting that both distributions were not similar nor associated. Unlike the southern African countries, about 12 of the models estimated less 10-daily rainfall than what was observed. However, after bias-correction, the models did improve significantly and all the models had a close linear relationship to the observations at rainfall values ranging from 0-125 mm/dekad, which is the range of most of the rainfall values. The relationship becomes more skewed from values ranging from 150-200 mm/dekad since the models estimated 50 mm more rainfall. Similar patterns are evident in cities such as Saint-Louis, Sedhiou and Tambacounda (Figure 9).

Mauritania- Similar patterns as cities in Senegal are evident in cities such as Nouakchott, Kiffa, Bassikounou and Tichit. Only few models estimated rainfall lesser than what was observed. However, after bias-correction, the distributions of both datasets are more linear. Generally, the models estimated 20 mm more rainfall in the cities of Nouakchott, Kiffa and Tichit but similar rainfall values in Bassikounou (See Appendix B).

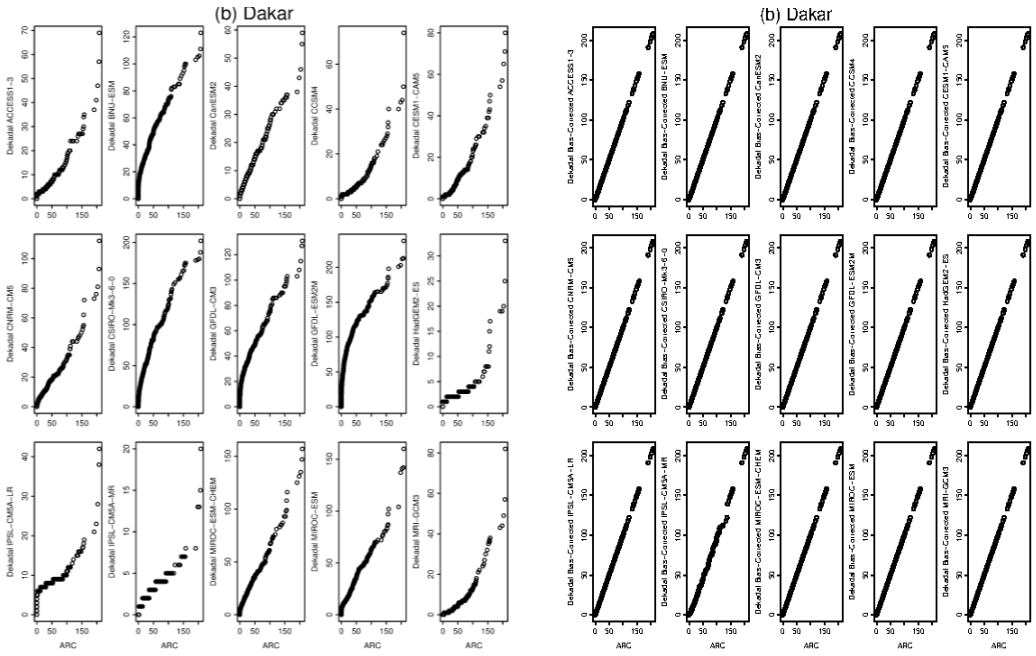

Figure 9: Q-Q plots of the 10-daily rainfall data in Dakar from 1989-2018 for 15 climate models against the reference observations. A straight line represents a linear relationship between the models and the observations.

4.5 Risk Modelling in Southern and West Africa

After evaluations, the rainfall data simulated by the climate models were used for risk modelling in the insurance impact software model, ARV. The empirical Cumulative Distribuiton Functions (CDF) are plotted for the total simulated rainfall in each of the four countries studied using Africa *RiskView* growing season dekads, the final drought index in each country, the estimated population affected and the estimated response costs; all representing the four main phases in ARC Ltd customization. A planting season's success is determined by the amount of water available during a growing season. For example, when the rainfall level is high in the counterfactual world (represented by the dashed line), the WRSI also becomes high. The WRSI ranges from 0-100; 0 indicates a bad growing season, 100 indicates an excellent growing season and any number below 100 indicates some water deficit during a growing season. When the rainfall levels and the WRSI are high, the population affected from a drought event and the cost for timely response become lower.

Malawi

Rainfall

The first column of Figure 10 below shows that the number of years with high rainfall levels from 1989-2018 are more in the counterfactual natural world than in the world with climate change. Although there are some differences in the models used, the multi-model ensemble which represents all possible realizations from the models is used as a reference. More emphasis is being placed on frequent low rainfall years as these are the ones that cause damage. For the ensemble results, about 35 % (0.35 on the y-axis) of years in the factual world have rainfall lower than the lowest rainfall year in the counterfactual world. Although the factual world has a few good years with high rainfall, the probability of high rainfall in most of the years is higher in the counterfactual world, which is important for general food security issues – more years with high rainfall values mean more surplus food to carry over the next year. There is a crossover in the distributions of years at 0.7 on the y-axis, where approximately 70 % of the years have rainfall values below 1000 mm/yr in both the factual and the counterfactual. This could be attributed to the fact that the counterfactual world is generally wetter. Overall, there is a probability of high and low rainfall in both worlds but there are more years with high rainfall levels in the counterfactual natural world, ranging from approximately 740 mm – 1200 mm than the factual world, ranging from approximately 600 mm – 1500 mm. The 300 mm more rainfall simulated in the factual world could be attributed to a few good rainfall years in the factual world.

Drought Index

The next column (Figure 10) shows the final drought index (WRSI), which is unitless, from 1989-2018. For the ensemble results, about 40 % (0.40 on the y-axis) of years in the factual world have a drought-index lower than the lowest drought-index year in the counterfactual world. And of course the counterfactual world has many more good years with high drought index, which is also important for general food security issues – more good years would mean more surplus food to carry over the next year. There is a similar overlap at 0.7 which extends to 1.0, where approximately 70-100 % of years in both the factual and the counterfactual have almost similar

drought-index values. This could be attributed to the general wetness in the counterfactual world. Overall, the final WRSI values for all years are higher in the counterfactual world, ranging from approximately 86-100 than the factual world with climate change, ranging from 76-100.

Estimated Population Affected

The third column (Figure 10) show*s* that the population affected from drought events from 1989-2018, as estimated in ARV, is lower for the counterfactual natural world than in the world with climate change. For the ensemble results, at least 2 million people *a*re affected in 70 % of the years, compared to only 0.90 million *people* in the counterfactual world. Therefore, almost two-times, more people *ar*e affected in the world with climate change at this exceedance point. Results are different for different percentiles of the distributions.

Estimated Response Cost

The same is evident for the response cost (last column of Figure 10) for assistance from 1989-2018, as the response cost is a simple multiplier of USD 42 per person. For the ensemble results, at least USD 100 million is needed for assistance in 70 % of the years in the factual world, compared to only USD 50 million in the counterfactual world. Additionally, the cost for timely response to drought events is about two-times more in the world with climate change at this threshold (Figure 10). Different results are likely for different percentiles of the distributions.

Malawi

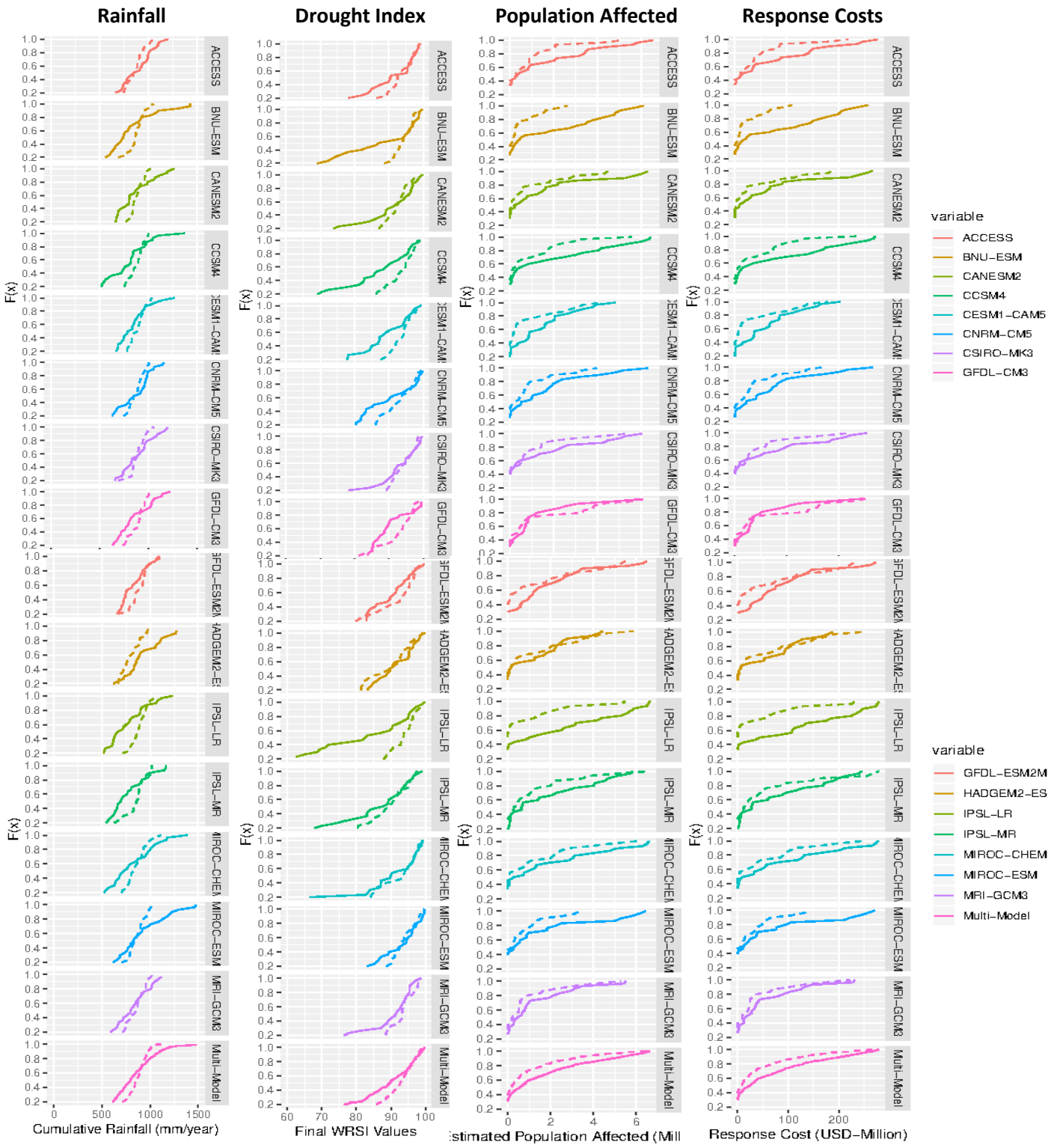

Figure 10: Empirical CDF of the final rainfall, drought index (WRSI), the estimated population affected and response cost for all 15 models and their multi-model ensemble in Malawi. From Left-Right (Rainfall, Drought Index, Estimated Population Affected, Estimated Response Cost). The solid lines represent the factual world and the dashed lines represent the counterfactual world.

Zimbabwe

Rainfall

The first column of Figure 11 below shows that there were more years with high rainfall levels from 1989-2018 in the counterfactual natural world than in the world with climate change. Although there are some differences in the models used, the multi-model ensemble which represents all possible realizations from the models is used as a reference. More emphasis is being placed on frequent low rainfall years as these are the ones that cause damage. For the ensemble results, about 30 % (0.30 on the y-axis) of years in the factual world have rainfall lower than the lowest rainfall year in the counterfactual world. Although the factual world has a few good years with very high rainfall, the probability of years with high rainfall values is higher in the counterfactual world, which is also important for general food security issues – more years with high rainfall values would mean more surplus food to carry over the next year. There is a crossover in the distributions of years at 0.4-0.8 on the y-axis, where approximately 40-80 % of the years have rainfall below 500 and 750 mm/yr in the factual and counterfactual. This could be attributed to the fact that the counterfactual world is generally wetter. Overall, there were more years with higher rainfall levels in the counterfactual natural world, ranging from approximately 450 mm – 800 mm than the factual world, ranging from approximately 325 mm – 1260 mm. The 460 mm more rainfall simulated in the factual world could be attributed to a few good rainfall years in the factual world. The rainfall is overall lower in Zimbabwe than Malawi in Southern Africa.

Drought Index

The next column (Figure 11) shows the final drought index (WRSI), which is unitless from 1989-2018. For the ensemble results, about 30 % (0.30 on the y-axis) of years in the factual world have a drought-index lower than the lowest drought-index year in the counterfactual world. Additonally, about 60-100 % of the years in the factual world has a drought-index as high as the drought-index in the counterfactual world. This could be attributed to the general wetness of the counterfactual world. However, the counterfactual world has more years with high drought-

index, which is also important for general food security issues – more years means more water available for food production and more food to carry over the next year. Overall, there are more years with high WRSI values in the counterfactual world, ranging from approximately 70-100 than the factual world, ranging from 55-100. The drought index is over all lower in Zimbabwe than Malawi in Southern Africa.

Estimated Population Affected

The third column (Figure 11) shows that the population affected from drought events from 1989-2018, as estimated in ARV, is lower for the counterfactual natural world than in the world with climate change. For the ensemble results, at least 3 million people are affected in 70 % of the years in the factual world, compared to only 2 million people in the counterfactual world. Therefore, about 1 million more people are affected in the world with climate change at this exceedance point. Results are different for different percentiles of the distributions. Overall, the population at risk in Zimbawe was higher than that of Malawi in Southern Africa.

Estimated Response Cost

The last column to the far right shows the distributions of estimated response costs from 1989-2018 (Figure 11). The same is evident for the response cost for assistance as the response cost is a simple multiplier of USD 40 per person. For the ensemble results, at least USD 120 million is needed for assistance in 70 % of the years in the factual world, compared to only USD 60 million in the counterfactual world. Additionally, the cost for timely response to drought events is about two-times more in the world with climate change at this threshold (Figure 11). Different results are likely for different percentiles of the distributions (Figure 11). Overall, the cost for responding to drought events is higher in Zimbabwe as compared to Malawi in Southern Africa.

Zimbabwe

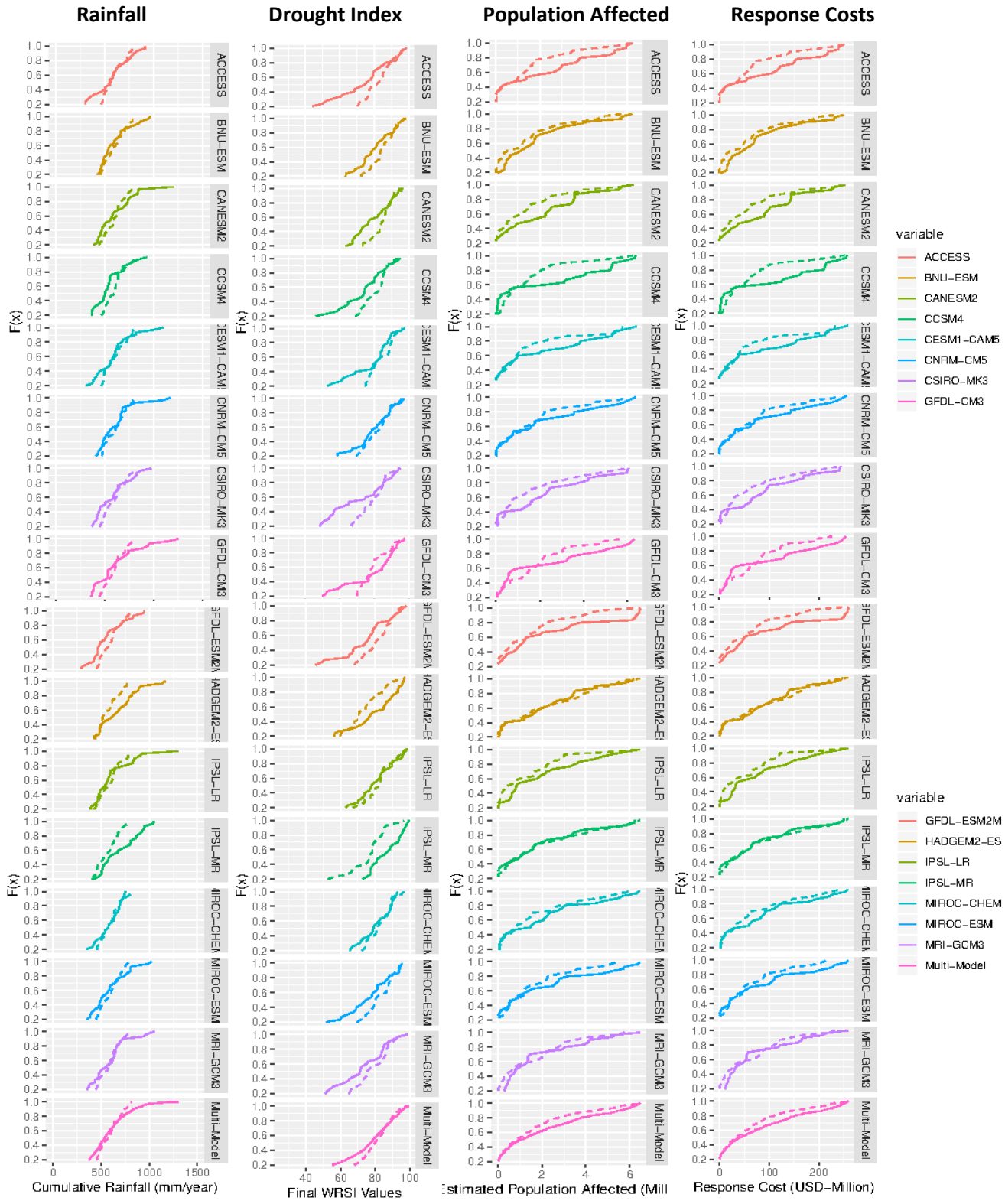

Figure 11: Empirical CDF of the final rainfall, drought index (WRSI), the estimated population affected and response cost for all 15 models and their multi-model ensemble in Zimbabwe. From Left-Right (Rainfall, Drought Index, Estimated Population Affected, Estimated Response Cost). The solid lines represent the factual world and the dashed lines represent the counterfactual world.

Senegal

Rainfall

The first column of Figure 12 below shows that there were more years with high rainfall levels from 1989-2018 in the counterfactual natural world than in the world with climate change. Although there are some differences in the models used, the multi-model ensemble which represents all possible realizations from the models is used as a reference. More emphasis is being placed on frequent low rainfall years as these are the ones that cause damage. For the ensemble results, about 20-40 % (0.20-0.40 on the y-axis) of years in the factual world have rainfall as low as the lowest rainfall years in the counterfactual world. However, about 100 % of the years in the factual world have rainfall levels as low as 80 % of the years in the counterfactual world, which is important for general food security issues – more years with high rainfall values mean more surplus food to carry over the next year. Overall, the rainfall levels were higher in the counterfactual natural world, ranging from approximately 400 mm – 1100 mm than the factual world, ranging from approximately 400 mm – 750 mm.

Drought Index

The next column (Figure 12) shows the final drought index (WRSI), which is unitless, from 1989-2018. For the ensemble results, about 20-40 % (0.20-0.40 on the y-axis) of years in the factual world have a drought-index as low as the lowest drought-index years in the counterfactual world. And of course the counterfactual world has many more good years with high drought index, which is also important for general food security issues – more years would mean more surplus food to carry over the next year. At 0.6 on the y-axis, about 60 % of the years have a drought index below 63 in the factual world, as compared to 75 in the counterfactual world. Overall, the final WRSI values are higher in the counterfactual world, ranging from approximately 38-98 than the factual world with climate change, ranging from 30-98.

Estimated Population Affected

The third column (Figure 12) shows that the population affected from drought events from 1989-2018, as estimated in ARV, is lower for the counterfactual natural world than in the world with climate change. For the ensemble results, at least 0.5 million people *a*re affected in 70 % of the years in the factual world, compared to only 0.35 million *people* in the counterfactual world. Therefore, about 0.15 million more people *a*re affected in the world with climate change at this exceedance point. Results are different for different percentiles of the distributions.

Estimated Response Cost

The last column to the far right show the distributions of estimated response costs from 1989-2018 (Figure 12). The same is evident for the response cost for assistance as the response cost is a simple multiplier of USD 50 per person. For the ensemble results, at least USD 25 million is needed for assistance in 70 % of the years in the factual world, compared to only USD 20 million in the counterfactual world. Additionally, the cost for timely response to drought events is USD 5 million more in the world with climate change at this threshold (Figure 10). Different results are likely for different percentiles of the distributions (Figure 12).

Senegal

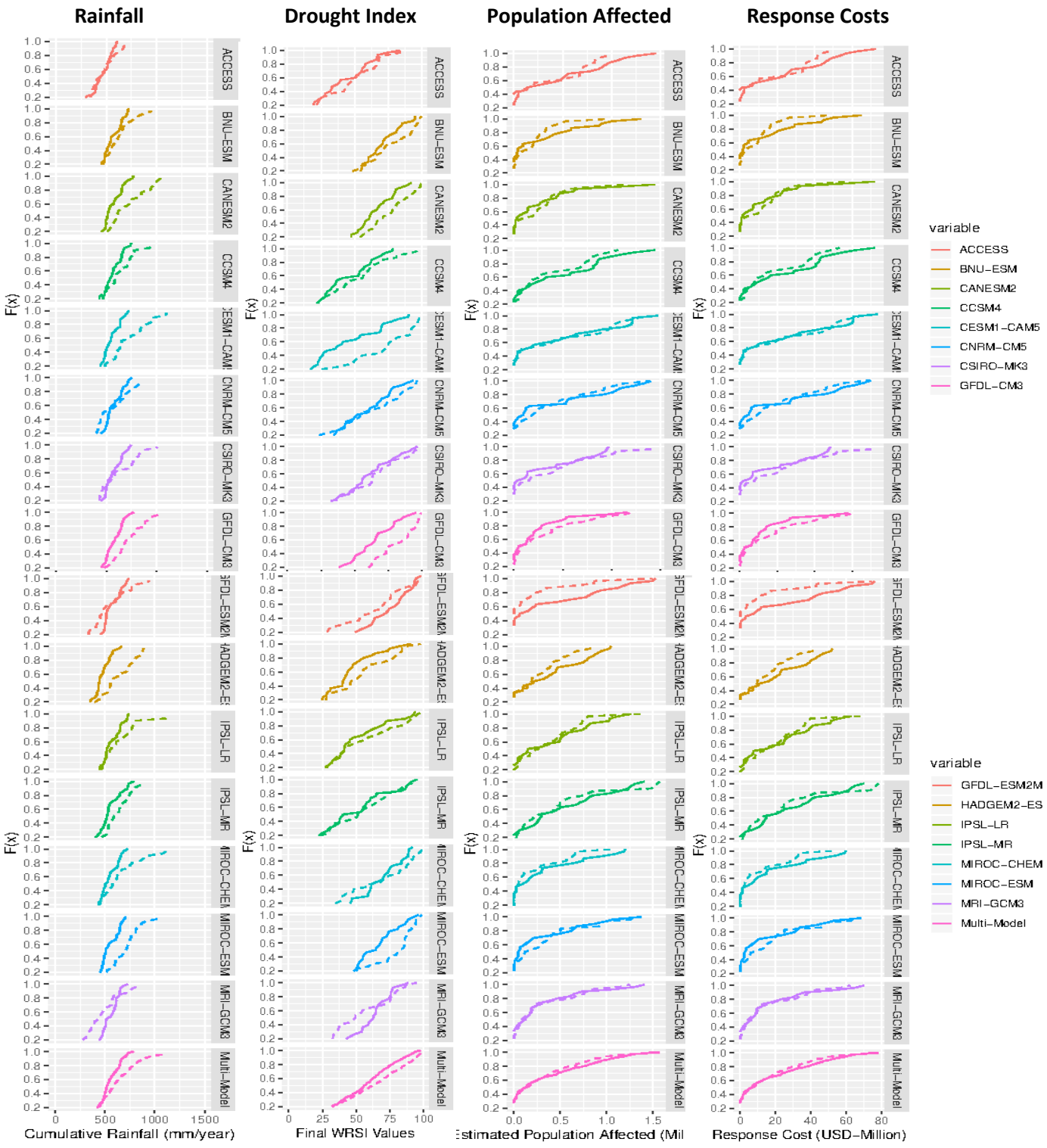

Figure 12: Empirical CDFs of the final rainfall, drought index (WRSI), the estimated population affected and response cost for all 15 models and their multi-model ensemble in Senegal. From Left-Right (Rainfall, Drought Index, Estimated Population Affected, Estimated Response Cost). The solid lines represent the factual world and the dashed lines represent the counterfactual world.

Mauritania

Rainfall

The first column (Figure 13) below shows there are more years with high rainfall levels from 1989-2018 in the counterfactual natural world than in the world with climate change. Although there are some differences in the models used, the multi-model ensemble which represents all possible realizations from the models is used as a reference. More emphasis is being placed on frequent low rainfall years as these are the ones that cause damage. For the ensemble results, about 30-70 % (0.30-0.70 on the y-axis) of years in the factual world have rainfall as low as the lowest rainfall years in the counterfactual world. However, the counterfactual world has many more good years with high rainfall, which is also important for general food security issues – more years with high rainfall values would mean more surplus food to carry over the next year. About 80 % of the years have rainfall levels below 150 mm in the factual world, as compared to 175 mm in the counterfactual world. Overall, the rainfall levels were higher in the counterfactual natural world, ranging from approximately 80 mm – 320 mm than the factual world, ranging from approximately 80 mm – 240 mm. The rainfall is overall lower in Mauritania than Senegal in West Africa.

Drought Index

The next column (Figure 13) shows the final drought index, WRSI, which is unitless from 1989-2018. For the ensemble results, about 20-70 % (0.20-0.70 on the y-axis) of years in the factual world have a drought-index similar to the years in the counterfactual world. And of course the counterfactual world has many more good years with high drought index, which is also important for general food security issues – more years, more surplus food to carry over the next year. At 0.9 on the y-axis, about 90 % of the years have a drought index below 50 in the factual world, as compared to 70 in the counterfactual world. Overall, the final WRSI values are higher in the counterfactual world, ranging from approximately 10-95 than the factual world with climate change, ranging from 10-75.

Estimated Population Affected

The third column (Figure 13) shows that the population affected from drought events from 1989-2018, as estimated in ARV, is lower for the counterfactual natural world than in the world with climate change. For the ensemble results, at least 0.875 million people are affected in 70 % of the years in the factual world, compared to only 0.75 million *people* in the counterfactual world. Overall, the population at risk in Mauritania was higher than that of Senegal in Southern Africa.

Estimated Response Cost

The last column to the far right show the distributions of estimated response costs from 1989-2018 (Figure 13). The same is evident for the response cost for assistance as the response cost is a simple multiplier of USD 50 per person. For the ensemble results, at least USD 50 million is needed for assistance in 70 % of the years in the factual world, compared to only USD 40 million in the counterfactual world. Thus, the cost for timely response to drought events is USD 10 million more in the world with climate change at this threshold (Figure 13). Different results are likely for different percentiles of the distributions (Figure 13). Overall, the cost for responding to drought events is higher in Mauritania as compared to Senegal in West Africa.

Mauritania

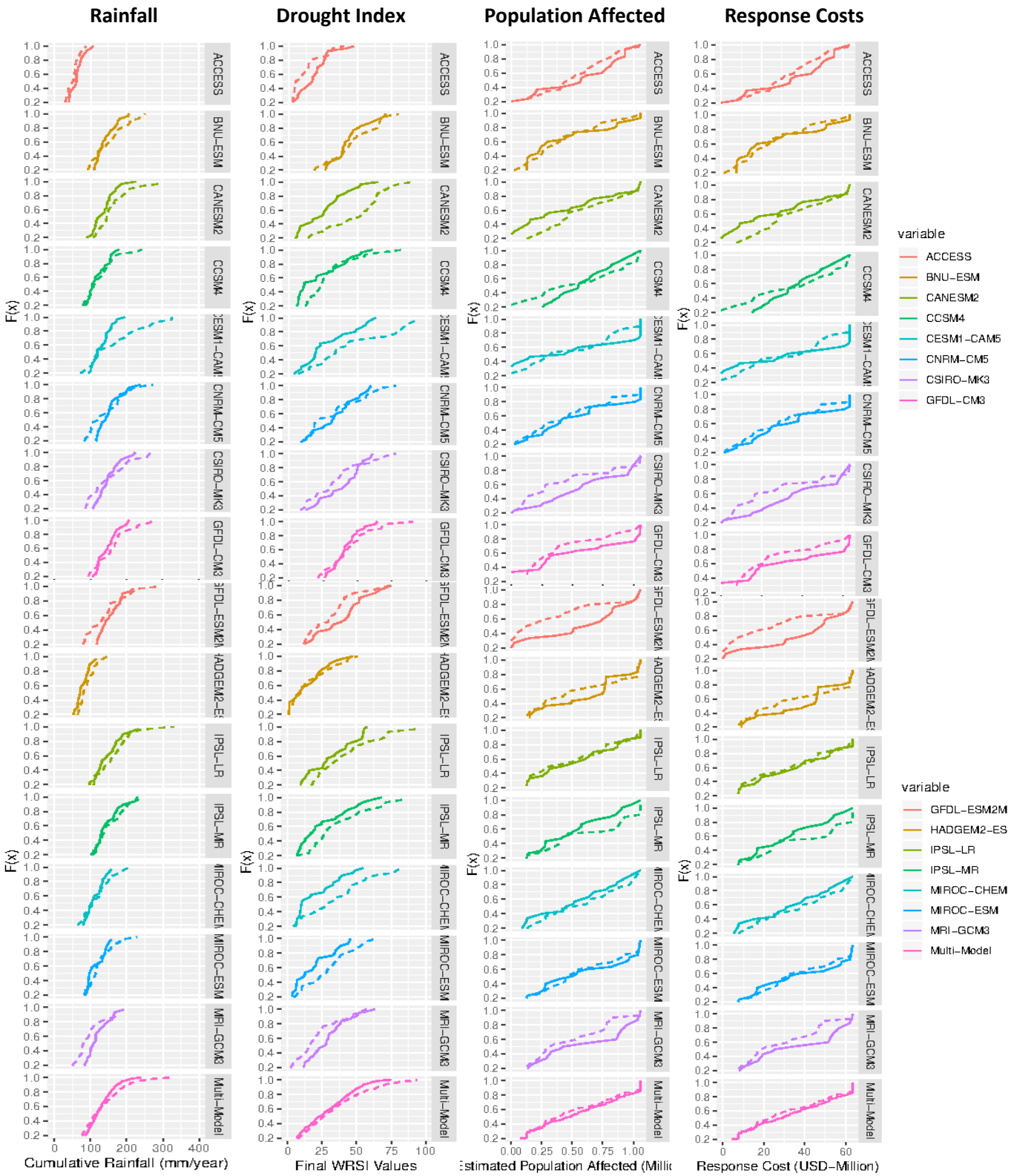

Figure 13: Empirical CDFs of the final rainfall, drought index (WRSI), the estimated population affected and response cost for all 15 models and their multi-model ensemble in Senegal. From Left-Right (Rainfall, Drought Index, Estimated Population Affected, Estimated Response Cost). The solid lines represent the factual world and the dashed lines represent the counterfactual world.

The Ratio of Population at Risk

The ratio of the population at risk represents the vulnerability and exposure level of people affected by a drought event in a world with and without climate change. This ratio is derived from the total number of people at risk over the entire period (1989-2018) for both the factual and the counterfactual simulation using each model. The box and whisker plotted below showed the ratio of people at risk in all four countries - the box represents the interquartile range of the risk ratio of all 15 models over 30 years; the whiskers are 1.5 times the interquartile range; however, there are some extreme values represented by the dots (Figure 14). The number, 1, on the y-axis is the threshold for people at risk. A risk-ratio above 1 indicates more people at risk in the factual world than the counterfactual world. Any number below one indicates less people at risk in the factual than the counterfactual world.

For **Malawi**, more than 90 % of the models showed that more people are at risk in the world with climate change than the world without climate change. The two outliers are models BNU-ESM with a risk-ratio of 3.94, and IPSL-LR, with a risk-ratio of 2.82, which both indicate higher percentage of people at risk in the factual world. Only one model, GFDL-CM3, had a risk ratio below 1, which indicates less people at risk in the factual than the counterfactual world (Figure 14).

For **Zimbabwe**, more than 85 % of the models showed that more people are at risk in the world with climate change than the world without climate change. All the models are in the same range; hence, there are no outliers. Only one model, HadGEM2-ESM, had a risk-ratio below 1, which indicates less people at risk in the factual than the counterfactual world (Figure 14).

For **Senegal**, more than 65 % of the models showed that more people are at risk in the world with climate change than the world without climate change. There is only one outlier, GFDL-ESM2M, with a risk-ratio of 2.17, which indicates higher percentage of people at risk in the factual world than the counterfactual world. Five of the models (CanESM2, CESM1-CAM5, CSIRO-MK3-6-0, GFDL-CM3, MIROC-ESM-CHEM) had risk-ratios below 1, which indicate less people at risk in the factual than the counterfactual world (Figure 14).

For **Mauritania**, about 80 % of the models showed that more people are at risk in the world with climate change than the world without climate change. There are two outliers: GFDL-ESM2M with a risk-ratio of 1.54, indicates higher percentage of people at risk in the factual than the counterfactual world and CanESM2, with a risk-ratio of 0.764 which indicates less people at risk in the factual than the counterfactual world, as compared to the rest of the models. Three of the models (CanESM2, IPSL-MR, MIROC-ESM-CHEM) had risk-ratios below 1, which indicate less people at risk in the factual than the counterfactual world (Figure 14).

Southern Africa

The risk-ratio of the median population at risk in Malawi is the highest at approximately 1.75 and this means more people are at risk in the world with climate change when it comes to food security than the rest of the three countries. Zimbabwe has a median risk-ratio of approximately 1.25 (Figure 14). There are more people at risk of food insecurity in the factual world, but the number of people is lesser than that of Malawi.

West Africa

Senegal and Mauritania have risk-ratios slightly above 1 and while this may not be as significant as the risk-ratios in the Southern African countries, they still show that more people are at risk in the factual world with climate change than the counterfactual world without climate change. The number of people at risk in Mauritania is 1.09, which is slightly lower than that of Senegal at 1.16 (Figure 14). For the actual impact, it has been shown that the number of people at risk in a world without climate change is less, hence anthropogenic climate change is affecting the impact level of drought on the livelihoods of people.

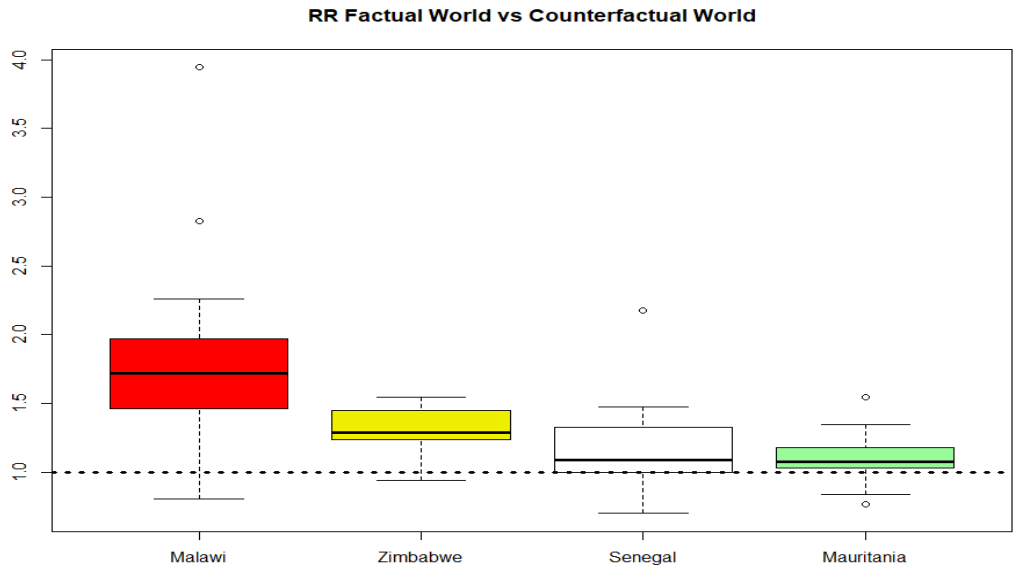

Figure 14: The ratio of population at risk in Malawi, Zimbabwe, Senegal and Mauritania. The box represents the interquartile range (upper and lower quartiles) of the risk-ratios; the thick solid lines in the boxes represent the median risk-ratios of all 15 climate models; the whiskers extend from from each quartile to the minimum and maximum. There are however some extreme values. The dots are outliers with extreme values far away from either end of the box. These outliers are due to different models simulating different results.

Chapter Five: Discussion and Conclusion

5.1 Introduction

This chapter discusses the results generated from this project in terms of their meaning and relevance for research, policy and practice. It starts off by giving a recap of the two specific objectives of this study, which were:

1. To use a weather or climate attribution approach to assess if the rainfall levels used in ARC Ltd risk models have changed due to human influence on the present-day climate.

2. To quantify how this changed probability translates into expected damage calculated in the risk model used by ARC Ltd to inform its underwriting calculations.

After summarizing the results in terms of these, this section then provides an overview of the potential business and ethical implications for insurance in the light of climate change and how attribution science can be used for parametric weather insurance modelling. It concludes by giving several recommendations for improving index-based or parametric weather insurance in the light of climate change and outlines the study's limitations and possibilities for future research that build on this dissertation.

5.2 Synthesis of the Key Results

The results from this dissertation showed that while the climate models overestimated as well as underestimated rainfall levels in different locations of West and Southern Africa, the models were shifted to represent what was observed through bias-correction. The key results showed that the rainfall levels over the last thirty years (1989-2018) in Malawi, Zimbabwe, Senegal and Mauritania were higher in a world without climate change than the world we live in with climate change. This has implications for crops production and yield as agriculture is mainly rain-fed in Africa (FAO, 2017), and less crop production leads to more population being affected by the lack of food. This study also showed that the number of people at risk of food insecurity due to

drought events and the cost for timely response for assistance were higher in the world we live in with climate change than a world without climate change. The risk-ratios calculated showed that the impact varied across countries as more climate change impacts were seen in the Southern African countries of Malawi and Zimbabwe than the West African countries of Senegal and Mauritania.

5.3 Weather to Impact Attribution

This study represents a cutting-edge science that transitions from weather event attribution (rainfall levels) to impact attribution (people affected and response costs). Not only was I interested in assessing the shift in rainfalls and drought events but also the actual socio-economic impacts incurred from those events to know if the impacts were made worse by, or likely caused by human-induced climate change. The gap in both risk profiles showed that less people were affected in a world without climate change; hence less response costs needed for assistance. The impacts on the two West African countries showed very little changes in both world scenarios and this could be due to the not so significant difference in rainfall simulated between the factual and counterfactual worlds in the models in this region. The impact of climate change on future trends was not assesed in this study but according to the IPCC report assessed to choose the case study countries (See Appendix D), consistent drying patterns were projected in both regions, which means the impacts of climate change will continue to increase (IPCC, 2014). The countries in Southern Africa had significant gaps in their risk profiles and according to Malawi Climate Action Report for 2016, climate change has had a major impact on drought events and the country is suffering from the negative effects. Additionally Brown et al. (2012) reported similiar case of climate change negatively affecting the agricultural sector in Zimbabwe.

5.3 Implications of Climate Change for Index-based or Parametric Insurance

5.3.1 Implications for Insurance Underwriting

From the drought-risk profiles shown for a world with climate change and a world without climate change in the countries studied, the response costs have increased due to climate change

already experienced and these costs underlie the basis of insurance premiums underwriting. To counteract the effects of high risks from weather and climate related events, insurance companies may increase the price of premiums, limit coverage or increase deductibles to respond to increases in risks because they are all-for-profit entities. Additionally, the implications of climate change on insurance premiums are inherently uncertain and this may lead to higher premiums as insurers are more likely to respond to the risk of underpricing and uncertainty with higher prices (Wolfrom & Yokoi-Arai, 2016). If premium prices get higher, developing countries may not be able to afford premiums and this will reduce client base levels for the insurance market. To help address constraints relating to the affordability of parametric-insurance for extreme weather and climate events risks, international policy options to support private or sovereign level insurance markets require considerations that are further discussed.

5.3.2 Impacts on Capital Markets and Global Reinsurers

International reinsurance markets play a critical role in absorbing losses from natural catastrophes (Wolfrom & Yokoi-Arai, 2016; Richards & Schalatek, 2017). All insurance schemes on all levels entirely rely on reinsurance companies to spread risks beyond the control of the insurance companies. When countries join the risk pool at ARC Ltd, some of the risks are absorbed by global reinsurers through risk transfer facilities (ARC, 2018a). The setup of the reinsurance affects how expensive the insurance will be to either individuals or governments (Richards & Schalatek, 2017). For instance, ARC Ltd covers drought in African countries and drought is more likely to affect more than one country at the same time and this places heavier responsibility on the insurance company. For example, ARC Ltd made a pay-out to all West African countries (Mauritania, Senegal and Niger) who joined the risk pool in 2014 due to the West African drought that occurred that year (ARC, 2018a). If for instance, the risks from ARC Ltd pools balance with those of the risks in the Caribbean Risk Pool, which covers earthquakes and hurricanes that are not related to drought, the costs will be lowered.

The capacity of those international reinsurers to absorb losses in the context of climate change will also depend on the capacity within those markets. For instance, Munich Re, one of the

world's biggest reinsurers blamed USD 18 billion of its losses to climate-related wildfire risks in the USA and insurers warned that climate change may make insurance unaffordable for most people (Neslen, 2019). If more losses are experienced from re-insurers, they may perhaps decrease the amount of risk they absorb from insurance companies. Richards & Schalatek (2017), referred to funds from reinsurers as *"global revolving solidarity fund"* and anything based on 'appeal' solely depends on the donor. There is this eagerness to know what climate change may mean for business in the nearest future as climate change cross-cut all sectors and levels. Not only does it affect the insurers and re-insurers market base levels but also the ability of governments and individuals to take up insurance and stay active in the insurance risk pools.

5.4 Ethical Implications of Climate Change on Parametric Insurance

As seen from the countries studies, the results indicate that the estimated number of people affected by a drought event in a given year and the response costs required to assist those people are higher in the real world than a world without human-induced climate change in all countries. This suggests that human-induced climate change is affecting the cost of parametric weather insurance and will continue to do so, at an even higher rate, if business continues as usual (more greenhouse gases are emitted). If premiums get higher for higher climate risks, then there may be fewer people taking up insurance because it is too expensive. If vulnerable developing countries are not able to afford premiums due to the cost of the added risk, it then brings us back to the question of 'is it fair that those in climate-vulnerable settings, not responsible for most of the damages, should bear the added cost from climate change"?

5.5 How can Attribution Science be Useful for Insurance

The lens of attribution science can be used to address the business and ethical implications of climate change on insurance uptake and the way forward is explained here. Using the two world (factual and counterfactual) scenarios from attribution science in the insurance impact model showed that the cost of responding to drought events, which underlie the basis of insurance premiums underwritings and negotiations, is higher in the world with climate change than the

world without climate change for the countries studied. Therefore, if the change in risks of extreme events due to human-induced climate change continues to increase, the cost of premiums will be added on. To address this, the lens of attribution science has the potential to apportion the cost of insurance between the background risk (counterfactual scenario) and the added risk from climate change (factual scenario). As discussed in chapter 2, the counterfactual world is void of greenhouse gas emissions and aerosols, therefore, the results would have no added cost from human activities. A proposal on how to blend finance to take care of both the natural background cost and the cost that is brought in by climate change is discussed with a worked example in section 5.7. Prior to section 5.7, background information on why there is a need for a blended financing mechanism and which finance needs to be blended are discussed below.

5.6 A Call for a Blended Financing Mechanism

5.6.1 Common but Differentiated Responsibilities

The UNFCCC aims to "*stabilize greenhouse gas concentrations in the atmosphere… allow ecosystems to adapt naturally to climate change… and ensure food production is not threatened"* (UNFCCC, 1992:9). An overarching principle of the convention is the principle of common but differentiated responsibilities, emphasized in article 4.1 of the UNFCCC, which states that *"all parties, considering their common but differentiated responsibilities and their specific national and regional development priorities, objectives and circumstances, shall develop and publish their national inventories… implement mitigation measures… and prepare for adaptation to the impacts of climate change."* (UNFCCC, 1992:10) and underpins major policies and proposals in the climate change space (UNFCCC, 1992, 2015). There are two fundamental elements within this principle; the first talks about the common responsibility of all to protect the environment, and the second distinguishes each one's contribution to that problem and responsibility thereof (UNFCCC). One broad, famous principle in the environmental and economic space that looked directly at those responsible for most of global emissions is the "polluter pays principle" (OECD, 1992) emphasized under Article 3.1 of the UNFCCC (UNFCCC, 1992; Khan, 2015). As its name

suggests, those responsible for pollution should be 'held liable for any harm or damage caused by that activity'. The different costs that would arise as insurance premiums from the factual and counterfactual in the countries studied showed that responsibility falls on both developed and developing nations. However, the shared-level of responsibility is different, weighing heavily on those responsible for most of the damages from human-induced climate change, as evident in the cost accrued from the counterfactual world in the countries studied. The IPCC Fourth Assessment-Report states that *"the continent of Africa accounts for the least amount of greenhouse gas emissions but will be the most vulnerable to climate change"* (IPCC, 2013). Therefore, existing policies concerning equity and justice in climate science, has outlined in the Paris Agreement of 2015 and WIM of the UNFCCC that direct compensation be given to vulnerable countries to address the socio-economic losses from climate change (UNFCCC, 2015; Richards & Schalatek, 2017).

5.7 Blending International Climate Funds for African Countries

The idea of using or blending international climate funds to pay for insurance premiums in developing countries is not a new idea but has only existed on a conceptual level. Proposals such as the Munich Climate Insurance Initiative and the Alliance of Small Island States which aimed to combine adaptation funding with insurance mechanisms in the context of climate change were put forward as part of the climate change negotiations (Richards & Schalatek, 2017). Attribution bonds have been called for to cover the probability of an extreme weather or climate events attributable to climate change (Estrin & Tan, 2016). Richards & Schalatek (2017) have argued that international funds should pay for insurance premiums for developing countries and that the payment plan should range from paying the full premiums to paying some proportion of the premiums depending on countries' vulnerability, capacity and the event attribution to climate change. But all these proposals and arguments have been just on the conceptual level. The African Risk Capacity proposed an idea of an Extreme Climate Facility (hereafter, XCF) as a means of leveraging funds for African countries dealing with intense and more frequent extreme events outside of what is known as "normal parameters". However, the XCF relies on private funding, and distribution of funds is based on availability (ARC, 2018a). While it is a great approach, it still

relies on appealing to donor agencies. This project, in its novelty, further stretched the idea of blending finance by providing a scientific evidence with the aid of attribution science.

Malawi

Using Malawi as a worked example, 90 % of the years in the world with climate change have response costs that are on average doubled from the world without climate change (Figure 10). Hence, the insurance premium will be higher by a certain factor, and this factor needs to be covered by other sources. Hence, the importance of blending funds.

The proposed idea of blending international funds such as the GCF for insurance premiums in Malawi, for example, will fill the gap of sitting on the conceptual level of funding 'loss and damage' from climate change in three ways: (i.) it would be based on a practical scientific evidence - this study showed that attribution science can be used to apportion the damage estimates used in insurance underwriting between that expected from a natural climate and that added through climate change. (ii.) Funds allocated would be based on a responsibility approach rather than solidarity or charity. (iii.) It would promote justice and equity by sharing common but differentiated responsibilities.

5.8 Climate Finance Gap in Africa

The biggest dedicated source of climate finance granting is the Green Climate Fund (GCF) tasked with providing support to developing countries to adapt to the adverse impacts of climate change (CFU, 2019). There is a huge gap when it comes to receiving funds for adaptation in Africa. The flow of funds to African countries are slow-paced and even though OECD (2018) reported that adaptation funds increased by 65 % from USD 7.8 billion in 2013 to USD 12.9 billion in 2017 to developing countries but sub-Saharan Africa still lags in receiving funds and most of the funds are still received as grants or loans (OECD, 2018). The results from the countries studied represent a key differentiation between what is known as adaptation fund and fund for loss and damage from human-induced climate change. The results showed that the impacts were outside of the 'normal parameters' of natural variabilities, hence climate change has had an impact on the risk profiles drawn. Therefore, climate funds should be given to cater for the added risk from climate

change and those funds should be known as 'loss and damage funds' that are based solely on responsibility rather than aid.

5.8.1 Addressing the Climate Finance Gap

According to the Climate Tracker info, one of the reasons why most African countries do not receive enough climate funding is the lack of proposals or "good enough" proposals to access funding. The need to use available funds and have additional funds that are not just available but accessible to support 'loss and damage' and adaptation is needed. Since the GCF works by having accredited entities in different countries through which countries are allowed direct access to climate finance, ARC Ltd may perhaps be an accredited entity for pan-African nations managing risks through ARC Ltd. As insurance is one promising way to access funds for loss and damage, the call for blending international funds to make insurance offered by ARC Ltd more affordable provides a platform where funds can be sourced directly through ARC Ltd serving as an accredited entity for countries participating in the risk pool. Such an initiative means that countries participating in the risk pool do not need to send separate proposals to access adaptation funds. By estimating the number of people affected and the response costs which underlie the basis of premium negotiations, the difference between the costs of premiums between a world with climate change and a world without climate change would then be paid to ARC Ltd through multi-lateral or bilateral climate funds, thereby reducing the premium costs for developing countries. It is noted that national ownership is central to the GCF approach; although ARC Ltd risk pool consists of multiple countries; their interests align with national climate policies and each participating country goes through a country-specific customization before joining the risk pool. Hence, funds gotten through ARC will still be accredited on a country level basis. The proposed idea of blending international climate finance with insurance premiums is not meant to replace any of the financing options currently available but to complement them in a more 'just way'.

From Solidarity to Responsibility for Loss and Damage Funding

The need to move from a solidarity-based to a responsibility-based approach is the overarching framework of this blended financing proposal. If new financing models are created to

differentiate cost from background natural variabilities and added climate change cost, the responsibility will be borne by both the developed and developing countries, thereby promoting common but differentiated responsibilities for dealing with climate and weather-related risks in insurance. Having blended financing model will enable countries to take up an initiative to protect its people from climate or weather-related disasters, which shows a sense of responsibility on their side and to get a proportion of the funds subsidized for risks they are not responsible for. With this approach, there will be a sense of entitlement that individual countries will have, making the entire process to not seem like another grant or donor aid to African countries. Developing countries can include their plan of actions for sovereign insurance in their National Adaption Plans, National Determined Contributions (NDCs) and other national policies and plans.

5.9 Challenges and Opportunities for Parametric Weather Insurance

As of present, vulnerable developing countries in climate vulnerable settings are the ones bearing the added cost from climate change. While this insurance scheme provides a financing bridge that is much needed for immediate and rapid response to food security crises on the continent, it does not cover full financing for a country to fully address the impacts from a drought event. As Richards & Schalatek (2017) put it, it is more like a “band-aid” to a much bigger injury challenge. There are several multilateral and bilateral funds and the proposal of creating a new international fund will pose a challenge and may perhaps prove difficult in terms of political agreement, operational challenges and time-frame. It is challenging in that it will take a while to be fully debated and operational. However, climate change poses an opportunity for new innovative market instruments to adapt to climate change and deal with catastrophic disasters beyond adaptation.

5.10 Conclusion

The very existence of ARC Ltd represents international cooperation and effort through the establishment of a multi-country risk pooling to adapt to climate change impacts. However,

climate risks are in turn affecting the efforts to properly adapt to climate change, limiting adaptation. The results have shown that climate change is affecting more people and increasing the response costs for assistance, which lead to higher premiums in all countries studied. There were significant gaps between the risk profiles in the Southern African countries of Malawi and Zimbabwe than the West African countries of Senegal and Mauritania. This suggests that human influence has played a significant role in drought events in southern Africa over the last thirty years, as simulated by the models. This agrees with the IPCC models projections that estimate drying patterns in Southern and East Africa as opposed to wetting patterns in West Africa. It should be noted that due to the geographical positioning of Senegal and Mauritania which form part of the Sahel, the response costs for assistance are higher due to the relatively low amount of rainfall received in the region.

Due to the increase in cost from human-induced climate change, new innovative strategies and efforts are needed to counteract this effect. Using the lens of attribution science to blend international climate funds such as the GCF for affordable premiums is proposed. When considering different potential sources for possible international funds, such a discussion must be based on a set of principles that recognize that the funding is not of solidarity or charity but of 'climate equity' where developed countries take responsibility for the damages that have been caused from the greenhouse gases emitted. While this 'proof of concept' has shown that climate change would impact on the cost of parametric insurance premiums, it should be noted that the results shown here are case-specific for each country and does not represent the entire sub-region or continent; different results are likely in other regions or countries. Additionally, further research works that build on this dissertation by using different model experiments and consider future trends are needed for more stringent policy applications.

5.11 Recommendations

Based on the findings of this study, the following are recommended:

1. A call for international support to look at the potential impacts of climate change on business, especially parametric weather insurance – and further calls to strengthen the quantification

of impacts, transparency procedures, methods and best practices for the implementation of insurance schemes, which were created to deal with weather-related risks.

2. At upcoming COP meetings, there should be a clear distinction between reports on financing adaptation options and financing loss and damage from human-induced climate change.

3. Blended financing models should be created at all levels for micro, meso and macro-scale parametric index-based insurance schemes. The flow of funds from the international to national and even more local level needs to be considered.

4. Additional research works beyond this study are essential. The research should consider the use of other model experiments other than CMIP5 (i.e. weather@home, C20C+) , with the use of many model ensembles to test for similar trends.

5.12 Limitations of the study

As a minor dissertation, this research was necessarily constrained by time, meaning that there are a number of limitations. The key ones are listed below:

1. The climate models used in this study are from a single experiment – the CMIP5 project. This limitation could have been overcome with the use of different model experiments such as weather@home and C20C+ model experiments but the research was constrained by time.

2. Since this study is a 'proof of concept', only one ensemble member per model was used. To overcome this limitation, all ensemble members could have been used to get a better representation of the models, but this could not be done due to time constraints. Therefore, to apply this concept more stringently, it is advisable that all ensembles from different model experiments be used.
3. The bias-correction did shift the models to have a better representation of what was observed but it was not perfect. To overcome this limitation, different bias-correction

methods other than quantile-quantile mapping could have been used. This project was a pioneer project and sought to test a “proof of concept”, therefore it needs to be built on further.

4. The models were not evaluated for interannual variability, so some of them may not be representing real world dry and wet seasons on a year to year basis that well.

5. Changes in evapotranspiration have not been considered in the insurance drought-risk modelling. And as warming becomes high all over the continent, evapotranspiration will likely add to drought risk. ARC insurance limited is still operating with static evapotranspiration values. To overcome this challenge, ARC Ltd is working on enabling the use of different evapotranspiration values that are representative of a specific country.

6. Reference List

ADB. 2019. Green Climate Fund. *African Development Bank Group.* Accessed (September 2019). Available: https://www.afdb.org/en/topics-and-sectors/initiatives-partnerships/green-climate-fund.

Adiku, S.G.K., Debrah-afanyede, E., Greatrex, H., Zougmore, R. & Maccarthy, D.S. 2017. Weather-Index Based Crop Insurance as a Social Adaptation to Climate Change and Variability in the Upper West Region of Ghana. *(189). Denmark.* Available: www.ccafs.cgiar.org.

Akter, S., Krupnik, T.J., Rossi, F. & Khanam, F. 2016. The Influence of Gender and Product Design on Farmers' Preferences for Weather-indexed Crop Insurance. *Global Environmental Change*. 38:217–229. DOI: 10.1016/j.gloenvcha.

Alderman, H. & Haque, T. 2007. Insurance Against Covariate Shocks: The Role of Index-based Insurance in Social Protection in Low-Income Countries of AFrica. (95). Washington, D.C. U.S.A.: The World Bank. DOI: 10.1596/978-0-8213-7036-0.

Allen, M. 2003. Liability for climate change. *Nature Publishing Group*. 421:891–892.

ARC. 2018a. African Risk Capacity: Transforming Disaster Risk Management & Financing in Africa. Accessed (June 2019). Available:https://africanriskcapacity.org.

ARC. 2018b. Terms of Reference of the Africa RiskView Technical Review Forum. *African Risk Capacity Sovereign Disaster Risk Solutions: A Specialized Agency of the African Union.*

ARC. 2019. African Risk Capacity Insurance Limited to Issue $ 738,835 payout to Cote d'Ivoire. Africa Risk Capacity Updates (September 12, 2019). Available:https://africanriskcapacity.org/page/2/.

ARC. n.d. Africa RiskView Technical Note Drought Methodology. *African Risk Capacity Sovereign Disaster Risk Solutions: A Specialized Agency of the African Union.* Available: support@africariskview.org

Bals, C., Warner, K. & Butzengeiger, S. 2006. Insuring the Uninsurable: Design Options for a Climate Change Funding Mechanism. *Climate Policy*. 6(6):637–647. DOI: 10.1080/14693062.2006.9685629.

Barnett, B.J., Barrett, C.B. & Skees, J.R. 2008. Poverty Traps and Index-Based Risk Transfer Products. *World Development*. 36(10):1766–1785. DOI: 10.1016/j.worlddev.2007.10.016.

Bellprat, O., Lott, F.C., Gulizia, C., Parker, H.R., Pampuch, L.A., Pinto, I., Ciavarella, A. & Stott, P.A. 2015. Unusual Past Dry and Wet Rainy Seasons over Southern Africa and South America from a Climate Perspective. *Weather and Climate Extremes*. 9(2015):36–46. DOI: 10.1016/j.wace.2015.07.001.

Binswanger-mkhize, H.P. 2012. Is There Too Much Hype about Index-based Agricultural Insurance ? *Journal of Development Studies*. 0388. DOI: 10.1080/00220388.2011.625411.

Brown, D., Chanakira, R.., Chatiza, K., Dhliwayo, M., Dodman, D., Masiiwa, M., Davison, M., Mugabe, P., et al. 2012. Climate change impacts, Vulnerability and adaptation options in Zimbabwe. *IIED Climat Change Working Paper Series. (3).* DOI: 10.1023/B:GEJO.0000003613.15101.d9.

Burke, M., De Janvry, A. & Quintero, J. 2010. Providing Index-based Agricultural Insurance to Smallholders: Recent progress and future promise. *World Bank.*

Cannon, A.J., Sobie, S.R. & Murdock, T.Q. 2015. Bias Correction of GCM Precipitation by Quantile Mapping: How Well do Methods Preserve Changes in Quantiles and Extremes? *Journal of Climate*. 28(17):6938–6959. DOI: 10.1175/JCLI-D-14-00754.1.

CCRIF. 2019. The Caribbean Catastrophe Risk Insurance Facility. Accessed (June 2019). Available: https://ccrif.org.

CFU. 2019. Global Climate Finance Architecture. Climate Funds Update, *Heinrich Böll Stiftung North America.* Accessed (September 2019). Available:https://climatefundsupdate.org/about-climate-finance/global-climate-finance-architecture/.

Chantarat, S., Mude, A.G., Barrett, C.B. & Carter, M.R. 2013. Designing Index-based Livestock Insurance. *The Journal of Risk and Insurance*. 80(1):205–237. DOI: 10.1111/j.1539-6975.2012.01463.x.

Christidis, N., Stott, P.A., Scaife, A.A., Arribas, A., Jones, G.S., Copsey, D., Knight, J.R. & Tennant, W.J. 2012. A New HadGEM3-A-Based System for Attribution of Weather and Climate-Related Extreme Events. *Journal of Climate*. 26:2756–2783. DOI: 10.1175/JCLI-D-12-00169.1.

Cole, S., Bastian, G.G., Vyas, S., Wendell, C. & Stein, D. 2012. The Effectiveness of Index-based Micro-insurance in Helping Smallholders Manage Weather-related Risks. *London: EPPI-Centre, Social Science Research Unit, Institute of Education, University of London.*

Dawson, T.P., Perryman, A.H. & Osborne, T.M. 2016. Modelling Impacts of Climate Change on Global Food Security. *Climatic Change*. 134(3):429–440. DOI: 10.1007/s10584-014-1277-y.

Dole, R., Hoerling, M., Perlwitz, J., Eischeid, J., Pegion, P., Zhang, T., Quan, X.W., Xu, T., et al. 2011. Was There a Basis for Anticipating the 2010 Russian Heat Wave ? *Geophysical Research Letters*. 38:1–5. DOI: 10.1029/2010GL046582.

Dow, K., Berkhout, F., Preston, B.L., Klein, R.J.T., Midgley, G. & Shaw, M.R. 2013. Limits to Adaptation. *Nature Climate Change*. 3(4):305–307. DOI: 10.1038/nclimate1847.

Durand, A., Hoffmeister, V., Weikmans, R., Gewirtzman, J., Natson, S., Huq, S. & Roberts, J.T. 2016. Financing Options for Loss And Damage: A Review and Roadmap*. Discussion Paper (21)*. Available: https://www.die-gdi.de/uploads/media/DP_21.2016.pdf.

Eden, J.M., Wolter, K., Otto, F.E.L. & Oldenborgh, G.J. Van. 2016. Multi-method Attribution Analysis of Extreme Precipitation in Boulde , Colorado. *Environmental Research Letters*. 11:1–9.

Eden, J.M., Kew, S.F., Bellprat, O., Lenderink, G., Manola, I., Omrani, H., Jan, G. & Oldenborgh, V. 2018. Extreme Precipitation in the Netherlands : An Event Attribution Case Study. *Weather and Climate Extremes*. 21:90–101. DOI: 10.1016/j.wace.2018.07.003.

Ernst & Young. 2008. Strategic Business Risk 2008. 20. Available: http://aaiard.com/11_2008/2008_Strategic_Business_Risk_-_Insurance.2.pdf.

Estrin, D. & Tan, S.V. 2016. Thinking Outside the Boat About Climate Change Loss and Damage: Innovative Insurance, Financial and Institutional Mechanisims to Address Climate Harm Beyond the Limits of Adaptation. In*ternational Workshop Report (24) (March 16-17, 2016). Washington, DC.*

FAO. 2015. Regional Overview of Food Insecurity: African Food Security Prospects Brighter than Ever. *Food and Agriculture Organization of the United Nations.* Accra.

FAO. 2017. Regional Overview Of Food Security and Nutrition in Africa 2017. The Food Security and Nutrition-conflict Nexus: Building Resilience for Food Security, Nutrition and Peace. *Food and Agriculture Organization of the United Nations.* Accra.

Fischer, E.M. & Knutti, R. 2015. Anthropogenic Contribution to Global Occurrence of Heavy-precipitation and High-temperature Extremes. *Nature Climate Change*. 5:560–564. DOI: 10.1038/NCLIMATE2617.

Funk, C., Husak, G., Michaelsen, J., Shukla, S., Hoell, A., Lyon, B., Hoerling, M.P., Liebmann, B., et al. 2013. E. Attribution of 2012 and 2003-12 Rainfall Deficits in Eastern Kenya and Southern Somalia. *Bulletin of American Meteorological Society*. (September):1–4.

Funk, C., Hoell, A., Shukla, S., Bladé, I., Liebmann, B., Roberts, J.B., Robertson, F.R. & Husak, G. 2014. Predicting East African Spring Droughts Using Pacific and Indian Ocean Sea Surface Temperature Indices. *Hydrology and Earth System Sciences*. 18:4965–4978. DOI: 10.5194/hess-18-4965-2014.

Gewirtzman, J., Natson, S., Richards, J.A., Hoffmeister, V., Durand, A., Weikmans, R., Huq, S. & Roberts, J.T. 2018. Financing Loss and Damage: Reviewing Options Under the Warsaw International Mechanism. *Climate Policy*. 18(8):1076–1086. DOI: 10.1080/14693062.2018.1450724.

Gommes, R. & Göbel, W. 2013. Beyond Simple, one-station Rainfall Indices. *In: The Challenges of Index-based Insurance for Food Security in Developing Countries.* 205-221.

Haustein, K., Otto, F.E.L., Uhe, P., Schaller, N., Allen, M.R., Hermanson, L., Christidis, N. & Mclean, P. 2016. Real-time Extreme Weather Event Attribution with Forecast Seasonal SSTs. *Environmental Research Letters*. 11(2016):1–12.

Hazell, P. 1992. The Appropiate Role of Agricultural Insurance in Developing Countries. *Journal of International Development*. 2(6):567–581. DOI: 10.1002/jid.3380040602.

Hegerl, G.C., Hoegh-Guldberg, O., Casassa, G., Hoerling, M., Kovats, S., Parmesan, C., Pierce, D. & Stott, P. 2010. Good Practice Guidance Paper on Detection and Attribution Related to Anthropogenic Climate Change*. In: Meeting Report of the IPCC Expert Meeting on Detection and Attribution Related to Anthropogenic Climate Change. The World Meteorological Organization. IPCC Working Group 1 Technical Support Unit, University of* Bern, Switzerland.

Herring, S.C., Hoerling, M.P., Peterson, T.C. & Stott, P.A. 2014. Explaining Extreme Events of 2013 from a Climate Perspective. *Bulletin of American Meteorological Society,* 95(9):1-96.

Herring, S.C., Hoerling, M.P., Kossin, J.P., Peterson, T.C. & Stott, P.A. 2015. Explaining Extreme Events of 2014 from a Climate Perspective. *Bulletin of American Meteorological Society,* 9(12):1-172.

Herring, S.C., Christidis, N., Hoell, A., Kossin, J.P., Shreck, C.J. & Stott, P.A. 2018. Explaining Extreme Events of 2014 from a Climate Perspective. *Bulletin of American Meteorological Society,* 99(1):1-157.

Hoeppe, P. 2016. Trends in Weather Related Disasters - Consequences for Insurers and Society. *Weather and Climate Extremes*. 11(2016):70–79. DOI: 10.1016/j.wace.2015.10.002.

Hoerling, M., Hurrell, J., Eischeid, J. & Phillips, A. 2006. Detection and Attribution of Twentieth-Century Northern and Southern African. *Bulletin of American Meteorological Society*. 19:3989–4008.

Hoerling, M., Kumar, A., Dole, R., Nielson-Gammon, J.W., Eischeid, J., Perlwitz, J., Quan, X.W., Zhang, T., et al. 2013. Anatomy of an Extreme Event. *American Meterorological Society*. 26:2811–2832. DOI: 10.1175/JCLI-D-12-00270.1.

IFAD. 2011. Weather Index-based Insurance in Agricultural Development: A Technical Guide. *International Fund for Agricultural Development, World Food Programme.*

IPCC. 2001. Climate Change 2001: The scientific Basis. *Contribution of Working Group 1 to the Third Assessment Report of the Intergovernmental Panel on Climate Change*. Cambridge University Press, Cambridge, United Kingdom and New York, USA, 881.

IPCC. 2013. Climate Change 2013*:* The physical Science Basis*. Working Group 1 Contribution to the Fourth Assesment Report of the Intergovernmental Panel on Climate Change*.

IPCC. 2014. Climate Change 2014: Synthesis Report. C*ontribution of Working Groups I, II and III to the Fifth Assessment Report of the Intergovernmental Panel on Climate Change.* Geneva, Switzerland, 155.

Khan, M. 2015. Polluter-Pays-Principle: The Cardinal Instrument for Addressing Climate Change. *Laws*. 4(3):638–653. DOI: 10.3390/laws4030638.

Kim, Y., Min, S., Stone, A., Shiogama, H. & Wolski, P. 2018. Multi-model Event Attribution of the Summer 2013 Heat Wave in Korea. *Weather and Climate Extremes*. 20(2018):33–44. DOI: 10.1016/j.wace.2018.03.004.

King, A.D. 2018. Natural Variability not Climate Change Drove the Record Wet Winter in Southeast Australia. *Bulletin of American Meteorological Society*. 99(1):139–143.

Knutson, T., Kossin, J.P., Mears, C., Perlwitz, J. & Wehner, M.F. 2017. Detection and Attribution of Climate Change 1. DOI: 10.7930/J01834ND.3.1.

Liesivaara, P. & Myyrä, S. 2015. Feasibility of an Area-Yield Insurance Scheme in the EU: Evidence from Finland. *Agricultural Economics Society*. 14(3):28–33. DOI: 10.1111/1746-692X.12096.

Linnerooth-bayer, J., Surminski, S., Bouwer, L.M., Noy, I. & Mechler, R. 2019. Loss and Damage from Climate Change. *Springer International Publishing.* DOI: 10.1007/978-3-319-72026-5.

Linnerooth-Bayer, J. & Hochrainer-Stigler, S. 2015. Financial Instruments for Disaster Risk Management and Climate Change Adaptation. *Climatic Change*. 133(1):85–100. DOI: 10.1007/s10584-013-1035-6.

Linnerooth-Bayer, J. & Mechler, R. 2006. Insurance for Assisting Adaptation to Climate Change in Developing Countries: A proposed strategy. *Climate Policy*. 6(6):621–636. DOI: 10.1080/14693062.2006.9685628.

Lott, F.C., Christidis, N. & Stott, P.A. 2013. Can the 2011 East African Drought be Attributed to Human-induced Climate Change ? *Geophysical Research Letters*. 40:1177–1181. DOI: 10.1002/grl.50235.

Marthews, T.R., Otto, F.E.L., Mitchell, D., Dadson, S.J. & Jones, R.G. 2015. 17 . The 2014 Drought in the Horn of Africa: Attribution of Meteorological Drivers. *Bulletin of American Meteorological Society*. 15:83–88. DOI: 10.1175/BAMS-D-15-00115.1.

Masih, I., Maskey, S. & Trambauer, P. 2014. A Review of Droughts on the African Continent : A Geospatial and Long-term Perspective. *Hydrology and Earth System Sciences*. 18(1):3635–3649. DOI: 10.5194/hess-18-3635-2014.

Massey, N., Jones, R., Otto, F.E.L., Aina, T., Wilson, S., Murphy, J.M., Hassell, D., Yamazaki, Y.H., et al. 2015. Weather@Home-Development and Validation of a Very Large Ensemble Modelling System for Probabilistic Event Attribution. *Quarterly Journal of the Royal Meteorological Society*. 141(690):1528–1545. DOI: 10.1002/qj.2455.

Mechler, R., Bouwer, L.M., Linnerooth-Bayer, J., Hochrainer-Stigler, S., Aerts, J.C.J.H., Surminski, S. & Williges, K. 2014. Managing Unnatural Disaster Risk from Climate Extremes. *Nature Climate Change*. 4(4):235–237. DOI: 10.1038/nclimate2137.

Mechler, R., Calliari, E., Bouwer, L.M., Schinko, T., Surminski, S., Linnerooth-bayer, J., Aerts, J., Botzen, W., et al. 2019. Loss and Damage from Climate Change. *Springer International Publishing*. DOI: 10.1007/978-3-319-72026-5.

Mills, E. 2009. A Global Review of Insurance Industry Responses to Climate Change. *Geneva Papers on Risk and Insurance: Issues and Practice*. 34(3):323–359. DOI: 10.1057/gpp.2009.14.

Mitchell, D., Heaviside, C., Vardoulakis, S., Huntingford, C., Masato, G., P Guillod, B., Frumhoff, P., Bowery, A., et al. 2016. Attributing Human Mortality during Extreme Heat Waves to Anthropogenic Climate Change. *Environmental Research Letters*. 11(7). DOI: 10.1088/1748-9326/11/7/074006.

Moss, R.H., Edmonds, J.A., Hibbard, K.A., Manning, M.R., Rose, S.K., Van Vuuren, D.P., Carter, T.R., Emori, S., et al. 2010. The Next Generation of Scenarios for Climate Change Research and Assessment. *Nature*. 463(7282):747–756. DOI: 10.1038/nature08823.

Müller, B. 2002. Equity in Climate Change: The Great Divide. *Ev 31*. Available: http://www.oxfordenergy.org/2002/03/equity-in-global-climate-change-the-great-divide/.

Müller, B., Johnson, L. & Kreuer, D. 2017. Maladaptive Outcomes of Climate Insurance in Agriculture. *Global Environmental Change*. 46:23–33. DOI: 10.1016/j.gloenvcha.2017.06.010.

Myers, S.S., Smith, M.R., Guth, S., Golden, C.D., Vaitla, B., Mueller, N.D., Dangour, A.D. & Huybers, P. 2017. Climate Change and Global Food Systems : Potential Impacts on Food Security and Undernutrition. *Annual Review of Public Health*. 38:259–77.

Neslen, 2019. Climate Change Could Make Insurance Too Expensive for People-Report. The Guardian (March 21, 2019). Available: https://www.theguardian.com/environment/2019/mar/21/climate-change-could-make-insurance-too-expensive-for-ordinary-people-report.

NOAA. 2019. Trends in Atmospheric Carbon Dioxide. *Earth System Research Laboratory Global Monitoring Division: National Oceanic and Atmospheric Administration.* Accessed: (October 2018). Available: https://www.esrl.noaa.gov/gmd/ccgg/trends/.

Novella, N.S. & Thiaw, W.M. 2013. African Rainfall Climatology Version 2 for Famine Early Warning Systems. *Journal of Applied Meteorology and Climatology*. 52(3):588–606. DOI: 10.1175/JAMC-D-11-0238.1.

O'Hare, G., Sweeney, J. & Wilby, R. 2005. Weather, Climate and Climate Change Human Perspectives. *Pearson Education Limited*. DOI: 10.1017/CBO9781107415324.004.

OECD. 1992. The Polluter-Pays Principle: OECD Analyses and Recommendations. Organization for Economic Cooperation and Development, Paris. DOI: 10.20595/jjbf.19.0_3.

OECD. 2018. Climate Finance from Developed to Developing Countries: Public Flows in 2013-17. Organization for Economic Cooperation and Development, *OECD Publishing.*

Otto, F.E.L. 2016. The Art of Attribution. *Nature Publishing Group*. 6(4):342–343. DOI: 10.1038/nclimate2971.

Otto, F., James, R. & Allen, M. 2014. The Science of Attributing Extreme Weather Events and its Potential Contribution to Assessing Loss and Damage Associated with Climate Change Impacts. Environmental Change Insitute, School of Geography, University of Oxford.

Otto, F.E.L., Massey, N., Oldenborgh, G.J. Van, Jones, R.G. & Allen, M.R. 2012. Reconciling Two Approaches to Attribution of the 2010 Russian Heat Wave. *Geophysical Research Letters*. 39:1–5. DOI: 10.1029/2011GL050422.

Otto, F.E.L., Jones, R.G., Halladay, K., Allen, M.R. & Otto, F.E.L. 2013. Attribution of Changes in Precipitation Patterns in African rainforests. *Philosophical Transactions of the Royal Society*. 368:1–10.

Otto, F.E.L., Boyd, E., Jones, R.G., Cornforth, R.J., James, R., Parker, H.R. & Allen, M.R. 2015. Attribution of Extreme Weather Events in Africa : A Preliminary Exploration of the Science and Policy Implications. 132:531–543. DOI: 10.1007/s10584-015-1432-0.

Otto, F.E.L., Wolski, P., Lehner, F., Tebaldi, C., Van Oldenborgh, G.J., Hogesteeger, S., Singh, R., Holden, P., et al. 2018. Anthropogenic Influence on the Drivers of the Western Cape drought 2015-2017. *Environmental Research Letters*. 13(12). DOI: 10.1088/1748-9326/aae9f9.

Pall, P., Aina, T., Stone, A., Stott, P.A., Nozawa, T., Hilberts, A.G.J., Lohmann, D. & Allen, M.R. 2011. Anthropogenic Greenhouse Gas Contribution to Flood Risk in England and Wales in autumn 2000 ´. *Nature*. 470:382–386. DOI: 10.1038/nature09762.

Parker, H.R., Lott, F.C., Cornforth, R.J., Mitchell, D.M. & Sparrow, S. 2017. A Comparison of Model Ensembles for Attributing 2012 West African rainfall. *Environmental Research Letters*. 12:1–10. DOI: 10.1088/1748-9326/aa5386.

Peterson, T.C., Stott, P.A. & Herring, S.C. 2012. Explaining Extreme Events of 2011 from a Climate Perspective. *Bulletin of American Meteorological Society.* DOI: 10.1175/BAMS-D-1.

Peterson, T.C., Hoerling, M.P., Stott, P.A. & Herring, S.C. 2013. Explaining Extreme Events of 2012 from a Climate Perspective. *Bulletin of American Meteorological Society*, 94(9):1–74.

Rahmstorf, S. & Coumou, D. 2011. Increase of Extreme Events in a Warming World. *Proceedings of the National Academy of Sciences of the United States of America*. 109(12):1–5. DOI: 10.1073/pnas.1101766108.

Richards, J.-A. & Schalatek, L. 2017. Financing Loss and Damage : A Look at Governance and Implementation Options. *Heinrich Böll Stiftung North America, Washington, D.C. U.S.A*.

Schaller, N., Kay, A.L., Lamb, R., Massey, N.R., Van Oldenborgh, G.J., Otto, F.E.L., Sparrow, S.N., Vautard, R., et al. 2016. Human Influence on Climate in the 2014 Southern England Winter Floods and their Impacts. *Nature Climate Change*. 6(6):627–634. DOI: 10.1038/nclimate2927.

Stone, D.A., Christidis, N., Folland, C., Perkins-Kirkpatrick, S., Perlwitz, J., Shiogama, H., Wehner, M.F., Wolski, P., et al. 2019. Experiment Design of the International CLIVAR C20C+ Detection and Attribution Project. *Weather and Climate Extremes*. 24:100206. DOI: 10.1016/j.wace.2019.100206.

Stott, P.A., Stone, D.A. & Allen, M.R. 2004. Human Contribution to the European Heatwave of 2003. 432. DOI: 10.1029/2001JB001029.

Stott, P.A., Allen, M., Christidis, N., Dole, R., Hoerling, M., Huntingford, C., Pall, P., Perlwitz, J., et al. 2013. Attribution of Weather and Climate-Related Extreme Events. 1–44.

Stott, P.A., Christidis, N., Otto, F.E.L., Sun, Y., Vanderlinden, J., Oldenborgh, G.J. Van, Vautard, R., Storch, H. Von, et al. 2016. Attribution of Extreme Weather and Climate-related Events. 7:23–41. DOI: 10.1002/wcc.380.

Tadesse, M.A., Shiferaw, B.A. & Erenstein, O. 2015. Weather Index Insurance for Managing Drought Risk in Smallholder Agriculture: Lessons and Policy Implications for sub-Saharan Africa. *Agricultural and Food Economics*. 3(1):1–21. DOI: 10.1186/s40100-015-0044-3.

Taylor, K.E. 2001. Summarizing Multiple Aspects of Model Performance in a Single Diagram. *Journal of Geophysical Research Atmospheres*. 106(D7):7183–7192. DOI: 10.1029/2000JD900719.

Taylor, K.E., Stouffer, R.J. & Meehl, G.A. 2012. An Overview of CMIP5 and the Experiment Design. *Bulletin of the American Meteorological Society*. 93(4):485–498. DOI: 10.1175/BAMS-D-11-00094.1.

Turvey, C.G. & Mclaurin, M.K. 2012. Applicability of the Normalized Difference Vegetation Index (NDVI) in Index-Based Crop Insurance Design. *Weather, Climate and Society*. 4:271–284. DOI: 10.1175/WCAS-D-11-00059.1.

Uhe, P., Philip, S., Kew, S., Shah, K., Kimutai, J., Mwangi, E., Oldenborgh, J. Van, Singh, R., et al. 2018. Attributing Drivers of the 2016 Kenyan Drought. *International journal of climatology*. 38(1):554–568. DOI: 10.1002/joc.5389.

UN. 2015. World Population Prospects: The 2015 Revision, Key Findings and Advance Tables. *Department of Economic and Social Affairs: United Nations, New York.* Working Paper No. (ESA/P/WP.241.).

UNDP. 2019. How Africa can Improve Mobilization of Climate Finance for Sustainable Development? *United Nations Development Programme, Africa*. Accessed (September 2019). Available: https://www.africa.undp.org/content/rba/en/home/blog/2019/how-africa-can-improve-mobilization-of-climate-finance-for-susta.html.

UNFCCC. 1992. United Nations Framework Convention on Climate Change. DOI: 10.2307/1903063.

UNFCCC. 2008. Mechanisms to Manage Financial Risks from Direct Impacts of Climate Change in Developing Countries. *United Nations Framework Convention on Climate Change,* 1–114.

UNFCCC. 2014. Report of the Conference of the Parties on its Nineteenth Session, held in Warsaw from 11 to 23 November 2013. U*nited Nations Framework Convention on Climate Change.*

UNFCCC. 2015. Paris agreement. *United Nations*

UNGA. 2015. Resolution Adopted by the General Assembly on 25 September 2015. U*nited Nations General Assembly, 57B6E3E44*.

van Asselt, H., Weikmans, R., Roberts, T. & Abeysinghe, A. 2016. Transparency of Action and Support under the Paris Agreement. European Capacity Building Initiative. Available: www.eurocapacity.org.

Vanhala, L. & Hestbaek, C. 2016. Framing Climate Change Loss and Damage in UNFCCC Negotiations. *Global Environmental Politics*. 16(4):111–129. DOI: 10.1162/GLEP_a_00379.

van Oldenborgh, G.J., van dier Wiel, K., Sebastian, A., Singh, R., Arrighi, J., Otto, F.E.L., Haustein, K., Sihan, L., et al. 2018. Attribution of Extreme Rainfall from Hurricane Harvey, August 2017. *Environmental Research Letters*. 13(2018):1–11.

Watson, C. & Schalatek, L. 2019. The Global Climate Finance Architecture. *Climate Funds Update*. (November 2018):5. Available: http://www.odi.org.uk/sites/odi.org.uk/files/odi-assets/publications-opinion-files/8685.pdf.

Wilcox, L.J., Yiou, P., Hauser, M., Lott, F.C., Jan, G., Ioana, V.O., Buwen, C. & Gabi, D. 2018. Multiple Perspectives on the Attribution of the Extreme European summer of 2012 to Climate Change. *Climate Dynamics*. 50(9):3537–3555. DOI: 10.1007/s00382-017-3822-7.

Winkler, K., Gessner, U. & Hochschild, V. 2017. Identifying Droughts Affecting Agriculture in Africa Based on Remote Sensing Time Series between 2000–2016 : Rainfall Anomalies and Vegetation Condition in the Context of ENSO. *Remote Sensing*. 9(831):1–26. DOI: 10.3390/rs9080831.

Wolfrom, L. & Yokoi-Arai, M. 2016. Financial Instruments for Managing Disaster Risks Related to Climate Change. *OECD Journal: Financial Market Trends*. 2015(1):25–47. DOI: 10.1787/fmt-2015-5jrqdkpxk5d5.

Wolski, P., Stone, D., Tadross, M., Wehner, M. & Hewitson, B. 2014. Attribution of Floods in the Okavango basin, Southern Africa. *JOURNAL OF HYDROLOGY*. 511(2014):350–358. DOI: 10.1016/j.jhydrol.2014.01.055.

Zhai, P., Zhou, B.Q. & Chen, Y. 2018. A Review of Climate Change Attribution Studies. *Journal of Meteorological Research*. 32(5). DOI: 10.1007/s13351-018-8041-6.

APPENDIX A: Descriptive Statistics Comparing 15 Models to a Reference Observation

West Africa (December-January-February Season

DJF-WA (Uncorrected)											
Models	Correlation	Mean	RMSE	Std.dev	CV	Corr/Rank	Mean/Rank	RMSE/Rank	Sd/Rank	CV/Rank	Average Rank
CCSM4	0.96	0.004	5.596	0.772	76.5	2	15	5	3	2	27
CESM1-CAM5	0.9494	0.2492	4.631	0.173	56.3	5	11	3	12	3	34
MRI-GCM3	0.7872	0.8858	10.65	0.8253	53	14	1	14	2	4	35
GFDL-CM3	0.9636	0.4937	6.489	0.4897	0.8	1	7	8	5	15	36
IPSL-CM5A-LR	0.9269	0.3096	4.799	0.4841	25.27	9	10	4	6	8	37
MIROC-ESM	0.9508	0.642	8.885	0.38	15.93	3	3	12	8	11	37
CNRM-CM5	0.8911	0.1762	4.096	0.4234	30	11	12	1	7	7	38
CanESM	0.9337	0.5313	6.592	0.5115	4.2	7	6	9	4	14	40
GFDL-ESM2M	0.9364	0.4193	5.953	0.3612	10	6	8	6	9	12	41
MIROC- CHEM	0.9503	0.565	7.347	0.171	25.18	4	4	11	13	9	41
HadGEM2-ES	0.888	0.119	27.93	8.567	755.1	12	14	15	1	1	43
CSIRO-MK3	0.5413	0.546	7.14	0.3591	41.2	15	5	10	10	5	45
IPSL-CM5A-MR	0.9053	0.4101	6.103	0.2968	19.2	10	9	7	11	10	47
BNU-ESM	0.8869	0.693	9.099	0.001	40.86	13	2	13	15	6	49
ACCESS	0.9302	0.1649	4.41	0.1284	4.4	8	13	2	14	13	50

DJF-WA (Bias-corrected)											
Models	Correlation	Mean	RMSE	Std.dev	CV	Corr/Rank	Mean/Rank	RMSE/Rank	Sd/Rank	CV/Rank	Average Rank
CanESM	0.9729	0.6028	7.21	0.4832	30.1	2	2	13	3	8	28
CCSM4	0.9774	0.394	5.449	0.1527	39.8	1	9	7	12	5	34
CESM1-CAM5	0.9724	0.4087	5.514	0.151	43.6	3	8	9	13	3	36
CNRM-CM5	0.9507	0.5374	6.629	0.472	14.1	7	5	10	4	12	38
GFDL-CM3	0.8747	0.6681	7.998	0.5477	36.3	14	1	14	2	7	38
BNU-ESM	0.9638	0.4108	5.429	0.4069	0.7	5	7	6	7	14	39
CSIRO-MK3	0.9427	0.5395	6.679	0.437	22.3	8	4	11	6	11	40
GFDL-ESM2M	0.9321	0.5685	6.951	0.4648	24	11	3	12	5	9	40
IPSL-CM5A-MR	0.9301	0.3632	5.477	0.309	105.6	12	11	8	8	2	41
HadGEM2-ES	0.894	0.304	24.84	7.44	547.1	13	12	15	1	1	42
IPSL-CM5A-LR	0.9389	0.372	4.846	0.1385	37.2	9	10	4	14	6	43
MIROC- CHEM	0.9632	0.2978	4.11	0.3005	0.38	6	13	1	9	15	44
MIROC-ESM	0.9671	0.2543	4.182	0.1835	9.5	4	14	2	11	13	44
MRI-GCM3	0.8447	0.4204	5.194	0.2841	23.5	15	6	5	10	10	46
ACCESS	0.9372	0.251	4.661	0.072	43.1	10	15	3	15	4	47

March-April-May Season

MAM-WA (Uncorrected)											
Models	Correlation	Mean	RMSE	Std.dev	CV	Corr/Rank	Mean/Rank	RMSE/Rank	Sd/Rank	CV/Rank	Average Rank
HadGEM2-ES	0.9664	0.0546	8.29	0.95	106.3	4	15	1	5	1	26
GFDL-ESM2M	0.9457	0.745	34.03	2.05	74.8	10	4	12	1	2	29
CCSM4	0.9661	0.424	20.25	1.188	53.7	5	6	11	4	4	30
GFDL-CM3	0.9702	0.141	10.52	0.805	58.1	2	14	5	7	3	31
MIROC-CHEM	0.9623	0.835	36.81	1.709	47.6	6	2	14	3	6	31
CSIRO-MK3	0.8985	0.974	43.18	1.983	51.1	13	1	15	2	5	36
CESM1-CAM5	0.9668	0.361	16.98	0.577	15.9	3	7	9	9	11	39
MIROC-ESM	0.9608	0.808	35.4	0.906	5.4	8	3	13	6	13	43
CNRM-CM5	0.9713	0.217	11.37	0.201	1.34	1	11	6	11	15	44
CanESM	0.9428	0.342	15.84	0.636	21.9	11	8	8	8	10	45
BNU-ESM	0.9537	0.453	20.09	0.129	22.28	9	5	10	13	9	46
ACCESS	0.9616	0.178	10.08	0.204	2.2	7	13	3	10	14	47
IPSL-CM5A-LR	0.8796	0.1945	9.568	0.095	36	14	12	2	14	7	49
MRI-GCM3	0.9188	0.2175	10.18	0.051	34.4	12	10	4	15	8	49
IPSL-CM5A-MR	0.8579	0.2745	12.66	0.1749	13.7	15	9	7	12	12	55

MAM-WA (Bias-corrected)											
Models	Correlation	Mean	RMSE	Std.dev	CV	Corr/Rank	Mean/Rank	RMSE/Rank	Sd/Rank	CV/Rank	Average Rank
IPSL-CM5A-MR	0.0625	0.3556	18.25	1.353	265.2	1	1	15	3	1	21
HadGEM2-ES	0.0327	0.11	11.56	1.797	152	8	7	11	1	2	29
MIROC- CHEM	0.0423	0.324	16.01	1.219	67.6	4	2	14	4	7	31
CanESM	0.0448	0.116	7.648	0.638	46.8	3	6	5	9	9	32
GFDL-ESM2M	0.0343	0.0448	7.807	1.708	78.9	7	13	6	2	5	33
IPSL-CM5A-LR	0.0542	0.2906	13.49	0.299	83.1	2	3	12	14	3	34
GFDL-CM3	0.0412	0.0577	8.483	0.688	79.1	5	12	8	8	4	37
MIROC-ESM	0.0408	0.28	14.15	0.81	41.4	6	4	13	6	10	39
CCSM4	0.0287	0.077	8.32	0.892	75.6	12	10	7	5	6	40
ACCESS	0.0309	0.095	8.551	0.735	58.4	11	8	9	7	8	43
MRI-GCM3	0.031	0.061	5.602	0.303	22.9	10	11	1	13	14	49
CESM1-CAM5	0.0325	0.022	5.98	0.392	36.2	9	15	2	12	12	50
CSIRO-MK3	0.0245	0.218	11.3	0.556	27.8	14	5	10	10	13	52
BNU-ESM	0.0197	0.031	6.106	0.446	40.2	15	14	3	11	11	54
CNRM-CM5	0.0247	0.0934	6.208	0.0588	3.8	13	9	4	15	15	56

June-July-August Season

JJA-WA (Uncorrected)											
Models	Correlation	Mean	RMSE	Std.dev	CV	Corr/Rank	Mean/Rank	RMSE/Rank	Sd/Rank	CV/Rank	Average Rank
HadGEM2-ES	0.7825	0.9114	14.57	0.5088	46.11	6	6	3	5	6	26
IPSL-CM5A-LR	0.5945	0.9995	10.99	0.5449	54.46	15	4	1	3	3	26
CanESM	0.8322	0.338	32.11	0.6	70.11	2	10	12	2	1	27
BNU-ESM	0.8282	0.313	30.32	0.5215	63.55	3	11	11	4	2	31
GFDL-ESM2M	0.8	2.083	97.11	0.803	13.46	4	1	15	1	14	35
IPSL-CM5A-MR	0.6188	0.9936	12.39	0.4505	44.69	14	5	2	7	7	35
MIROC- CHEM	0.6996	1.224	24	0.3855	49.79	12	3	8	9	4	36
MRI-GCM3	0.6218	0.828	19.47	0.4582	34.57	13	7	5	6	10	41
CSIRO-MK3	0.8373	0.806	72.75	0.429	20.87	1	8	14	8	13	44
CNRM-CM5	0.7698	0.497	46.26	0.2127	47.39	7	9	13	11	5	45
MIROC-ESM	0.7267	1.24	24.43	0.1629	32.51	10	2	9	13	11	45
CCSM4	0.7671	0.188	19.59	0.283	39.62	8	14	6	10	8	46
ACCESS	0.7476	0.173	19.42	0.1473	27.33	9	15	4	14	12	54
CESM1-CAM5	0.7124	0.266	28.01	0.2025	36.99	11	12	10	12	9	54
GFDL-CM3	0.7857	0.213	22.23	0.085	10.58	5	13	7	15	15	55

JJA-WA (Bias-corrected)											
Models	Correlation	Mean	RMSE	Std.dev	CV	Corr/Rank	Mean/Rank	RMSE/Rank	Sd/Rank	CV/Rank	Average Rank
MRI-GCM3	0.997	0.141	9.216	0.182	7.29	1	1	3	6	12	23
BNU-ESM	0.9513	0.1	10.62	0.1571	23.34	3	5	6	7	4	25
CESM1-CAM5	0.9116	0.0177	8.163	0.2806	26.77	13	12	1	2	2	30
HadGEM2-ES	0.9607	0.121	12.98	0.1416	23.4	2	3	14	8	3	30
CNRM-CM5	0.9429	0.093	11	0.1338	20.74	7	7	8	9	6	37
IPSL-CM5A-LR	0.9493	0.129	12.97	0.1055	20.77	4	2	13	13	5	37
CCSM4	0.9305	0.0367	8.48	0.1885	15.76	11	11	2	5	9	38
IPSL-CM5A-MR	0.9321	0.013	36.47	1.71	174.6	9	13	15	1	1	39
GFDL-CM3	0.9317	0.079	12.07	0.215	12.6	10	9	10	3	10	42
MIROC- CHEM	0.8907	0.0995	10.8	0.1989	11.04	15	6	7	4	11	43
ACCESS	0.9293	0.115	12.11	0.114	20.51	12	4	11	12	7	46
CanESM	0.948	-0.108	12.53	0.1173	20.36	5	15	12	11	8	51
GFDL-ESM2M	0.9375	0.043	9.581	-0.048	0.5	8	10	4	15	15	52
CSIRO-MK3	0.9471	0.003	9.591	0.0181	2.11	6	14	5	14	14	53
MIROC-ESM	0.9015	0.0866	11.93	0.1251	4.21	14	8	9	10	13	54

September-October-November Season

SON-WA (Uncorrected)											
Models	Correlation	Mean	RMSE	Std.dev	CV	Corr/Rank	Mean/Rank	RMSE/Rank	Sd/Rank	CV/Rank	Average Rank
GFDL-CM3	0.9603	0.224	19.37	0.978	61.6	1	13	7	3	3	27
HadGEM2-ES	0.926	0.3847	26.16	0.563	154.1	6	3	13	4	1	27
GFDL-ESM2M	0.9451	1.067	64.36	1.671	29.2	5	1	15	2	6	29
CCSM4	0.951	0.374	24.11	0.468	6.9	3	4	9	7	10	33
CNRM-CM5	0.9454	0.364	24.15	0.539	12.8	4	7	10	5	7	33
CSIRO-MK3	0.8076	0.669	43.22	1.812	68.5	15	2	14	1	2	34
MIROC-ESM	0.9213	0.369	24.28	0.538	12.4	7	5	11	6	8	37
IPSL-CM5A-LR	0.9105	0.24	16.16	0.2523	39.68	12	12	3	10	4	41
IPSL-CM5A-MR	0.9202	0.247	16.47	0.1933	35.33	9	11	4	12	5	41
BNU-ESM	0.9522	0.25	16.97	0.168	6.54	2	10	5	13	12	42
MIROC-CHEM	0.9201	0.367	23.97	0.237	9.54	10	6	8	11	9	44
CanESM	0.9207	0.002	9.972	0.069	6.7	8	15	2	14	11	50
CESM1-CAM5	0.9146	0.364	24.3	0.391	2	11	7	12	8	13	51
MRI-GCM3	0.8599	0.3162	19.35	0.3133	0.4	14	9	6	9	15	53
ACCESS	0.8971	0.0385	8.731	0.0488	1.08	13	14	1	15	14	57

SON-WA (Bias-corrected)											
Models	Correlation	Mean	RMSE	Std.dev	CV	Corr/Rank	Mean/Rank	RMSE/Rank	Sd/Rank	CV/Rank	Average Rank
BNU-ESM	0.9814	0.0769	8.34	0.088	17.8	8	10	2	5	6	31
CESM1-CAM5	0.9858	0.097	9.271	0.0807	16.18	5	7	8	4	7	31
MRI-GCM3	0.9828	0.1289	9.198	0.08	5.6	7	4	7	3	11	32
GFDL-ESM2M	0.9883	0.085	9.893	0.0381	11.31	4	9	10	1	9	33
IPSL-CM5A-LR	0.9905	0.177	12.01	0.133	3.75	2	3	11	8	12	36
IPSL-CM5A-MR	0.9921	0.099	24.03	2.309	201.1	1	6	15	15	1	38
CNRM-CM5	0.9788	0.038	7.374	0.063	2.4	10	13	1	2	14	40
CanESM	0.9843	0.1271	9.806	0.1315	0.51	6	5	9	7	15	42
GFDL-CM3	0.9901	0.058	12.07	0.648	55.7	3	11	12	13	3	42
HadGEM2-ES	0.9664	0.2749	21.13	0.698	134.2	11	1	14	14	2	42
CCSM4	0.9799	0.086	9.136	0.172	7.8	9	8	6	10	10	43
MIROC-ESM-CHEM	0.9616	0.0242	8.701	0.123	15.1	13	14	4	6	8	45
MIROC-ESM	0.9664	0.0196	8.484	0.227	25.1	11	15	3	12	5	46
CSIRO-MK3	0.9336	0.0547	9.113	0.216	28.6	15	12	5	11	4	47
ACCESS	0.9558	0.1892	12.48	0.1678	2.6	14	2	13	9	13	51

Southern Africa

December-January-February Season

DJF-SA (Uncorrected)											
Models	Correlation	Mean	RMSE	Std.dev	CV	Corr/Rank	Mean/Rank	RMSE/Rank	Sd/Rank	CV/Rank	Average Rank
HadGEM2-ES	0.8445	0.143	43.85	2.244	183.9	1	13	5	1	1	21
BNU-ESM	0.791	0.506	69.46	0.2661	51.28	8	5	11	2	3	29
CanESM	0.837	0.272	39.11	0.1552	33.56	3	11	4	3	8	29
IPSL-CM5A-LR	0.8313	0.441	60.58	0.1297	39.59	4	7	9	6	4	30
IPSL-CM5A-MR	0.82	0.433	60.47	0.1341	39.56	5	8	8	4	5	30
GFDL-ESM2M	0.7849	0.588	80.65	0.1013	56.59	9	1	15	9	2	36
CCSM4	0.8404	0.522	72.02	0.023	32.75	2	3	14	14	9	42
CESM1-CAM5	0.7713	0.354	49.26	0.1073	34.06	11	10	6	8	7	42
GFDL-CM3	0.8037	0.367	52.58	0.134	17.03	7	9	7	5	14	42
ACCESS	0.8098	0.481	66.41	0.092	26.24	6	6	10	11	10	43
MIROC-ESM	0.6059	0.523	71.59	0.0595	38.25	14	2	13	13	6	48
MIROC-CHEM	0.602	0.51	70.83	0.122	25.71	15	4	12	7	11	49
MRI-GCM3	0.7755	0.129	22.07	0.093	19.65	10	14	2	10	13	49
CNRM-CM5	0.6856	0.222	34.8	0.0869	25.28	13	12	3	12	12	52
CSIRO-MK3	0.7536	0.056	18.86	0.0037	5.69	12	15	1	15	15	58

DJF-SA (Bias-corrected)											
Models	Correlation	Mean	RMSE	Std.dev	CV	Corr/Rank	Mean/Rank	RMSE/Rank	Sd/Rank	CV/Rank	Average Rank
IPSL-CM5A-MR	0.9825	0.0863	43.27	2.563	289.9	1	4	15	1	1	22
HadGEM2-ES	0.9646	0.0943	18.85	0.291	42.5	10	3	13	2	2	30
GFDL-ESM2M	0.9683	0.0089	7.136	0.1494	14.18	9	15	1	4	3	32
CanESM	0.9804	0.052	10.4	0.089	3.5	2	9	6	5	12	34
CESM1-CAM5	0.9704	0.022	7.147	0.0666	8.64	8	12	2	7	5	34
MRI-GCM3	0.9706	0.9485	9.199	0.0199	3.3	7	1	5	11	13	37
ACCESS	0.9722	0.0779	12.29	0.0333	4.8	6	6	9	10	8	39
CCSM4	0.9771	0.0203	8.479	0.059	3.96	3	13	4	8	11	39
IPSL-CM5A-LR	0.977	0.028	7.979	0.0149	4.19	4	11	3	13	10	41
GFDL-CM3	0.9612	0.0148	10.5	0.081	9.7	12	14	7	6	4	43
CNRM-CM5	0.9742	0.0387	11.05	0.002	4.2	5	10	8	15	9	47
CSIRO-MK3	0.9553	0.145	21.22	0.1583	1.55	13	2	14	3	15	47
MIROC-ESM	0.9445	0.083	13.4	0.016	6.18	14	5	12	12	7	50
BNU-ESM	0.963	0.0773	12.86	0.0531	2.6	11	7	11	9	14	52
MIROC-ESM-CHEM	0.9305	0.074	12.72	0.003	7.17	15	8	10	14	6	53

March-April-May Season

MAM-SA (Uncorrected)											
Models	Correlation	Mean	RMSE	Std.dev	CV	Corr/Rank	Mean/Rank	RMSE/Rank	Sd/Rank	CV/Rank	Average Rank
HadGEM2-ES	0.8267	0.2082	25.1	1.078	162.5	7	13	3	1	1	25
BNU-ESM	0.8328	0.794	58.42	0.295	27.8	5	1	15	4	7	32
IPSL-CM5A-MR	0.8705	0.626	46.67	0.181	27.4	2	4	12	7	8	33
ACCESS	0.8618	0.645	48.82	0.411	14.19	3	3	13	3	12	34
CESM1-CAM5	0.7673	0.415	32.2	0.1778	41.88	9	8	8	8	2	35
CSIRO-MK3	0.8297	0.362	28.47	0.0937	33.46	6	11	5	11	6	39
IPSL-CM5A-LR	0.8596	0.566	42.97	0.039	33.65	4	6	10	14	5	39
CCSM4	0.8025	0.681	50.18	0.051	37.5	8	2	14	13	3	40
CanESM	0.8875	0.173	18.42	0.0307	17.37	1	14	2	15	10	42
CNRM-CM5	0.6553	0.328	25.92	0.1391	35.17	14	12	4	9	4	43
GFDL-CM3	0.7452	0.451	35.51	0.237	14.77	10	7	9	6	11	43
GFDL-ESM2M	0.7391	0.576	44.38	0.46	7.38	11	5	11	2	15	44
MIROC-ESM	0.709	0.385	30.65	0.246	10.04	13	10	6	5	14	48
MIROC- CHEM	0.7277	0.402	31.83	0.052	24.91	12	9	7	12	9	49
MRI-GCM3	0.6234	0.05	11.96	0.0958	13.92	15	15	1	10	13	54

MAM-SA (Bias-Corrected)											
Models	Correlation	Mean	RMSE	Std.dev	CV	Corr/Rank	Mean/Rank	RMSE/Rank	Sd/Rank	CV/Rank	Average Rank
CanESM	0.9467	0.0555	9.801	0.285	24.29	7	7	6	4	5	29
IPSL-CM5A-LR	0.9439	0.094	10.34	0.2534	31.75	8	5	8	5	3	29
CESM1-CAM5	0.9282	0.04	8.19	0.2882	31.53	12	8	5	3	4	32
CCSM4	0.9324	0.025	6.582	0.2087	22.81	9	11	1	6	6	33
HadGEM2-ES	0.9227	0.3143	27.78	0.746	154.6	15	1	15	2	2	35
GFDL-ESM2M	0.9653	0.0021	7.091	0.1785	17.68	2	14	3	8	10	37
IPSL-CM5A-MR	0.947	0.0008	24.06	1.654	165.6	6	15	14	1	1	37
CNRM-CM5	0.9666	0.0652	11.09	0.112	19	1	6	11	11	9	38
ACCESS	0.9293	0.039	7.198	0.1648	19.64	11	9	4	9	8	41
MIROC- CHEM	0.9246	0.032	10.08	0.1952	21.98	13	10	7	7	7	44
MRI-GCM3	0.9606	0.1084	11.68	0.0844	2.7	3	4	12	12	15	46
CSIRO-MK3	0.9565	0.162	14.15	0.007	13.33	4	2	13	15	13	47
GFDL-CM3	0.9529	0.017	10.45	0.123	14.2	5	12	9	10	12	48
BNU-ESM	0.9245	0.113	10.85	0.0745	16.82	14	3	10	13	11	51
MIROC-ESM	0.9323	0.0068	7.037	0.0439	3.74	10	13	2	14	14	53

June-July-August Season

JJA-SA (Uncorrected)											
Models	Correlation	Mean	RMSE	Std.dev	CV	Corr/Rank	Mean/Rank	RMSE/Rank	Sd/Rank	CV/Rank	Average Rank
HadGEM2-ES	0.8662	0.905	11.33	3.005	110.2	1	7	9	2	1	20
ACCESS	0.717	1.615	18.28	2.112	19	4	2	14	3	8	31
GFDL-ESM2M	0.3496	1.148	13.7	3.105	91.1	13	5	11	1	2	32
CNRM-CM5	0.6552	1.044	12.09	1.672	30.7	7	6	10	7	6	36
MRI-GCM3	0.4898	0.509	6.526	1.715	79.9	12	11	5	6	3	37
BNU-ESM	0.664	2.055	23.06	1.877	5.82	5	1	15	4	13	38
CSIRO-MK3	0.8075	0.0395	2.37	0.38	43.7	2	15	1	15	5	38
GFDL-CM3	0.6516	1.479	16.78	1.731	10.2	8	3	13	5	11	40
IPSL-CM5A-LR	0.5978	0.726	8.498	1.042	18.3	9	9	7	10	9	44
MIROC-ESM	0.3331	0.499	6.329	1.172	44.9	14	13	4	9	4	44
IPSL-CM5A-MR	0.6577	0.78	8.989	0.956	9.9	6	8	8	11	12	45
CanESM	0.7402	0.605	7.123	0.591	0.83	3	10	6	14	15	48
CCSM4	0.5716	1.37	15.44	1.404	1.4	10	4	12	8	14	48
CESM1-CAM5	0.5709	0.505	6.155	0.722	14.4	11	12	3	13	10	49
MIROC- CHEM	0.3171	0.466	5.81	0.878	28.1	15	14	2	12	7	50

JJA-SA (Bias-corrected)											
Models	Correlation	Mean	RMSE	Std.dev	CV	Corr/Rank	Mean/Rank	RMSE/Rank	Sd/Rank	CV/Rank	Average Rank
MIROC-CHEM	0.1514	1.034	2.1	0.904	84.1	2	11	3	4	3	23
CCSM4	0.0926	1.046	2.209	0.832	75.1	5	9	5	5	4	28
HadGEM2-ES	0.0471	1.585	8.721	3.332	173.3	12	1	15	1	2	31
IPSL-CM5A-LR	0.1047	1.063	1.824	0.573	48	4	8	2	9	8	31
ACCESS	0.0865	1.378	5.113	1.24	62.5	7	2	14	3	6	32
IPSL-CM5A-MR	0.1375	0.9889	4.019	2.114	214.9	3	14	12	2	1	32
MIROC-ESM	0.1568	1.024	2.475	0.712	67.1	1	12	7	7	5	32
GFDL-CM3	0.0866	1.146	2.948	0.74	51.9	6	5	10	6	7	34
GFDL-ESM2M	0.0712	1.143	2.639	0.542	34.9	9	6	8	11	11	45
MRI-GCM3	0.0385	1.218	3.293	0.656	36	14	4	11	8	9	46
CSIRO-MK3	0.0728	1.3	4.05	0.572	20.9	8	3	13	10	13	47
BNU-ESM	0.0483	1.039	2.116	0.356	30.5	10	10	4	13	12	49
CNRM-CM5	0.0335	1.127	2.755	0.533	36	15	7	9	12	9	52
CanESM	0.0481	1.01	1.482	0.018	0.8	11	13	1	15	15	55
CESM1-CAM5	0.0419	0.8227	2.352	0.0867	11	13	15	6	14	14	62

September-October-November Season

SON-SA (Uncorrected)											
Models	Correlation	Mean	RMSE	Std.dev	CV	Corr/Rank	Mean/Rank	RMSE/Rank	Sd/Rank	CV/Rank	Average Rank
HadGEM2-ES	0.8625	0.8	55.55	2.327	84.9	10	2	14	1	1	28
CCSM4	0.9069	0.734	48.28	0.271	26.71	1	4	12	9	3	29
MIROC-ESM	0.8943	0.229	17.7	0.356	10.4	6	13	2	7	7	35
BNU-ESM	0.8831	0.895	58.46	0.184	37.51	7	1	15	12	2	37
CESM1-CAM5	0.9028	0.323	22.75	0.188	10.2	2	9	7	11	8	37
GFDL-ESM2M	0.8947	0.595	39.98	0.492	6.45	5	5	11	4	12	37
CNRM-CM5	0.8342	0.485	33.84	0.634	10	11	6	10	3	9	39
GFDL-CM3	0.895	0.41	28.68	0.463	3.7	4	8	8	5	14	39
MIROC- CHEM	0.9017	0.188	14.75	0.009	15.11	3	15	1	15	5	39
IPSL-CM5A-MR	0.8809	0.257	19.54	0.092	13.11	8	12	4	13	6	43
IPSL-CM5A-LR	0.88	0.221	18.64	0.342	9.9	9	14	3	8	10	44
ACCESS	0.8218	0.768	50.78	0.743	1.41	12	3	13	2	15	45
CanESM	0.8211	0.299	21.14	0.053	18.91	13	11	5	14	4	47
MRI-GCM3	0.8131	0.443	29.48	0.387	3.86	14	7	9	6	13	49
CSIRO-MK3	0.6954	0.301	22.23	0.202	7.58	15	10	6	10	11	52

SON-SA (Bias-corrected)											
Models	Correlation	Mean	RMSE	Std.dev	CV	Corr/Rank	Mean/Rank	RMSE/Rank	Sd/Rank	CV/Rank	Average Rank
HadGEM2-ES	0.9474	0.466	33.85	1.649	80.8	10	2	15	2	2	31
IPSL-CM5A-MR	0.946	0.2358	22.89	1.8	266.4	13	3	14	1	1	32
MIROC- CHEM	0.9522	0.1917	15.26	0.31	62.1	7	5	13	4	3	32
ACCESS	0.9384	0.945	8.059	0.288	22.1	14	1	7	6	6	34
CNRM-CM5	0.963	0.135	13.15	0.309	15.3	5	8	9	5	7	34
CCSM4	0.9715	0.014	6.356	0.0511	6.38	2	14	1	11	10	38
CSIRO-MK3	0.9282	0.07	10.15	0.343	25.5	15	9	8	3	4	39
CESM1-CAM5	0.9767	0.0507	7.259	0.008	6.2	1	10	3	15	11	40
GFDL-ESM2M	0.9667	0.0049	7.446	0.104	11	4	15	4	9	8	40
MIROC-ESM	0.9542	0.1728	13.3	0.019	23.2	6	7	10	13	5	41
MRI-GCM3	0.947	0.201	14.18	0.116	7.09	12	4	12	8	9	45
GFDL-CM3	0.9513	0.035	7.559	0.065	2.9	8	12	5	10	12	47
BNU-ESM	0.9712	0.032	7.881	0.047	1.5	3	13	6	12	14	48
CanESM	0.9495	0.0409	7.226	0.0135	2.9	9	11	2	14	12	48
IPSL-CM5A-LR	0.9473	0.177	13.66	0.1724	0.6	11	6	11	7	15	50

Appendix B:Q-Q Plots Showing Distributions of 15 Models and a Reference Observation in Four Cities in Malawi, Zimbabwe, Senegal and Mauritania

Malawi Top(Uncorrected); Bottom (Bias-corrected)

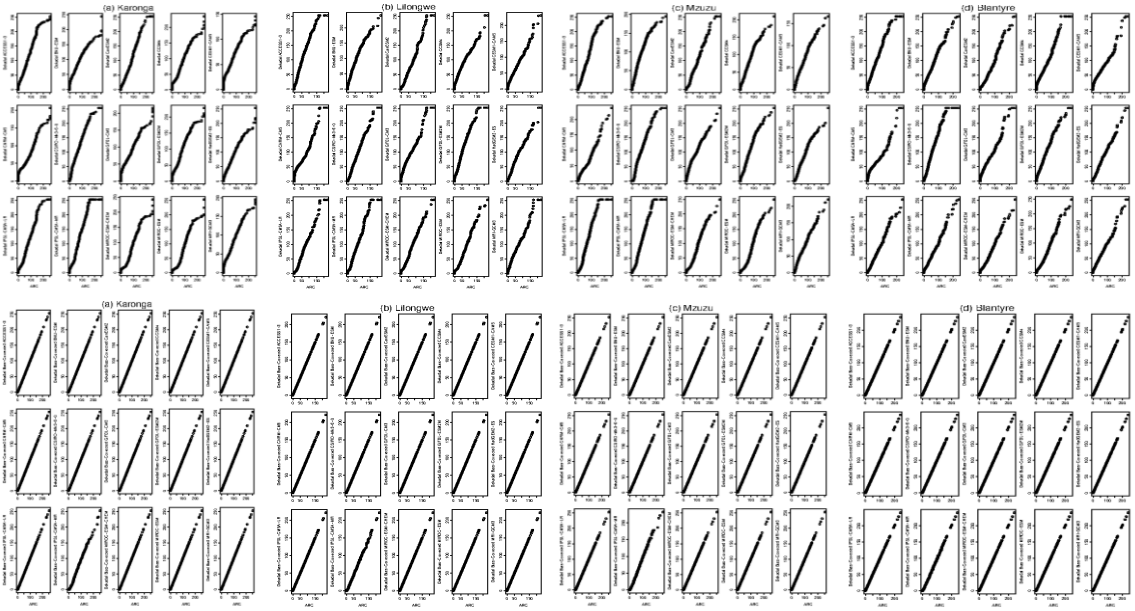

Zimbabwe Top(Uncorrected); Bottom (Bias-corrected)

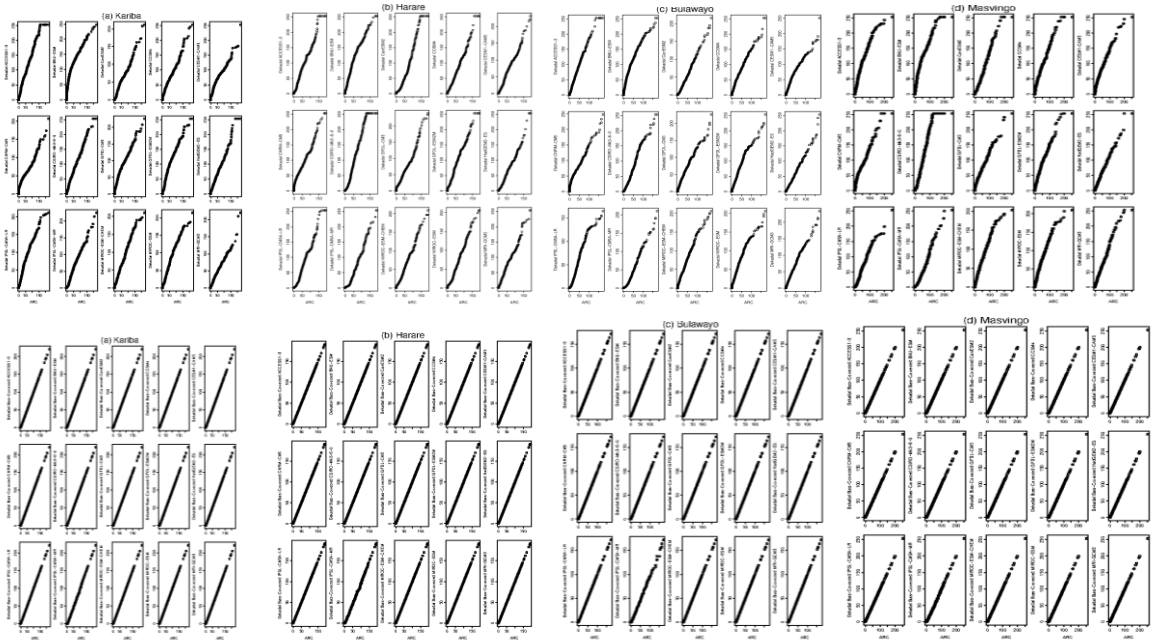

Senegal Top(Uncorrected); Bottom (Bias-corrected)

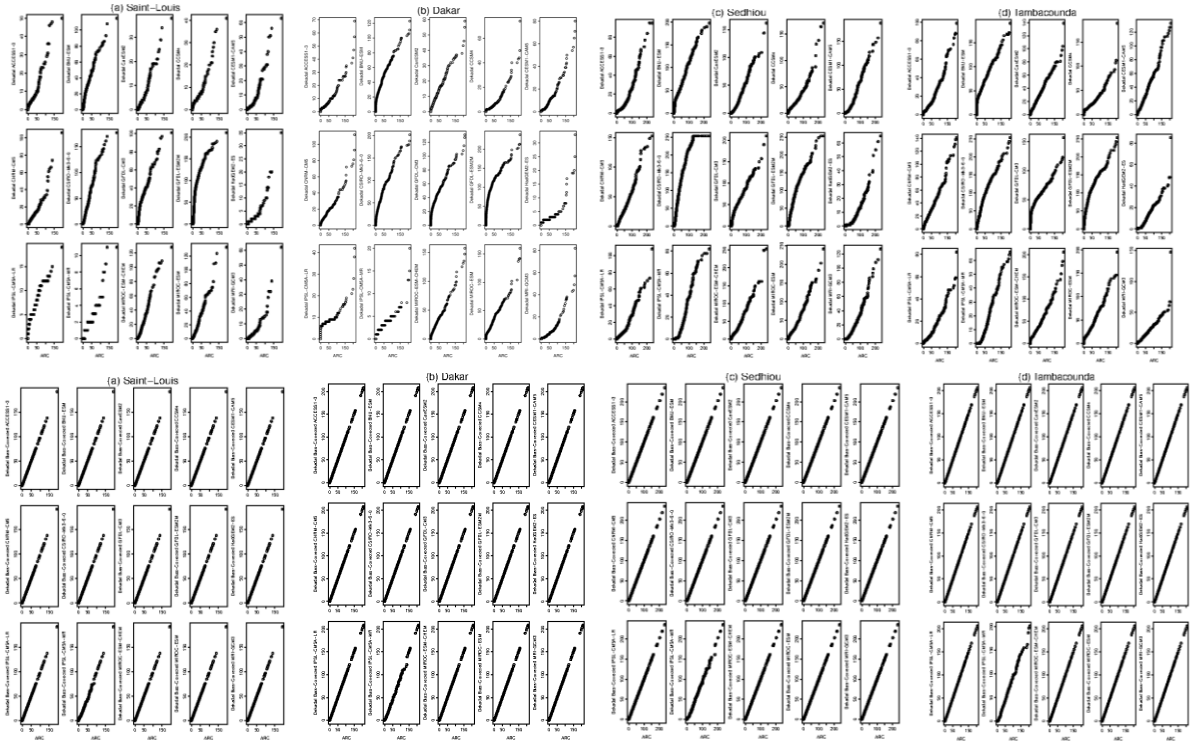

Mauritania Top(Uncorrected); Bottom (Bias-corrected)

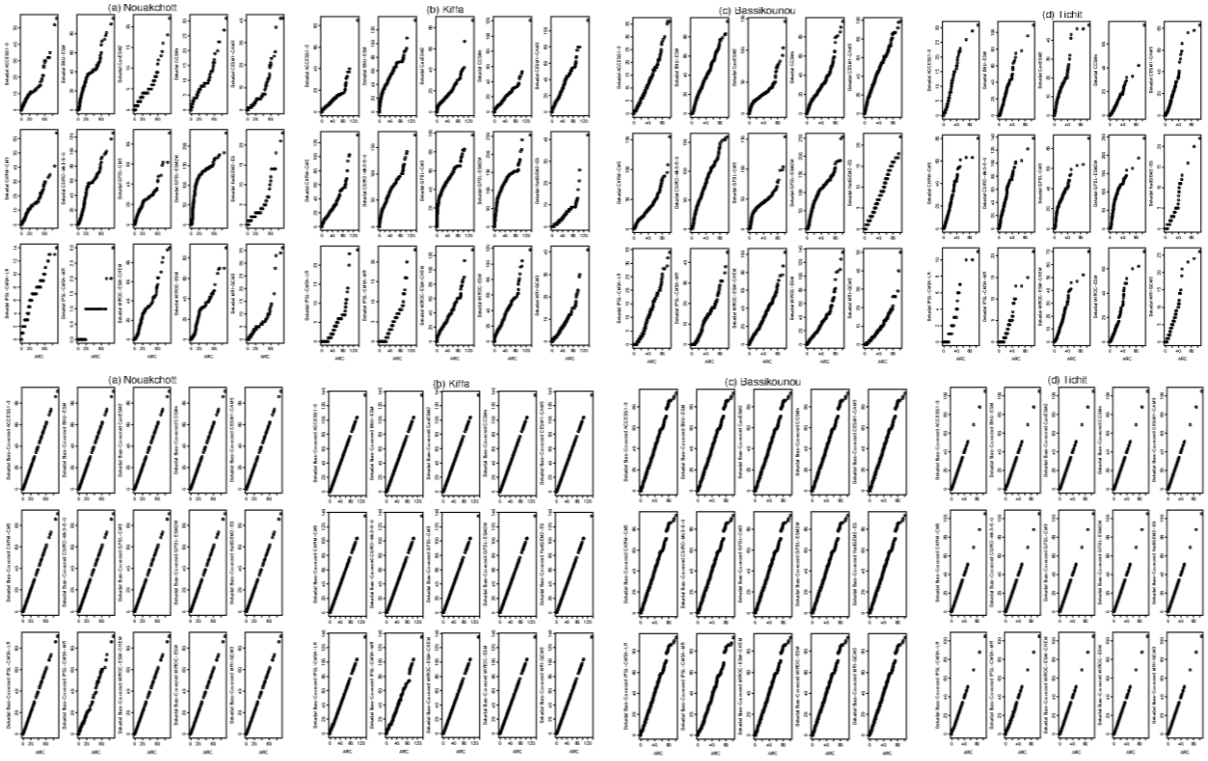

Appendix C: Kolmogorov-Smirnov Non-parametric Test for Distribution

Null Hypothesis (Ho): P-value

Alternate Hypothesis (H1): P-value

Malawi

Models	Karonga (Uncorrected)	Karonga (Bias-corrected)	Lilongwe (Uncorrected)	Lilongwe (Bias-corrected)	Mzuzu (Uncorrected)	Mzuzu (Bias-corrected)	Blantyre (Uncorrected)	Blantyre (Bias-corrected)
ACCESS	P < 2.2e-16	P=1	P < 2.2e-16	P=1	P < 2.2e-16	P=1	P < 2.2e-16	P=1
BNU-ESM	P < 2.2e-16	P=1	P < 2.2e-16	P=1	P < 2.2e-16	P=1	P < 2.2e-16	P=1
CanESM	P < 2.2e-16	P=1	P < 2.2e-16	P=1	P < 2.2e-16	P=1	P < 2.2e-16	P=1
CCSM4	P < 2.2e-16	P=1	P < 2.2e-16	P=1	P < 2.2e-16	P=1	P < 2.2e-16	P=1
CESM1-CAM5	P < 2.2e-16	P=1	P < 2.2e-16	P=1	P < 2.2e-16	P=1	P < 2.2e-16	P=1
CNRM-CM5	P < 2.2e-16	P=1	P < 2.2e-16	P=1	P= 0.005	P=1	P < 2.2e-16	P=1
CSIRO-MK3	P= 1.024e-09	P=1	P = 0.0013	P=1	P=2.02e-08	P=1	P < 2.2e-16	P=1
GFDL-CM3	P < 2.2e-16	P=1	P < 2.2e-16	P=1	P < 2.2e-16	P=1	P < 2.2e-16	P=1
GFDL-ESM2M	P < 2.2e-16	P=1	P < 2.2e-16	P=1	P < 2.2e-16	P=1	P < 2.2e-16	P=1
HadGEM2-ES	P < 2.2e-16	P=1	P < 2.2e-16	P=1	P= 4.06e-07	P=1	P < 2.2e-16	P=1
IPSL-CM5A-LR	P < 2.2e-16	P=1	P < 2.2e-16	P=1	P=1.33e-12	P=1	P < 2.2e-16	P=1
IPSL-CM5A-MR	P < 2.2e-16	P= 0.305	P < 2.2e-16	P= 0.216	P < 2.2e-16	P= 0.1483	P < 2.2e-16	P= 0.1635
MIROC- CHEM	P < 2.2e-16	P=1	P < 2.2e-16	P=1	P < 2.2e-16	P=1	P < 2.2e-16	P=1
MIROC-ESM	P < 2.2e-16	P=1	P < 2.2e-16	P=1	P < 2.2e-16	P=1	P < 2.2e-16	P=1
MRI-GCM3	P < 2.2e-16	P=1	P < 2.2e-16	P=1	P < 2.2e-16	P=1	P < 2.2e-16	P=1

Zimbabwe

Models	Kariba (Uncorrected)	Kariba (Bias-corrected)	Harare (Uncorrected)	Harare (Bias-corrected)	Bulawayo (Uncorrected)	Bulawayo (Bias-corrected)	Masvingo (Uncorrected)	Masvingo (Bias-corrected)
ACCESS	P < 2.2e-16	P=1	P < 2.2e-16	P=1	P < 2.2e-16	P=1	P < 2.2e-16	P=1
BNU-ESM	P < 2.2e-16	P=1	P < 2.2e-16	P=1	P < 2.2e-16	P=1	P < 2.2e-16	P=1
CanESM	P < 2.2e-16	P=1	P < 2.2e-16	P=1	P < 2.2e-16	P=1	P < 2.2e-16	P=1
CCSM4	P < 2.2e-16	P=1	P < 2.2e-16	P=1	P < 2.2e-16	P=1	P < 2.2e-16	P=1
CESM1-CAM5	P < 2.2e-16	P=1	P < 2.2e-16	P=1	P < 2.2e-16	P=1	P < 2.2e-16	P=1
CNRM-CM5	P < 2.2e-16	P=1	P < 2.2e-16	P=1	P < 2.2e-16	P=1	P < 2.2e-16	P=1
CSIRO-MK3	P = 1.467e-05	P=1	P < 2.22e-16	P=1	P= 1.97e-07	P=1	P < 2.2e-16	P=1
GFDL-CM3	P < 2.2e-16	P=1	P < 2.2e-16	P=1	P < 2.2e-16	P=1	P < 2.2e-16	P=1
GFDL-ESM2M	P < 2.2e-16	P=1	P < 2.2e-16	P=1	P < 2.2e-16	P=1	P < 2.2e-16	P=1
HadGEM2-ES	P < 2.2e-16	P=1	P < 2.2e-16	P=1	P < 2.2e-16	P=1	P < 2.2e-16	P=1
IPSL-CM5A-LR	P= 2.45e-14	P=1	P=1.97e-07	P=1	P=0.0003	P=1	P = 6.534e-07	P=1
IPSL-CM5A-MR	P=1.806e-05	P= 0.3056	P < 2.2e-16	P= 0.148	P=5.16e-07	P= 0.236	P < 2.2e-16	P= 0.197
MIROC- CHEM	P < 2.2e-16	P=1	P < 2.2e-16	P=1	P < 2.2e-16	P=1	P < 2.2e-16	P=1
MIROC-ESM	P < 2.2e-16	P=1	P < 2.2e-16	P=1	P < 2.2e-16	P=1	P < 2.2e-16	P=1
MRI-GCM3	P= 4.782e-12	P=1	P < 2.2e-16	P=1	P < 2.2e-16	P=1	P < 2.2e-16	P=1

Senegal

Models	Saint-Louis (Uncorrected)	Saint-Louis (Bias-corrected)	Dakar (Uncorrected)	Dakar (Bias-corrected)	Sedhiou (Uncorrected)	Sedhiou (Bias-corrected)	Tambacounda (Uncorrected)	Tambacounda (Bias-corrected)
ACCESS	P < 2.2e-16	P=1	P < 2.2e-16	P=1	P < 2.2e-16	P=1	P < 2.2e-16	P=1
BNU-ESM	P = 0.0450	P=1	P < 2.2e-16	P=1	P = 4.365e-10	P=1	P < 2.2e-16	P=1
CanESM	P < 2.2e-16	P=1	P= 2.069e-06	P=1	P = 1.34e-13	P=1	P = 3.239e-06	P=1
CCSM4	P < 2.2e-16	P=1	P < 2.2e-16	P=1	P = 3.453e-14	P=1	P = 2.449e-10	P=1
CESM1-CAM5	P < 2.2e-16	P=1	P= 2.363e-09	P=1	P = 4.782e-12	P=1	P=1.356e-09	P=1
CNRM-CM5	P = 1.338e-12	P=1	P= 7.372e-05	P=1	P = 1.792e-09	P=1	P = 4.979e-05	P=1
CSIRO-MK3	P = 8.946e-05	P=1	P < 2.2e-16	P=1	P < 2.2e-16	P=1	P < 2.2e-16	P=1
GFDL-CM3	P= 0.00825	P=1	P = 1.024e-09	P=1	P = 0.0095	P=1	P = 2.025e-08	P=1
GFDL-ESM2M	P = 8.66e-15	P=1	P= 2.54e-14	P=1	P = 3.273e-10	P=1	P < 2.2e-16	P=1
HadGEM2-ES	P < 2.2e-16	P=1	P < 2.2e-16	P=1	P < 2.2e-16	P=1	P < 2.2e-16	P=1
IPSL-CM5A-LR	P < 2.2e-16	P=1	P < 2.2e-16	P=1	P < 2.2e-16	P=1	P < 2.2e-16	P=1
IPSL-CM5A-MR	P < 2.2e-16	P= 1.83e-10	P < 2.2e-16	P= 0.9671	P < 2.2e-16	P= 0.02141	P < 2.2e-16	P= 0.482
MIROC- CHEM	P = 4.08e-05	P=1	P < 2.2e-16	P=1	P = 0.008	P=1	P < 2.2e-16	P=1
MIROC-ESM	P = 2.069e-06	P=1	P < 2.2e-16	P=1	P = 0.0045	P=1	P < 2.2e-16	P=1
MRI-GCM3	P < 2.2e-16	P=0.9962	P = 3.45e-14	P=1	P < 2.2e-16	P=1	P < 2.2e-16	P=1

Mauritania

Models	Nouakchott (Uncorrected)	Nouakchott (Bias-corrected)	Kiffa (Uncorrected)	Kiffa (Bias-corrected)	Bassikounou (Uncorrected)	Bassikounou (Bias-corrected)	Tichit (Uncorrected)	Tichit (Bias-corrected)
ACCESS	P < 2.2e-16	P=1	P = 8.66e-15	P=1	P < 2.2e-16	P=1	P = 8.66e-15	P=1
BNU-ESM	P = 0.0214	P=1	P = 2.449e-10	P=1	P = 0.0796	P=1	P = 0.1798	P= 3.337 e-05
CanESM	P < 2.2e-16	P=1	P = 2.025e-08	P=1	P = 1.558e-08	P=1	P=0.2812	P=1
CCSM4	P = 2.069e-06	P=1	P = 1.338e-12	P=1	P = 0.0243	P=1	P = 4.395e-08	P=1
CESM1-CAM5	P < 2.2e-16	P=1	P < 2.2e-16	P=1	P = 9.382e-08	P=1	P = 1.97e-07	P=1
CNRM-CM5	P = 0.0109	P=1	P = 2.725e-05	P=1	P = 0.1974	P=1	P = 0.3877	P=1
CSIRO-MK3	P = 5.811e-10	P=1	P < 2.2e-16	P=1	P= 6.546e-12	P=1	P = 1.732e-14	P=1
GFDL-CM3	P= 0.2581	P=1	P = 2.109e-15	P=1	P= 6.996e-13	P=1	P = 4.365e-10	P=1
GFDL-ESM2M	P < 2.2e-16	P=1	P < 2.2e-16	P=1	P < 2.2e-16	P=1	P < 2.2e-16	P=1
HadGEM2-ES	P < 2.2e-16	P=1	P < 2.2e-16	P=1	P < 2.2e-16	P=1	P < 2.2e-16	P=1
IPSL-CM5A-LR	P = 1.66e-11	P=1	P < 2.2e-16	P = 6.25e-06	P < 2.2e-16	P=3.11e-09	P < 2.2e-16	P= 2.2e-16
IPSL-CM5A-MR	P < 2.2e-16	P < 2.2e-16	P < 2.2e-16	P=0 1.97e-07	P < 2.2e-16	P= 1.189e-05	P < 2.2e-16	P= 2.2e-16
MIROC- CHEM	P = 0.00039	P=1	P < 2.2e-16	P=1	P = 0.0005	P=1	P = 3.337e-05	P=1
MIROC-ESM	P = 1.204e-07	P=1	P < 2.2e-16	P=1	P = 7.372e-05	P=1	P = 0.0006	P=1
MRI-GCM3	P < 2.2e-16	P=1	P = 1.221e-14	P=1	P < 2.2e-16	P=1	P < 2.2e-16	P=0.4178

Appendix D: Country Selection from IPCC Observations and Projections

Annual precipitation Change over Africa

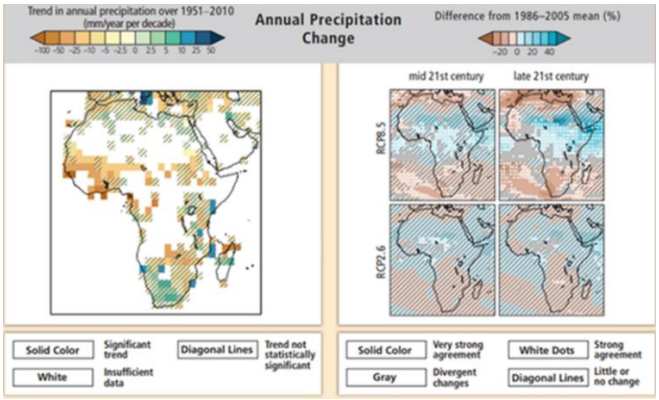

The figures above show maps of observed and projected changes in annual precipitation over Africa from 1951–2010, derived from a linear trend. [WGI AR5 Figures SPM.2 and 2.29]. For the observed data (left panel), trends have been calculated where sufficient data permit a robust estimate (i.e., only for grid boxes with greater than 70% complete records and more than 20% data availability in the first and last 10% of the time period). For the projections (right panel), annual average temperature changes and average percent changes in annual mean precipitation are calculated using CMIP5 multi-model for 2046–2065 (mid-century) and 2081–2100 (late century) under RCP2.6 and 8.5, relative to 1986–2005. Other areas are white. Solid colors indicate areas where trends are significant at the 10% level. Diagonal lines indicate areas where trends are not significant.

Seasonal Mean Precipitation Change Globally (RCP 8.5)

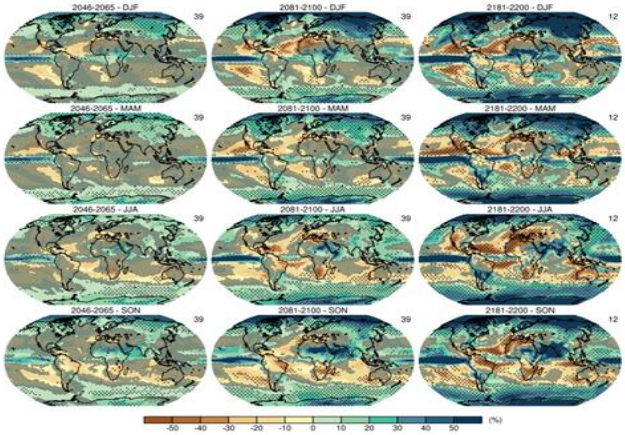

The figure on the left shows a multi-model ensemble mean of projected changes in the seasonal mean precipitation for 2045–2065, 2081–2100 and 2181–2200 relative to 1986–2005 under RCP8.5 forcing scenario for the four seasons. [WGI AR5 Figure 12.22]. The number of CMIP5 models used is indicated in the upper right corner.

Appendix E: Main Parameters used in ARV for each Country

Country	Reference Crops	Season Start	Season End	1st Dekad Criterion	2nd Dekad Criterion	3rd Dekad Criterion	Aggregation Method	Aggregation Period	Threshold	WRSI reduction	WRSI Benchmark	Cost per person
Malawi	Maize	11 Nov	31 May	25 mm	0	0	Maximum	5 years	100 mm	3 points	Median	USD 42
Zimbabwe	Maize	25 Sept	28 Feb	20 mm	5 mm	5mm	First	10 years	100 mm	3 points	Mean	USD 40
Senegal	Groundnut	11 May	20 Nov	20 mm	5 mm	5 mm	Maximum	10 years	100 mm	3 points	Median	USD 50
Mauritania	Sorghum	11 June	31 Nov	20 mm	5 mm	5 mm	First	5 years	60 mm	0 points	Mean	USD 60

Appendix F: Bias-Correction Script

```
# This script applies a Q-Q mapping approach to bias-correct

# CMIP5 rainfall data over Africa for Historical forcings (Hist)

# and Historical with Natural forcings (Nat).

rm(list=ls()) # cleaning up

# Load required libraries

library(ncdf4)

library(fields)

# Load library ends here

# set work directory

setwd("/home/rodoulami/lustre/AXAPostDoc-Projects/supervision/MSc_students/Sylvia/analysis02")

################################################

# load and set observed data

Obsdata <- nc_open("dkd.data/dkd.data01/obs/pr_dkd_CPC_ARC2_nomissing.19890101-20181231.nc") # loading
ncdf file

prOb    <- ncvar_get(Obsdata, "precOb")

lat     <- ncvar_get(Obsdata, "lat")

lon     <- ncvar_get(Obsdata, "lon")

timeOb  <- ncvar_get(Obsdata, "time")

# nctimegpcc<-ncvar_get(ncdata, "time") #months since 1891-01-15

ntsOb <- length(timeOb)  # Get the number of time steps in data

nyOb  <- ntsOb/36       # Get the number of years of data. It doesn't work if the last year is not full, i.e. if it doesn't
have 36 dekads

nj    <- length(lat)

ni    <- length(lon)

prOb_bydekad <- array(prOb,dim = c(ni,nj,nyOb,36)) #array

# Done with loading and setting of observation data

################################################

# Number of files to bias-correct (nfile) for each forcing

# The number of file must be the same for historiacal and

# natural forcing.
```

```
nfile = 15
# Open and read the text file with the full list of input data
# to bias-correct.
indata <- read.table("AllFiles01.txt", header = FALSE)
# Paths to the location of the input data
inputHist = "rgd.data/hist/"
inputNat  = "rgd.data/histNat/"
################################################
# Loading data: Open and read model historical data
for (k in 1:nfile) {
 Histdata <- nc_open(paste0(inputHist,indata[k,1]))
 prH   <- ncvar_get(Histdata, "prec")
 lat   <- ncvar_get(Histdata, "lat")
 lon   <- ncvar_get(Histdata, "lon")
 timeH <- ncvar_get(Histdata, "time")
 ntsH <- length(timeH)
 nyH  <- ntsH/36
 nj   <- length(lat)
 ni   <- length(lon)
 prH_bydekad <- array(prH,dim = c(ni,nj,nyH,36)) #array
# Done with loading model historical data
################################################
# Loading data: Open and read model natural data
 Natdata <- nc_open(paste0(inputNat,indata[k,2]))
 prN   <- ncvar_get(Natdata, "prec")
 lat   <- ncvar_get(Natdata, "lat")
 lon   <- ncvar_get(Natdata, "lon")
 timeN <- ncvar_get(Natdata, "time")
 ntsN <- length(timeN)
 nyN  <- ntsN/36
 nj   <- length(lat)
 ni   <- length(lon)
```

```
prN_bydekad <- array(prN,dim = c(ni,nj,nyN,36)) #array
# Done with loading model historicalNat data
################################################
################ BIAS CORRECTION ################
################################################
# Bias correcting data: Q-Q mapping
# this is done month by month or dekad by dekad
# creating arrays filled with NaN to store bias-corrected data
  prH_bc_QQ <- array(NaN, c(ni,nj,nyH,36))
  prN_bc_QQ <- array(NaN, c(ni,nj,nyN,36))

  prH_bc_rnd <- array(NaN, c(ni,nj,nyN,36))
  prN_bc_rnd <- array(NaN, c(ni,nj,nyN,36))

  prH_bc_lim <- array(NaN, c(ni,nj,nyN,36))
  prN_bc_lim <- array(NaN, c(ni,nj,nyN,36))

  prH_bc_int <- array(NaN, c(ni,nj,nyN,36))
  prN_bc_int <- array(NaN, c(ni,nj,nyN,36))

# Bias-correction starts here
 for (m in 1:36) {
 for (j in 1:nj) {
 for (i in 1:ni) {
 ecdfH  <- ecdf(prH_bydekad[i,j,,m])

 # calculate quantiles for all dataset
  qH  <- ecdfH(prH_bydekad[i,j,,m])
  qN  <- ecdfH(prN_bydekad[i,j,,m])  # qN uses the ecdfH
 # translate quantiles into values
# type is important in the line below.
# type=1 calculates quantiles from the empirical distribution.
```

```
    # Othewise a smooth, fitted distribution is used.
      prH_bc_QQ[i,j,,m] <- quantile(prOb_bydekad[i,j,,m], qH, na.rm = T, type = 1)
      prN_bc_QQ[i,j,,m] <- quantile(prOb_bydekad[i,j,,m], qN, na.rm = T, type = 1)
}
# Bias correction ends here
##################################################
# Setting the bias-corrected values
# to ARC requirements for historical
 prH_bc_QQ <- round(prH_bc_QQ,0)      # Round the bias-corrected values
 prH_bc_QQ <- as.integer(prH_bc_QQ)    # Set the bias-corrected values as integers
 prH_bc_QQ[prH_bc_QQ>253] <- 253      # Set the bias-corrected values greater than
# 253 mm to 253 mm to satisfy ARC requirements
# Setting the bias-corrected values
# to ARC requirements for Natural
 prN_bc_QQ <- round(prN_bc_QQ,0)      # Round the bias-corrected values
 prN_bc_QQ <- as.integer(prN_bc_QQ)    # Set the bias-corrected values as integers
 prN_bc_QQ[prN_bc_QQ>253] <- 253      # Set the bias-corrected values greater than
# 253 mm to 253 mm to satisfy ARC requirements
# Paths to the location where to save output data
 outputHist = "bc.data/bc.data02/hist"
 outputNat  = "bc.data/bc.data02/histNat/"
##################################################
# Saving bias-corrected output data
# Prepare bias-corrected model outputs for historical
 precH <- array(prH_bc_QQ, dim = c(ni,nj,ntsH))   # because it was an 4d array, and we need a 3d array
# Define dimensions
 xdim = ncdim_def('lon', 'degrees_east', lon)
 ydim = ncdim_def('lat', 'degrees_north', lat)
 tdim = ncdim_def('time', 'days since 0001-01-01', timeH)
 mv <- as.integer(-999999999)   #-9.99999979021477e+33
# Define variables
```

```
  varx <- ncvar_def("precH", "mm per dekade", list(xdim,ydim,tdim),mv,longname="Rainfall q-q Bias-correction for
Historical ", prec="integer")

  bcH.out <- nc_create(paste0(outputHist,indata[k,3]), list(varx) ) # Create netcdf output file

# Write variables into netcdf output file

  for(it in 1:ntsH) {

    ncvar_put(bcH.out, varx, precH[,,it], start=c(1,1,it), count=c(-1,-1,1) )

  }

  nc_close(bcH.out)  # Close netcdf output file

# Prepare bias-corrected model outputs for historicalNat

  precN <- array(prN_bc_QQ, dim = c(ni,nj,ntsN))  # because it was an 4d array, and we need a 3d array

# Define dimensions

  xdim = ncdim_def('lon' ,'degrees_east', lon)

  ydim = ncdim_def('lat' ,'degrees_north', lat)

  tdim = ncdim_def('time' ,'days since 0001-01-01', timeN)

  mv <- as.integer(-999999999)   #-9.99999979021477e+33

# Define variables

  vary <- ncvar_def( "precN", "mm per dekade", list(xdim,ydim,tdim),mv,longname="Rainfall q-q Bias-correction for
Nataural", prec="integer")

  bcN.out <- nc_create(paste0(outputNat,indata[k,4]), list(vary) ) # Create netcdf output file

# Write variables into netcdf output file

  for(it in 1:ntsN) {

  ncvar_put(bcN.out, vary, precN[,,it], start=c(1,1,it), count=c(-1,-1,1) )

  }

  nc_close(bcN.out) # Close netcdf output file

} # end of for model in models "for (k in 1:nfile)"
```